A Tale of Waves and Eddies in a Sea of Rotating Turbulence

by

Amrik Sen

B.Tech., National Institute of Technology, Silchar, 2006

M.S., University of Colorado, Boulder, 2009

Doctoral Dissertation

A thesis submitted to the

Faculty of the Graduate School of the

University of Colorado in partial fulfillment

of the requirements for the degree of

Doctor of Philosophy

Department of Applied Mathematics

2014

This thesis entitled:

A Tale of Waves and Eddies in a Sea of Rotating Turbulence

written by Amrik Sen

has been approved for the Department of Applied Mathematics

_____

Dr. Annick Pouquet

_____

Prof. Keith Julien

_____

Prof. Pablo Daniel Mininni

_____

Prof. Tom Manteuffel

_____

Prof. Bengt Fornberg

Date _____

The final copy of this thesis has been examined by the signatories, and we find that both the content and the form meet acceptable presentation standards of scholarly work in the above mentioned discipline.

Sen, Amrik (Ph.D., Applied Mathematics)

A Tale of Waves and Eddies in a Sea of Rotating Turbulence

Thesis directed by Dr. Annick Pouquet

Abstract

In this thesis, we investigate several properties of rotating turbulent flows. First, we ran several computer simulations of rotating turbulent flows and performed statistical analysis of the data produced by an established computational model using Large Eddy Simulations (LES). This enabled us to develop deeper phenomenological understanding of such flows, e.g. the effect of anisotropic injection in the power laws of energy and helicity spectral densities, development of shear in specific rotating flows and evidence of wave-vortex coupling. This served as a motivation for detailed theoretical investigations. Next, we undertook a theoretical study of nonlinear resonant wave interactions to deduce new understanding of rotating flow dynamics. The latter analysis pertained to the highly anisotropic regime of rotating flows. To the best of our knowledge, the application of wave-turbulence theory to asymptotically reduced equations in the limit of rapidly rotating hydrodynamic flows is presented here for the first time and aims to further our understanding of highly anisotropic turbulent flows. A coupled set of equations, known as the wave kinetic equations, for energy and helicity is derived using a novel symmetry argument in the canonical description of the wave field sustained by the flow. A modified wave turbulence schematic is proposed and includes scaling law solutions of the flow invariants that span a hierarchy of slow manifold regions where slow inertial waves are in geostrophic balance with non-linear advection processes. A brief summary of the key findings of this thesis is presented in Table 1.

To my mother, ***Sanjukta***

for being the best teacher ever.

Acknowledgements

At the outset, I would like to acknowledge the support of my parents. My thoughts and ideas are a manifestation of theirs in all forms and shape. Secondly, I am extremely grateful for the constant encouragement of my friends, my life as a graduate student is incomplete without them. Special note of thanks to Jason Hammond, Ashar Ali, Matthew Reynolds, Steve Chestnut, Anthony Rasca and Ted Galanthay. I would also like to mention that during my stay in Colorado for the past seven years, I have developed many friendships outside the university and Colorado itself became home to me. Special thanks are due to Chern Lim and Russ Anthony for their friendship and contribution in making me a better athlete and sportsman despite the demands and rigor of graduate school. They and many other friends from the Boulder Badminton Club have further convinced me that *a healthy mind resides in a healthy body.* My interests outside academic research have spanned from biking, trail running, badminton to following live local music and volunteering in a tutoring program for advanced placement tests with high school kids, all of which have enriched my life in many ways. I have also had the opportunity to teach in the capacity of an instructor, both at CU Boulder and at FRCC (Westminster), to a wide student audience from engineering to nursing graduates, an experience I have thoroughly cherished and enjoyed. Their enthusiasm and inquisitiveness to learn has strengthened my faith in education. I would conclude here by quoting from an inscription on the walls of the George Norlin library here at the University of Colorado, Boulder campus: *"Enter here the timeless fellowship of the human spirit"*.

January 1, 2014 Amrik Sen

Contents

Chapter

Tables

Table

Figures

Figure

Summary of new results of this thesis

Ch. No.	Sec. no.	Remark
2	2.2 2.3.3	Inverse cascade energetics in rotating turbulence simulations: spectra and phenomenology, anisotropic injection builds shear in rotating flows.
5*	5.2, 6.1	Coupled energy-helicity equations are derived for the first time for asymptotically reduced hydrodynamic equations that are valid in the slow manifold. Symmetry arguments are used in the canonical description to extend the results of the special non-helical flow to the general fully helical flow. Energy and helicity spectral power laws are obtained.

Table 1: A summary of the key findings of this dissertation research. Items in asterisk (*) denote work accomplished post comprehensive exam.

Chapter 1

Introducing a world of *Waves, Eddies* and *Turbulence*

"To create one's own world takes courage."

Georgia O'Keeffe

In this chapter, we present a historical as well as an application based introduction to the troika, viz., *waves*, *eddies* and *turbulence*, that together form the centerpiece of this doctoral research work. The primary question we attempt to answer in this dissertation is the following, **how does the wave-eddy interplay drive the flow of energy across scales in rotating turbulent flows?** To accomplish this goal, we have analyzed results of computational simulations and employed theoretical investigations of the governing fluid equations. Before we present the detailed analysis of rotating turbulent flows, we introduce the reader to the role of waves, eddies and turbulence in the context of several natural systems pertaining to geophysical and astrophysical applications.

1.1 Waves, eddies and their interplay in nature

Waves are efficient carriers of energy and angular momentum. Hence, their ubiquitous occurrence in different natural systems has an important physical significance. The study of waves has spanned a broad spectrum of applied fields. These studies have broadened our understanding of climate in meteorology [26, 27]. Historically, meteorologists have studied atmospheric disturbances modeled by the nonlinear vorticity equation[52, 53]. These studies were aimed at forecasting

weather phenomena and atmospheric circulations [104, 31]. *Atmospheric Rossby waves*, as they are better known, emerge due to shear in rotating flows. These waves were first invented by Carl-Gustaf Arvid Rossby, who described their motion. Specifically, it was shown that easterly waves have diminishing velocity with increasing wavelength, while the situation reversed for westerly currents [94]. This is only a historical perspective of the significance of studying wave phenomena in the context of atmospheric meteorology and we will comment a little more on some of the recent investigations in this field in a while after we mention the role of waves in other fields of science.

Atmospheric studies are often not confined to our planet earth because several physical processes on earth are impacted, either directly or indirectly, by phenomena happening outside our thin atmosphere. In this regard, one of the primary subjects of research investigation is the Sun and its atmosphere. More specifically, the study of the Sun's corona and its highly ionized plasma state. In the corona, kinetic and magnetohydrodynamic (henceforth referred to as MHD) waves transport energy from the chromosphere to the outer corona and the solar wind and thereby sustain the solar corona [78, 23]. Kinetic models of the solar corona have revealed the possibility of coronal particle acceleration and heating by high-frequency waves, although previous studies had only detected prevalence of weak MHD waves. However, a recent observational study by McIntosh et. al. [80] has shown the existence of large amplitude Alfvénic waves of the order of $20kms^{-1}$ and the periods of the order of $100 - 500s$ in the quiet solar atmosphere with sufficient energy reserves to pump the solar corona. Mathematical models and simulations further support this proposition [55, 128].

Beyond the earth and the sun lies the large expanding universe and the scientific realm of astrophysics. Here, we will mention a few areas in astrophysics where the role of waves (often gravity waves) is important, one such field being the study of accretion discs. Accretion discs are a ubiquitous phenomenon in astrophysics, from planetary formation, Saturn's rings, black holes that swallow stars to the Milky Way's spiral structure. The focal point of accretion disk theory is to understand how angular momentum is transported in the radially outward direction so that matter can *accrete* onto the central gravitating body. In this context, Lovelace et. al. [73] consider a thin

(2D) non-magnetized Keplerian accretion disk based on the vorticity equation [96] to show that a certain Rossby wave instability mechanism results in the formation of multiple Rossby vortices after *breaking* of the waves, the vortices then coalesce after a few revolutions. This may explain the transport of angular momentum in the radially outward direction. Moreover, simulation studies like that of Arras et. al. [2] have shown that quasi-periodic oscillations (QPOs) associated with accreting neutron star and black hole binaries are triggered by magneto-rotational instabilities. Further, observational studies have demonstrated wave bending and warping phenomena in binary star systems [105]. While the role of waves in these examples has significant influence in the actual dynamics of the respective processes, the question one may ask is how are these waves produced? How do they couple with the dynamics of vortices and turbulence?

Eddies are *swirling* of a fluid and are representative of vortical motions. Sometimes, standing or solitary wave modes may be analogous with vortical coherent structures that abound in geophysical and planetary dynamics. The two best examples that come to mind are the *polar vortex* in the earth's stratosphere prominent in the winter and the *Great Red Spot* (GRS) on Jupiter's southern equatorial belt. Unlike waves which serve as carriers of energy and momentum, vortices are invariably reserves (pool) of momentum, mass and energy. Together, they are the powerhouse of many natural systems and detail understanding of their interplay (technically, interaction) is key to unraveling the mystery of several physical processes of this universe. In this introductory section, we will only mention a few examples of wave-vortex interplay as a motivation of this thesis work.

Earlier, in the introductory paragraph, we mentioned that long wave disturbances in the earth's atmosphere affect the climate. A logical starting point is to understand how such waves may be generated at the first place? Instabilities and orographic asymmetries are known sources of wave generation. Another possible source is tropical cyclones that radiate Rossby waves due to existence of large scale potential vorticity gradients in the atmosphere, this theory has been supported by numerical simulations by K. D. Krouse et. al. [68]. This is not surprising as supported by a common and simple experiment by throwing a stone on water in a pond would show that surface gravity

waves are generated in the radial direction. Numerical simulations using the quasi-geostrophic vorticity equation in a beta plane have shown that stratospheric planetary wave activities can be sustained by forcing from tropospheric baroclinic eddies [107]. The occurrence of vortex islands in models of protoplanetary nebula are considered to be sources of Rossby waves, the latter can be generated as a result of vorticity gradients as has been shown vía computer simulations by Davis et. al. [36]. A recent theoretical and numerical study has shown that internal waves in the deep ocean may be generated by resonant interactions between tidal oscillations and geostrophic eddies as long as the horizontal length scales of the tidal currents and the eddies are comparable [70]. These length scales are normally not comparable except near coastlines where topographic effects can play a role. These studies clearly emphasize the interplay between waves and eddies in atmospheric and planetary flows and their impact in atmospheric and planetary circulations in general. Numerical experiments by Bigot and Galtier [11] have shown the coupling of 3D wave modes and 2D vortical modes in the presence of a strong magnetic field and can explain the co-existence of waves and vortices in astrophysical plasmas.

A confluence of a classical hydrodynamic theory with a relatively modern quantum mechanical theory is the field of superfluid flows. This will help us understand complex fluid motions in both low temperature fluids and ordinary fluids. A recent study by L'vov et. al. describe the nature of interaction between hydrodynamic eddies and Kelvin waves in superfluid turbulence [123]. Hopefully, these examples have reinforced the fact that the interplay of waves and eddies in a variety of physical systems is an important phenomena and understanding the mechanism of their interaction is of fundamental significance. It must also be said that most of the examples presented here thus far, involve another complex phenomena intertwined with the story of waves and eddies. This complex phenomena is *turbulence* and is known as the last unsolved problem in classical physics. In the subsequent paragraphs, we informally introduce the history and science associated with the study of turbulence.

Turbulence is a quintessential problem in nonlinear physics. The complexity of a turbulent fluid flow is elucidated by the prevalence of a multitude of interacting scales [43] that exchange

energy amongst themselves [66] and manifest interesting physical structures [39].

1.1.1 Eddies and turbulence

So what exactly is *turbulence*? This question can be perhaps best answered by quoting Lewis Fry Richardson's famous couplet [102]: *'Big whirls have little whirls that feed on their velocity, and little whirls have lesser whirls and so on to viscosity.'* Thus, Richardson's notion of turbulence is that of a flow composed of *eddies* of different scales exchanging energy among themselves, thereby resulting in smaller eddies from larger ones. This cascading of energy into smaller eddies continues until a sufficiently small scale whence the viscosity of the fluid effectively dissipates the kinetic energy into internal energy of the fluid system. The story of classical turbulence is thus a fascinating tale of *cascading eddies*. This story was beautifully captured in a sketch by Leonardo Da Vinci a few hundred years before it was put in words by Richardson (see Figure 1.1.1). In this sense, turbulence is ubiquitous; from the profile of smoke rising from a cigarette to atmospheric circulation, and from flow in gas turbines to blood flow in human body.

1.1.2 Waves and turbulence

So, is the story of turbulence a story of eddies alone? An interesting extension of the problem of turbulence is to examine the flow by imposing an anisotropic effect like a direction specific magnetic field or an imposed global rotation. In this thesis we will study the latter as a canonical framework for studying turbulence. We will formulate our examination of wave-eddy dynamics in fluid flows within this set up.

The introduction of rotation through a Coriolis term in the governing equations and its effect on the geometrical features that develop in the flow, have been studied for over a century now [56, 101, 117]. Consider, the nondimensionalized incompressible Navier-Stokes equations (the governing equations) with global rotation, $\mathbf{\Omega} = \Omega\hat{z}$, as follows:

$$\partial_t \mathbf{u} + (\mathbf{u}\cdot\nabla)\mathbf{u} + \frac{1}{Ro}\hat{z}\times\mathbf{u} = -\frac{1}{Ro}\nabla P + \frac{1}{Re}\nabla^2\mathbf{u} + \mathbf{f}, \tag{1.1}$$

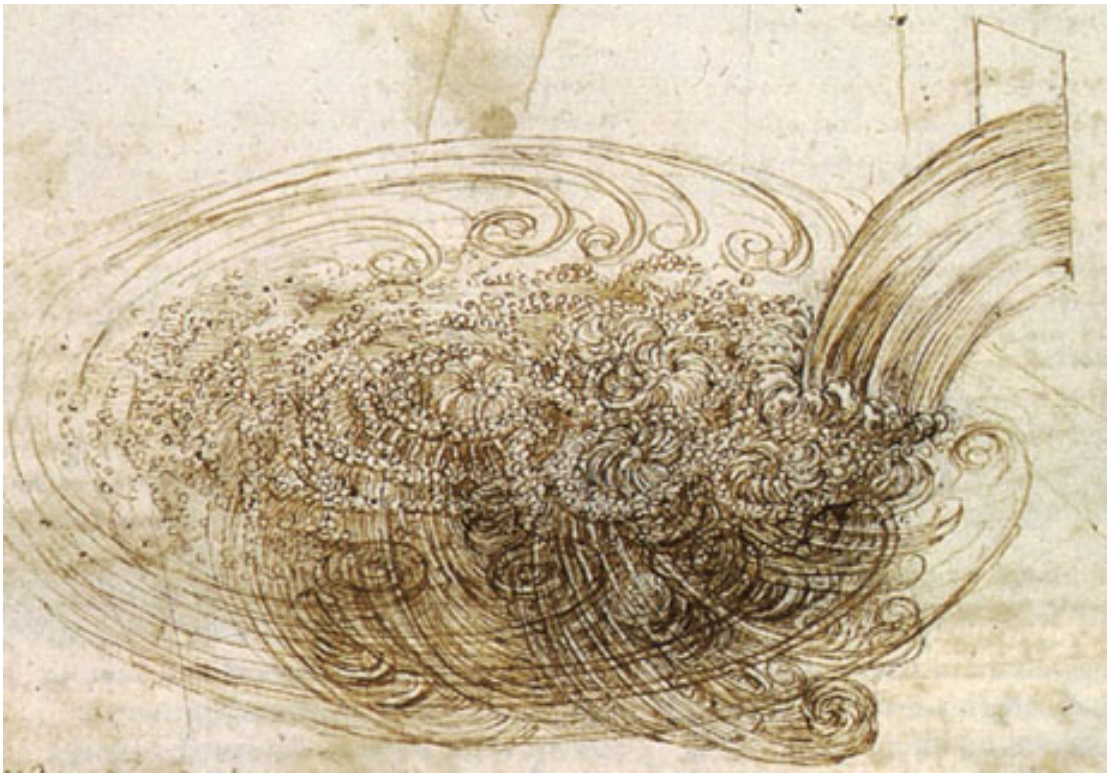

Figure 1.1: Leonardo Da Vinci's illustration of the swirling flow of turbulence. The sketch elucidates that water flowing out of an orifice has eddying motions of different scales (*courtesy: The Royal Collection ©2004, Her Majesty Queen Elizabeth II*).

$$\nabla \cdot \mathbf{u} = 0, \tag{1.2}$$

where $\mathbf{u}$ is the instantaneous velocity field, P is the pressure term, $\mathbf{f}$ is an external force per unit mass, the Rossby number is $Ro = \frac{U_0}{2L_0\Omega}$ (where U_0 and L_0 are, respectively, normalized velocity and length scales taken to be unity), and the Reynolds number is $Re = \frac{U_0 L_o}{\nu}$ (where ν is the kinematic viscosity). To understand the role of global rotation in the flow dynamics, consider a steady state,

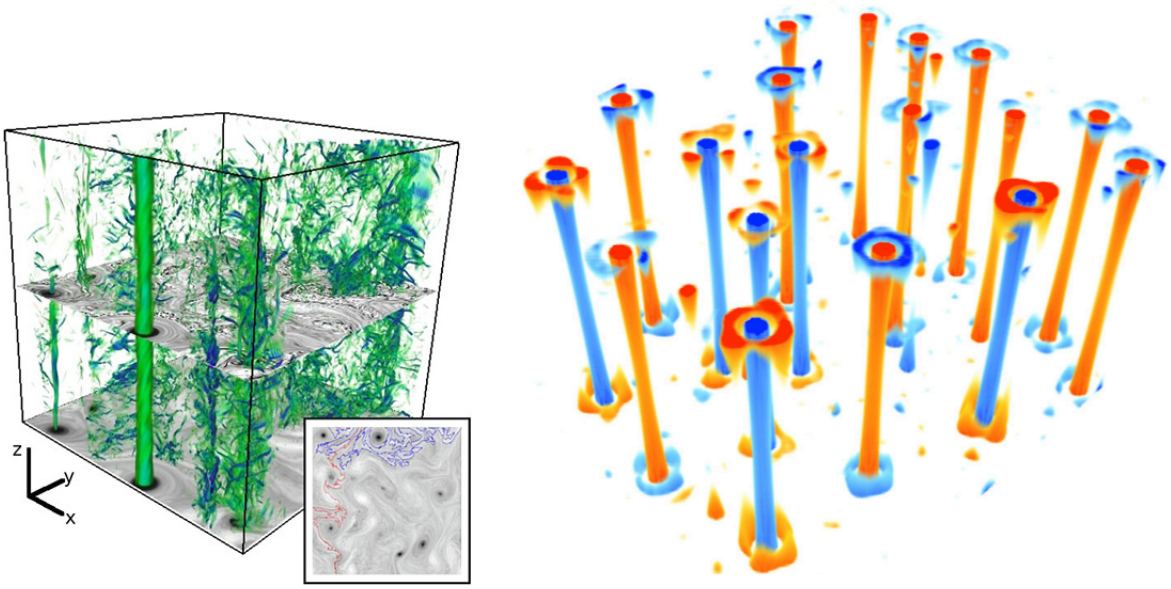

Figure 1.2: Left: Perspective volume rendering of vorticity intensity in a snapshot of a 1536^3 rotating turbulent helical flow (*courtesy: NCAR* and [121]). Right: Convective Taylor Columns from simulations of Rayleigh-Beénard convection using reduced equations [51].

inviscid, weakly (negligibly) nonlinear approximation of the governing equation (1.1) in the absence of external forces. This results in a balance between the Coriolis term and the gradient of pressure: $\hat{z} \times \mathbf{u} = -\nabla P$, whence the curl of this expression along with the incompressibility condition (1.2) gives us the following relation:

$$(\hat{z} \cdot \nabla)\mathbf{u} = 0. \tag{1.3}$$

Equivalently, this means $\mathbf{u} = \mathbf{u}(x, y)$, i.e. the velocity field is independent of z under the effect of rapid global rotation. This is known as the *Taylor-Proudman* theorem [49]. The implication of this theorem is the observed emergence of columnar structures in rotating turbulent flows (see

Figure 1.1.2). Morevover, the linear, inviscid, time-dependent equation is known to have *wave* solutions,

$$\mathbf{u} = \mathbf{U}e^{i\omega t}, \tag{1.4}$$

$$P = \mathcal{P}e^{i\omega t}, \tag{1.5}$$

where ω is the wave frequency, $\mathbf{U}$ and $\mathcal{P}$ are, respectively, the velocity and pressure amplitudes. The *waves* in the flow are of the *dispersive* type [130] and the dispersion relation is given by,

$$\omega_s(\mathbf{k}) = 2\Omega s\frac{k_z}{k}, \tag{1.6}$$

where k_z is the z-component of the wave vector, $\mathbf{k}$ and $s = \pm 1$. In the subsequent chapters we observe that the effect of the waves, through the dispersion relation, appears in the nonlinear energy transfer term and thereby plays a key role in the nonlinear transfer of energy across scales.

Rotating turbulence is thus a theater of *waves* and *eddies* interacting with each other at different spatial and temporal scales. The nature of their interaction is thus key to unraveling the mystery of rotating turbulent flows. This manuscript is an attempt in that direction.

1.2 Brief survey of rotating turbulence in the atmospheres, laboratory and computer simulations

We would like to emphasize that fluid turbulence is a matured field with several contributions leading to a vast body of work that has been archived in the research literature. Here we briefly mention a few research efforts that served as a motivation of this thesis work. Several other work is cited in relevant parts of the thesis in the subsequent chapters.

1.2.1 Rotating turbulence in geophysical and planetary atmospheres

Rotating fluid flow is ubiquitous in nature, from atmospheric and oceanic phenomena to planetary dynamics. The interplay between waves and vortical eddies makes for interesting dynamics both from fundamental physical point of view and also in furthering our understanding about several geophysical and planetary processes. Here, we will mention two such recent findings

that served as a motivation to understand wave-vortex interactions which is the main subject of this dissertation. The first is a study of the role of planetary waves in generating and sustaining the stratospheric polar vortex [72]. Another evidence of wave-vortex interplay in planetary science is an observational study about the manner in which planetary wave disturbances on Jupiter's atmosphere are severely impacted by the presence of large vortices like the Great Red Spot (GRS) [111]. Analysis of Cassini satellite data from the Jovian atmosphere has shown evidence of energy exchange between vortical eddies and the mean wind flow in the rich turbulent atmosphere of the planet [106]. It is important to note that in the atmosphere, the wave dynamics due to rotation is often coupled with density stratification effects and thereby interactions between different types of waves like gravity waves are possible especially through near resonant interactions. A detailed presentation of rotating turbulence in the context of geophysical and planetary applications can be found in the literature [124, 81]. Another interesting study on the role of rotation in accretion disks can be found in the paper by Dubrulle et. al. [38].

1.2.2 Rotating turbulence in the laboratory

The interesting observational studies mentioned above and similar studies in the past have always enthused researchers to attempt to simulate similar environments in a controlled laboratory environment since the pioneering work by G. I. Taylor who first showed the emergence of columnar eddies in a rotating tank in the laboratory. These experimental studies have enabled further understanding of rotating turbulent flows and related processes like vortex generation methods [125], resonant wave propagation and decay [13, 15]. The role of instability mechanisms in generating vortices in rotating fluid systems is described in a very simple and easily accessible manner in an article in the Hands-on Oceanography [91].

1.2.3 Rotating turbulence in computer simulations

Here, we mention three recent simulations of rotating turbulent flows and statistical analysis of the simulation data therein. First, is a high resolution (1536^3) direct numerical simulation of

rotating helical turbulence by Mininni and Pouquet [83], [83] and detailed investigation on the role of helical forcing on the flow dynamics. Another simulation of decaying rotating turbulence is the work by Thiele and Muller [122]. In both these papers, the authors have obtained power laws for the anisotropic energy spectrum that are in agreement with the analysis presented later in this thesis. Finally, it is worth mentioning computational simulations of asymptotically reduced model for rotating convective flow by Julien et. al. [61] and the statistical analysis of different flow regimes therein. Computational studies of reduced equations have acquired a useful place in the literature as they are valid for flow regimes that are still unattainable by simulations of the full incompressible Navier-Stokes equations. The theoretical wave turbulence investigation presented in the subsequent chapters in this thesis is based on asymptotically reduced equations of Julien and Knobloch [58].

1.3 Dimensional analysis and power laws in turbulence: the legacy of Kolmogorov

Since turbulence is basically chaotic motion of fluid under certain physical constraints, it is impossible to deterministically predict the dynamics of flow field variables (e.g., velocity, vorticity, etc.). Hence a statistical approach is necessary to answer questions like: what is the average decay rate of energy across scales in a turbulent flow? This entails the nature of energy cascade across scales and their possible physical implications. Thus a useful quantity of interest is the isotropic total energy spectrum, $E(k) = \frac{1}{2}\sum_{k\leq|\mathbf{k}|<k+1}|\mathbf{u}(\mathbf{k})|^2$ and is such that the total energy is $E = \sum_k E(k)$. $E(k)$ represents the energy contained in a feature (e.g., eddies) of scale, $l_k \sim \frac{1}{k}$. Kolmogorov's theory [43] is based on a wide separation of viscous and global (box) scales and over a range of wave modes (known as the *inertial* range) where the flux of energy, $\Pi(k)$, given by $\partial_t E(k) = -\partial_k \Pi(k)$, is constant. Dimensional analysis then gives:

$$E(k) \sim \epsilon^{2/3} k^{-5/3}, \tag{1.7}$$

which is valid for all k in the inertial range. Here, ϵ is the rate of energy dissipation. The result expressed in equation (1.7) is valid for two-dimensional flows in the *inverse cascade* range of the spectrum. But the Kolmogorov phenomenology can be extended to the case of decaying rotating turbulence and a constant flux solution for the inertial range energy spectrum can be obtained by equating the inertial wave time scale ($\tau_\Omega = \frac{1}{\Omega}$) with the nonlinear (eddy turn-over) time scale ($\tau_{NL} = \sqrt{k^3 E(k)}$). The Kolmogorov solution for rotating turbulence, in the absence of external forces, is [136]:

$$E(k) \sim (\Omega\epsilon)^{1/2} k^{-2}. \tag{1.8}$$

Scaling law solutions to stationary and non-stationary energy spectra in turbulent flows have been studied by many researchers since the pioneering work by Kolmogorov in 1941. Two interesting papers by Heisenberg in the late 1940s, elaborated later by Chandrasekhar [25], explain how simple explicit solutions for the energy spectrum can be obtained both for the stationary and non-stationary case, by solving a certain second order differential equation. These solutions agree with the predictions of Kolmogorov theory and provide a historical perspective to the significance of scaling law solutions to spectra of turbulence.

1.4 Two dimensional turbulence: a competition between scales

Before we delve into forced rotating turbulent flows, it is useful to review our understanding of two dimensional turbulence in the presence of external forces. It must be emphasized that since the flow is restricted to two dimensions, there is no Coriolis term in the governing equations. This entails an absence of *waves* in the system and hence it is a story of *eddies*. Forced two dimensional turbulence has several unique characteristics, perhaps the most interesting aspect being the reversal in the energy flux resulting in an *inverse cascade* of energy to large scales. This reversal of energy flux is explained in detail in this section. The conceptual explanations of this section are based on the works of Batchelor [7] and the review paper on two dimensional turbulence of Boffetta and Ecke [12]. The following sections underline the role of invariants in the flow dynamics.

1.4.1 Direct cascade of enstrophy

Inviscid two dimensional turbulence, in the absence of external forces, has two fundamental invariants, viz., *energy* and *enstrophy.* However, it must be mentioned that there are an infinitely many *Casimir* invariants in 2D turbulence (i.e. any continuously differentiable function of the vorticity field is conserved) [19] that are conceptual extensions of the two fundamental invariants mentioned here. Energy is as defined in the previous section. Enstrophy, Z is defined as follows: $Z = \frac{1}{2}\bar{\zeta^2} = \frac{1}{2}\sum_{\mathbf{k}} |\zeta_{\mathbf{k}}|^2$, where the over-bar denotes spatial average.[1] Real physical flows have finite viscosity and therefore it is essential to consider the dissipation of energy in the limit of small viscosity for turbulent flows. Again, in the absence of external forces and considering finite non-zero viscosity, the evolution of energy and enstrophy is given by the following equations:

$$\partial_t E = -2\nu Z \equiv \epsilon_\nu(t), \tag{1.9}$$

$$\partial_t Z = -2\nu P \equiv \eta_\nu(t), \tag{1.10}$$

where $P := \int k^4 E(k) dk$ is called the *Palinstrophy.* Equation (1.10) implies a decaying Z and thus it bounds enstrophy from above (initial condition). Therefore, equation (1.9) implies that $\epsilon_\nu \to 0$ as $\nu \to 0$. This is unlike three dimensional turbulence where enstrophy Z is not bounded from above as equation (1.10) has a source term in the case of three dimensional flows. In fact, in three dimensional turbulence, Z is magnified due to vortex stretching. However, in 2D turbulence, spatial gradient of vorticity, $\nabla\zeta$ increases due to prolongation of isovorticity lines. This is explained formally as follows. The governing equation for two dimensional flows in the absence of forcing can be written in terms of vorticity, ζ, as follows:

$$D_t\zeta = \partial_t\zeta + \mathbf{u}\cdot\nabla\zeta = \nu\nabla^2\zeta. \tag{1.11}$$

Taking the gradient of equation (1.11) and using appropriate vector calculus identities[2] along with the incompressibility condition gives us an equation for the evolution of vorticity gradient,

$$\partial_t(\nabla\zeta) = -\nabla\mathbf{u}\cdot\nabla\zeta + \nu\nabla^2(\nabla\zeta). \tag{1.12}$$

[1] Note: ω is used to denote wave frequency and $\zeta = \nabla\times\mathbf{u}$ is used to denote vorticity.
[2] $\nabla(\mathbf{a}\cdot\mathbf{b}) = (\mathbf{a}\cdot\nabla)\mathbf{b} + (\mathbf{b}\cdot\nabla)\mathbf{a} + (\mathbf{a}\times\nabla\times\mathbf{b}) + (\mathbf{b}\times\nabla\times\mathbf{a})$ and $\nabla\times\nabla\mathbf{a} = 0$

Multiplying equation (1.12) by $(\nabla\zeta)$ and averaging over spatial dimensions, we arrive at a transport equation for mean squared vorticity gradient and the resulting nonlinear term comprising of the product of the gradient of velocity and vorticity represents the amplification rate of vorticity gradients by prolongation of isovorticity lines. This means that if the 2D turbulence is initiated with vorticity and vorticity gradients on comparable length scales, the prolongation of the isovorticity lines will amplify the vorticity gradients thereby transporting enstrophy (mean square vorticity) to smaller scales. This is known as the direct cascade of enstrophy to smaller scales and plays a major role in the direction of energy cascade as is explained in the next section.

1.4.2 Dual cascade of energy

Two dimensional turbulence with non-trivial external forcing exhibits dual cascade of energy, i.e. energy cascades both towards smaller and larger scales. The spectrum scales with the respective inertial range wavenumbers as follows:

$$E(k) \sim \epsilon^{2/3} k^{-5/3}, \quad \forall k \ll k_f, \tag{1.13}$$

$$E(k) \sim \eta^{2/3} k^{-3}, \quad \forall k \gg k_f, \tag{1.14}$$

where k_f is the forcing wavenumber and ϵ and η are, respectively, the rate of energy dissipation at viscous and box scales. It is important to note that in the limit of infinite Reynolds number, as $k \to \infty$, we have $E(k) = \frac{Z(k)}{k^2} \to 0$, i.e. energy transfer to the smallest scale is inhibited by the direct cascade of enstrophy.

However, an interesting question is: why does the energy cascade to large scales at all? We will see that the key to this question is directly related to the fact that the other invariant of the system, viz., enstrophy, cascades to smaller scales only. The simplest and yet convincing explanation for the reversal of energy flux to larger scales is based on Fjørtoft's argument [41]. Consider that there are only three interacting wave modes in the system, $\mathbf{k}, \mathbf{p}, \mathbf{q}$ such that $k < p < q$. For simplicity, say $p = 2k$ and $q = 3k$. Let us also denote by $\delta E(k)$ the differential energy in wave mode $\mathbf{k}$ over a fixed incremental time span such that $\delta E(k) < 0$ implies a loss of energy by mode $\mathbf{k}$ in that time

interval and vice versa. Then, the conservation of energy and enstrophy entail the following:

$$\delta E(k) + \delta E(p) + \delta E(q) = 0, \tag{1.15}$$

and

$$\delta Z(k) + \delta Z(p) + \delta Z(q) = 0, \tag{1.16}$$

where $\delta Z(k) = k^2 \delta E(k)$. Equations (1.15) and (1.16) result in $\delta E(k) = -\frac{5}{8}\delta E(p)$ and $\delta E(q) = -\frac{3}{8}\delta E(p)$. So if the intermediary wave mode $\mathbf{p}$ loses energy, i.e. $\delta E(p) < 0$ then $\delta E(k) > \delta E(q) > 0$. This means more energy goes to the larger scale, $\mathbf{k}$ than the smaller scale, $\mathbf{q}$ and thereby elucidating the inverse energy cascade. However, it is interesting to note that $\delta Z(q) = -\frac{27}{8}k^2\delta E(p)$ and $\delta Z(k) = -\frac{5}{8}k^2\delta E(p)$ and thus if $\delta E(p) < 0$, we have $\delta Z(q) > \delta Z(k)$. This is a clear indication of a direct cascade of enstrophy. It is easy to check that if the enstrophy cascades to larger scales, it is impossible to have an inverse cascade of energy based on the above arguments. The pioneering work in two-dimensional turbulence is the work by Robert Kraichnan and is a useful reference [66].

Therefore, in order to have an inverse cascade of any one of the invariants of the system, it is imperative to have a purely direct cascade of the other invariant of the system. We will see later in the following chapter that in the case of forced rotating flows, a new invariant, *helicity* (alignment of velocity and vorticity, i.e. $\mathbf{u} \cdot \zeta$) plays the role of the enstrophy to enable the inverse cascade of energy. However, a naive and direct application of this argument, to the case of 3D turbulence, is contested by Kraichnan [67] because unlike enstrophy, helicity at any given mode $\mathbf{k}$, denoted by $H(\mathbf{k})$, is not exactly determined by $E(\mathbf{k})$ (or equivalently by $u_{\mathbf{k}}$). It is merely bounded from above by $E(\mathbf{k})$ by the relation: $|H(\mathbf{k})| \leq k|E(\mathbf{k})|$. Moreover, since maximal helicity is not conserved, the equality in the above relation does not necessarily hold true for any $\mathbf{k}$ even in the case of a maximally helical initial state. This means that the invariance of helicity is not a sufficient condition for the reversal in energy flux to larger scales and this is what makes the study of 3D rotating turbulence an interesting and difficult one. It must be noted that helicity is identically zero in two dimensional flows.

1.5 Summary

In this introductory chapter, we have stated the motivating factors of this thesis. We have also presented a brief overview of 2D turbulence. Two dimensional turbulence is a matured research field having occupied the minds of several researchers over more than two centuries. A broader narrative on 2D turbulence can be found in several review articles on the topic [64, 116] and that of Fornberg [42] for a computational perspective.

Chapter 2

Rotating Turbulence I: Phenomenology and Simulations

"It is important to express oneself...provided the feelings are real and are taken from your own experience."

Berthe Morisot

In the previous chapter, we have introduced, albeit briefly, the problem of turbulence with background rotation. We will see, from what follows here and the latter chapters, that the many interesting challenges posed by background rotation stem from the presence of *inertial Waves* that interact with the *vortical Eddies* and thereby alter the dynamics and energetics of the flow system. For e.g., it is well known that rotation decreases the rate of energy decay [21, 89]. Rotation also introduces a new invariant of the system, viz., *helicity*. Helicity is a measure of the alignment of velocity and vorticity and is non-trivial in a 3D flow unlike in the 2D case. The new invariant has been shown to further decrease the energy decay rate only in the presence of background rotation but does not affect the energy decay in the absence of rotation [119]. The fact that non-trivial helicity retards the nonlinear energy transfer across scales has been long conjectured by Kraichnan [67]. This can be easily checked by re-writing the nonlinear transfer term in the governing equation, $(\mathbf{u}\cdot\nabla)\mathbf{u}$ in terms of the *Lamb vector*, $\zeta\times\mathbf{u}$ and noting that in the maximally helical case when velocity and vorticity are perfectly aligned, i.e. $\mathbf{u}\cdot\zeta=1$, we have $\zeta\times\mathbf{u}=0$ and the deductions thereof. Moreover, helicity is also responsible for departure in mirror symmetry in homogeneous isotropic turbulence [79, 99].

The current manuscript does not discuss the role of helicity on turbulent flows although

some passing references to the role of helicity in the context of the simulations performed is made. Interested readers should refer to the paper by Moffatt [87] for a topological perspective of helicity and to the recent papers by Mininni and Pouquet [83, 84] for a phenomenological treatment of the role of helicity in rotating flow dynamics based on direct numerical simulations.

In this chapter, we will discuss the particular case of rotating turbulent flows in the presence of different types of external forces and the resulting energetics and physical features that result from it. We will begin with a brief discussion on rotating turbulence based on important work in the past and then present the case of forced rotating turbulence in the subsequent sections.

2.1 Towards axisymmetric turbulence: historical perspective

2.1.1 The Craya-Herring helical basis

One of the first papers to present a novel theoretical framework for analyzing rotating (axisymmetric) turbulence was one by Herring in 1974 [54]. This paper introduced the *Craya-Herring basis* [32, 54], a suitable basis of the wavefields that populate rotating flows. The Craya-Herring basis vectors are two of the three eigenvectors of the two-point velocity correlation tensor that have non-trivial eigenvalues, denoted by $(\mathbf{e}_{\mathbf{k}}^{(1)}, \mathbf{e}_{\mathbf{k}}^{(2)})$ that lie in a plane perpendicular to the direction of wave propagation. Craya [32] showed that helicity manifests itself as a purely imaginary number proportional to the product of these basis vectors. The construction of the non-trivial eigenvalues imply that if the statistical properties of the velocity field are invariant to an arbitrary rotation of the coordinate axes about the axis of rotation, then so are the statistics of these two eigenvalues. Hence, the physical importance of this basis in the context of axisymmetric flows. It must be said here that the third eigenvector is the wave vector, $\mathbf{k}$ that is in the direction of propagation of the wave and has a zero eigenvalue. The incompressibility condition then conveniently becomes, $\mathbf{k} \cdot u_{\mathbf{k}} = 0$. In his paper [54], Herring uses the direct interaction approximation as a closure strategy to compute the two-point velocity correlation tensor and based on numerical results, shows the progress of axisymmetric turbulence to isotropy at smaller scales (larger wavenumbers).

Lesieur [71] proposed a small modification of this basis formulation by constructing a new set of complex-conjugate pair of eigenvectors, known as the *helical basis vectors*, as a linear combination of the nontrivial Craya-Herring basis vectors in a complex plane as follows: $\mathbf{N_k} = \mathbf{e}_\mathbf{k}^{(2)} - i\mathbf{e}_\mathbf{k}^{(1)}$ and $\mathbf{N}_\mathbf{k}^* = \mathbf{e}_\mathbf{k}^{(2)} + i\mathbf{e}_\mathbf{k}^{(1)} = \mathbf{N}_{-\mathbf{k}}$. In this formulation of the helical basis vectors, $\mathbf{N_k}e^{i\mathbf{k}\cdot\mathbf{x}}$ is the eigenvector of the curl operator. The Craya-Herring helical basis, denoted by $(\mathbf{N_k}, \mathbf{N}_\mathbf{k}^*, \mathbf{k})$, has since attained wide recognition in theoretical representations of axisymmetric turbulence.

2.1.2 Anisotropic effects and closure strategies

Earliest works on theoretical spectral space analysis of rotating turbulence can be referred to Cambon et. al. [21]. The need for wave space analysis arises from the fact that earlier efforts based on the Reynolds stress tensor, $\mathcal{T}$ is not suitable for studying anisotropic effects because $\mathcal{T}$ remains fairly spherical or symmetric in the three principal components as noted in simulations. On the other hand, the spectral approach separates the linear and nonlinear (resulting from the convolution in spectral space) contribution. The latter may be modeled based on a Eddy Damped Quasi-Normal Markovian (EDQNM) approximation or its variants as in [22] that retain the anisotropic structure of the relevant operators. The *quasi normal* approximation enables one to write the fourth order moments as a sum of second order moments and fourth order cumulant. The latter is then taken to be proportional to the third order moment. This forms the basis of a closure strategy. The trace of the second order spectral tensor, representing the energy spectral density, is proportional to the nonlinear transfer term (third order moments approximated by the sum of the second order moments and the cumulant approximation, due to the quasi normal approximation). Cambon et. al. [22] decompose the second order spectral tensor in terms of three scalars, viz., energy, helicity and the polarization anisotropy, the latter is a complex scalar function measuring the extent of anisotropy in the flow. Evolution equations for each of these terms in terms of the respective nonlinear triadic transfer presents the wave space build up of the three corresponding spectra.

Formally, the evolution equation for energy in wave space, is:

$$\left(\partial_t + 2\nu k^2\right) E(k,t) = T(k,t), \tag{2.1}$$

where the transfer term on the right hand side is an integral over all triads of the form $\mathbf{k} = \mathbf{p} + \mathbf{q}$ that satisfy the resonance condition: $\omega_{\mathbf{k}} = \omega_{\mathbf{p}} + \omega_{\mathbf{q}}$. Here, $\omega_k = 2\Omega\frac{k_z}{k}$ is the dispersion relation. It must be noted that, $T(k,t)$ in its original form is proportional to the third order moment of the velocity field in spectral space. Equation (2.1) is written in closed form by the closure strategy mentioned above.

It must be mentioned here that the aforementioned anisotropic closure mechanism is not unique. In fact, the simulations presented in the next section are performed using a Large Eddy Simulation (LES) model that is a variant of the EDQNM closure methodology that assumes isotropy at small scales. The technique is discussed in more detail in the next section.

The angular dependence of the spectra is captured by this formalism as the flow gradually becomes two-dimensional. The particular spectral laws for decaying rotating turbulence can be found in the papers by Cambon [21, 22]. The nonlinear transfer term is non-trivial only when the resonance condition is satisfied by the interacting triads. As far as the direction of the energy transfer is concerned, [21, 14] show that the resultant (secondary) wave number in the triad configuration is shallower (more 2D) than the two primary wave numbers when the resonance condition is satisfied. This is based on the instability assumption, described by Waleffe [126, 127], that entails the direction of energy flow amongst the three wave numbers in the triad configuration. Hence, owing to rotation, the energy is gradually concentrated near the two dimensional manifold (or *slow manifold*) with weak dependence along the rotation axis.

2.2 External forcing, inverse energy cascade and large scale dynamics

An interesting feature of rotating turbulent flows is the transfer of energy to large scales on application of external forcing [112, 114, 28]. In physical space, this manifests as growth in core size of the columnar structures. This is the main focus of this chapter and subsequent sections of

this chapter are based on the recent paper by Sen et. al. [109].

2.2.1 Scaling laws at large scales: recent findings

There has been little consensus about the scaling of the energy spectrum at large scales. The numerical simulation of [114] reports a steep $\sim k_\perp^{-3}$ spectrum whereas [112, 28] show a more conventional $\sim k_\perp^{-5/3}$ scaling that is reminiscent of two-dimensional (2D) Kolmogorov-Kraichnan-Batchelor-Leith (KKBL) phenomenology for an inverse cascade of energy [66] (also see [33]). In [113], a model is used to show that a $\sim k_\perp^{-5/3}$ spectrum for the 2D modes (also called "slow modes") results when triadic interactions between the 2D and the 3D ("fast") modes are discounted for artificially, but a $\sim k_\perp^{-3}$ spectrum is observed when all interactions are accounted for. Besides, a $\sim k_\perp^{-3}$ law for the horizontal kinetic energy spectra is also observed in a rapidly rotating Rayleigh-Bénard convection using a reduced model [61].

In what follows we attempt to clarify some of the aforementioned issues related to the scaling index of the energy spectrum. To this end, an LES model is used that models the smaller scales based on energy and helicity contributions to the eddy viscosity and the eddy noise terms in the EDQNM equations and explicitly solves the governing equations for larger scales. Details are mentioned below. A large parameter study, with different types of external forcing functions, is performed.

2.2.2 Numerical simulations and sub-grid scale modeling of turbulence

The simulations of this section were performed using a highly scalable Fortran 90-95 pseudo-spectral code that integrates the Navier-Stokes equations (1.1) and (1.2) in a rotating frame of reference with periodic boundary conditions. Detail discussions of the parallelized code, called GHOST (acronym for Geophysical High Order Suite for Turbulence), can be found in the papers of Baerenzung et. al. [3, 4] and Mininni et. al. [86]. The model is briefly summarized below.

First, the larger resolved scales are computed by integrating the following equation:

$$\left[\frac{\partial}{\partial t} + k^2\left(\frac{1}{\mathcal{R}e} + \nu_{k|k_c}\right)\right]\mathbf{u}_\alpha(\mathbf{k},t) = T_\alpha^<(\mathbf{k},t) - \frac{1}{\mathcal{R}o}P_{\alpha\beta}\,\varepsilon_{\beta\gamma\zeta}\mathbf{u}_\zeta(\mathbf{k},t) + \mathbf{f}_\alpha(\mathbf{k},t), \tag{2.2}$$

which is the Fourier transform of (Eq. 1.1) (barring the newly introduced subgrid model term, $\nu_{k|k_c}$). The Greek subindices denote cartesian components of the vectors and tensors and Einstein summation convention is assumed. The term $T_\alpha^<(\mathbf{k},t)$ is the Fourier transform of the nonlinear term in Eq. (1.1) over all modes with $k < k_c$. Here, $k_c = N/2$, where N is the domain resolution. This term is computed using the pseudo-spectral method. The eddy viscosity term, $\nu_{k|k_c}$ is related to the subgrid model and is computed based on parameters that are modeled from the unresolved scales. $P_{\alpha\beta}(\mathbf{k}) = \delta_{\alpha\beta} - \frac{k_\alpha k_\beta}{k^2}$ is the classical projection operator on the solenoidal velocity field that lies in a plane perpendicular to the wave vector, $\mathbf{k}$ and $\varepsilon_{\beta\gamma\zeta}$ is the antisymmetric tensor associated with the curl operator (Levi-Civita symbol).

The isotropic energy spectrum $E(k,t)$ and the helicity spectrum $H(k,t)$ up to wavenumber $3k_c$ (including unresolved scales) are then obtained through data fitting and extrapolation from the resolved scales. Next, the isotropic energy spectrum $E(k,t)$ for the unresolved scales is evolved based on the following:

$$(\partial_t + 2\nu k^2)E(k,t) = -2\nu_{k|k_c}k^2E(k,t) - 2\tilde{\nu}_{k|k_c}k^2H(k,t) + T_E^<(k,t) + \frac{\hat{T}_E^{pq}(k,t)}{4\pi k^2}. \tag{2.3}$$

An equivalent balance equation for the unresolved helicity spectrum $H(k,t)$ is solved if the helicity of the flow is non-zero (note: when $H \equiv 0$, we have $\tilde{\nu} \equiv 0$). Here, $\nu_{k|k_c}$ and $\tilde{\nu}_{k|k_c}$ are terms prescribed by the model as before, $T_E^<(k,t)$ represents the energy transferred to unresolved scales from the resolved scales and $\hat{T}_E^{pq}$ represents the energy and helicity interactions at wavenumbers $p, q > k_c$. The analytical forms of the above terms come from a two-point analysis of an integro-differential equations originating from the EDQNM closure for isotropic Navier-Stokes turbulence. Finally, eddy-noise (upscaling of energy towards the resolved scales from the unresolved scales) is added to the velocity field based on a reconstruction of Eq. (2.3).

2.2.3 External forcing functions

The primary goal of this section is to study the effect of external forcing mechanism on the large scale dynamics of the flow, especially the nature of the energy spectrum for all wave numbers, $k < k_f$, where k_f is the forcing wavenumber. Especially, the role of spectral anisotropy of the forcing function is studied in detail. The different categories of forcing functions studied are described below.

(1) **Taylor-Green forcing:** The Taylor-Green (TG) forcing function [118] is as follows:

$$\begin{aligned}\mathbf{f}_{\mathrm{TG}} = f_0 \left[\sin(k_{TG}x)\cos(k_{TG}y)\cos(k_{TG}z)\hat{x}\right. \\ \left. - \cos(k_{TG}x)\sin(k_{TG}y)\cos(k_{TG}z)\hat{y}\right], \end{aligned} \tag{2.4}$$

where f_0 is the forcing amplitude taken to be 5.0. $\mathbf{f}_{\mathrm{TG}}$ has only two components, i.e. in the $x-y$ plane and hence injects zero helicity. In spectral space, it injects energy into a few purely 3D modes. Eq. (2.4) includes products of three trigonometric terms in each component, i.e. a product of three modes in spectral space, the effective forcing wave number is $k_f = \sqrt{3}\min\{k_{TG}\}$ which is taken to be approximately 40 in the simulations. Thus, the 2D mode projection of the forcing wavenumber is $k_{\perp,f} = \sqrt{2}\min\{k_{TG}\} \approx 30$.

(2) **Arnold-Beltrami-Childress forcing:** The Arnold-Beltrami-Childress (ABC) forcing function [1, 29] is as follows:

$$\begin{aligned}\mathbf{f}_{\mathrm{ABC}} = f_0 \left\{\left[B\cos(k_f y) + C\sin(k_f z)\right]\hat{x}\right. \\ + \left[A\sin(k_f x) + C\cos(k_f z)\right]\hat{y} \\ \left. + \left[A\cos(k_f x) + B\sin(k_f y)\right]\hat{z}\right\}, \end{aligned} \tag{2.5}$$

with $A = 0.9$, $B = 1$ and $C = 1.1$. ABC forcing is an eigenfunction of the curl operator and injects maximum helicity (i.e., $\mathbf{f}_{ABC}$ and $\nabla \times \mathbf{f}_{ABC}$ are co-linear). The ABC forcing excites only two 2D modes in the Fourier shell with $k = k_f$ (in the k_x and k_y axis in Fourier space) and one 3D mode (in the k_z axis).

(3) **Isotropic random forcing:** In this case, all modes in spherical Fourier shells between $k_f = 40$ and 41 were fired with the same amplitude but random phases. The procedure described in [100] was used to correlate phases and change the helicity of the forcing from zero to maximal. This results in isotropic forcing independent of the amount of helicity. As a result, more energy is injected into 3D modes compared to 2D modes. This forcing is denoted by $\mathbf{f}_{\mathrm{RND}}$.

(4) **Anisotropic random forcing:** In this case, we introduce a new parameter, β in order to control the extent of anisotropy in the forcing. We define a new forcing function by multiplying each mode in the random forcing (described above) by a factor that concentrates the effective forcing near the 2D manifold,

$$\mathbf{f}_{\mathrm{ANI}}(\mathbf{k}) = \left(1 - \frac{k_z}{k_f}\right)^{\beta} \mathbf{f}_{\mathrm{RND}}(\mathbf{k}). \tag{2.6}$$

The simple case, when $\beta = 0$, corresponds to isotropic forcing.

The simulations were started from a flow at rest and without rotation and integrated up to ten large-scale turnover times ($\tau_f = L_f/U \approx 10$) until a turbulent steady state with a reasonably well developed direct energy cascade was attained. Next, at a time arbitrarily re-labeled $t = 0$, rotation was turned on and the simulation was continued for at least 250 τ_f turnover times.

2.2.4 Definitions: spectra and flux of energy

The definitions in this section are reproduced from the papers, [85, 109]. The isotropic total energy spectrum is computed in the simulations as:

$$E(k) = \frac{1}{2} \sum_{k \le |\mathbf{k}| < k+1} |\mathbf{u}(\mathbf{k})|^2, \tag{2.7}$$

and is such that the total energy is $E = \sum_k E(k)$. We can also define an axisymmetric energy spectrum:

$$e(k_\perp, k_\parallel) = \frac{1}{2} \sum |\mathbf{u}(\mathbf{k})|^2 = e(k, \theta_k), \tag{2.8}$$

where in the latter expression, θ_k is the colatitude in Fourier space with respect to the rotation axis. The sum in Eq. (2.8) is over the following wave numbers: $(k_\perp, k_\parallel)$ s.t. $k_\perp \leq |\mathbf{k} \times \hat{\mathbf{z}}| < k_\perp + 1$; $k_\parallel \leq k_z < k_\parallel + 1$. The axisymmetric energy spectrum is such that the total energy in 2D modes is $E_{2D} = \sum_{k_\perp} e(k_\perp, k_\parallel = 0) = \sum_k e(k, \theta_k = \pi/2)$. As a result, we refer to $e(k_\perp, k_\parallel = 0)$ as the energy spectrum of the 2D modes. The spectrum $e(k_\perp, k_\parallel)$ can be further decomposed into a perpendicular and parallel components as follows:

$$e(k_\perp, k_\parallel) = e_\perp(k_\perp, k_\parallel) + e_\parallel(k_\perp, k_\parallel), \tag{2.9}$$

where the first term corresponds to the energy spectrum of only the horizontal components of the velocity (u and v), and the second to the vertical component (w).

Reduced perpendicular and parallel spectra can then be defined as:

$$E(k_\perp) = \sum_{k_\parallel} e(k_\perp, k_\parallel), \tag{2.10}$$

and

$$E(k_\parallel) = \sum_{k_\perp} e(k_\perp, k_\parallel) \tag{2.11}$$

respectively. As for the energy, $E = \sum_{k_\perp} E(k_\perp) = \sum_{k_\parallel} E(k_\parallel)$. We then introduce the isotropic and perpendicular energy spectra of the 3D modes:

$$E_{3D}(k) = E(k) - e(k, \theta_k = \pi/2), \tag{2.12}$$

and

$$E_{3D}(k_\perp) = E(k_\perp) - e(k_\perp, k_\parallel = 0). \tag{2.13}$$

Finally, we associate energy fluxes with the energy spectra $E(k)$, $E(k_\perp)$, and $E(k_\parallel)$. These are defined from the transfer functions as follows:

$$T(k) = -\sum_{k \leq |\mathbf{k}| < k+1} \mathbf{u}^\star(\mathbf{k}) \cdot \widehat{(\mathbf{u} \cdot \nabla \mathbf{u})}_\mathbf{k}, \tag{2.14}$$

$$T(k_\perp) = -\sum_{k_\perp \leq |\mathbf{k} \times \hat{z}| < k_\perp + 1} \mathbf{u}^\star(\mathbf{k}) \cdot \widehat{(\mathbf{u} \cdot \nabla \mathbf{u})}_\mathbf{k}, \tag{2.15}$$

and

$$T(k_\parallel) = -\sum_{k_\parallel \le k_z < k_\parallel + 1} \mathbf{u}^\star(\mathbf{k}) \cdot (\widehat{\mathbf{u}\cdot\nabla\mathbf{u}})_{\mathbf{k}}, \tag{2.16}$$

where the superscript $\widehat{\ }$ denotes Fourier transformed quantities. Then, the fluxes are as follows:

$$\Pi(k) = -\sum_{k'=0}^{k} T(k') \tag{2.17}$$

$$\Pi(k_\perp) = -\sum_{k'_\perp=0}^{k_\perp} T(k'_\perp), \;\; \Pi(k_\parallel) = -\sum_{k'_\parallel=0}^{k_\parallel} T(k'_\parallel) \tag{2.18}$$

These fluxes represent energy per unit of time across spheres in Fourier space with radius k, cylinders with radius $k_\perp$ and planes with $k_\parallel$ = constant, respectively. In particular, note that $\Pi(k_\parallel = 0)$ represents energy transferred from 2D to 3D modes when positive, and from 3D to 2D modes when negative.

Similarly, we can write definitions for helicity. Although, enstrophy is not an invariant in 3D flows, we will establish some connections between enstrophy and helicity later. 2D and 3D enstrophy are defined in the following ways:

$$Z_{2D} = \frac{1}{2} \sum_{\mathbf{k}\ s.t.\ k_z=0, |\mathbf{k}|\neq 0} |\omega|^2, \tag{2.19}$$

$$Z_{3D} = \frac{1}{2} \sum_{\mathbf{k}\ s.t.\ k_z, |\mathbf{k}|\neq 0} |\omega|^2, \tag{2.20}$$

2.2.5 Simulation results for energy spectra

Table (2.1) describes various simulation runs with the respective parameters and scaling index of the energy spectrum. The perpendicular spectrum $E(k_\perp)$, the spectrum of 3D modes $E_{3D}(k_\perp)$ and the spectrum of the horizontal kinetic energy of the 2D modes, $e_\perp(k_\perp, k_\parallel = 0)$, at late times are all shown in Fig. 2.1 for the TG, ABC, RND1 and RND4 runs. The ABC run shows a spectrum $e_\perp(k_\perp, k_\parallel = 0) \sim k_\perp^{-5/3}$ and $E(k_\perp) \sim k^{-1}$ at large scales. All the other runs have $e_\perp(k_\perp, k_\parallel = 0) \sim k_\perp^{-3}$. The build up of the energy spectrum is clearly shown in Sen et. al. [109] indicating a cascading phenomenon due to *local transfer* of energy across scales towards low wave

Table 2.1: Table of the runs with the total relative helicity of the flow $\rho_H := \frac{H(k)}{kE(k)}$, the anisotropy exponent β, the forcing scale Rossby and Reynolds numbers, Ro_f and Re_f, the energy injection rate ϵ, and the power law index in the inverse cascade range of the horizontal kinetic energy spectrum of the 2D modes. TG, ABC, RND, and ANI respectively stand for Taylor-Green, ABC, random, and random anisotropic forcing. Note that ρ_H is the relative helicity of the flow at the time when the inverse cascade starts, i.e. at t=0 in the run with rotation. All runs use a grid with $N = 256$ points, a forcing wavenumber $k_f = 40$, an imposed rotation $\Omega = 35$, and a kinematic viscosity $\nu = 2 \times 10^{-4}$.

Run	ρ_H	β	$\mathcal{R}o_f$	$\mathcal{R}e_f$	ϵ	index
TG	8×10^{-3}	–	0.045	390	0.030	≈ -3
RND1	9×10^{-3}	–	0.045	390	0.047	≈ -3
RND2	8×10^{-2}	–	0.044	390	0.050	≈ -3
RND3	5×10^{-1}	–	0.046	420	0.047	≈ -3
RND4	7×10^{-1}	–	0.044	420	0.047	≈ -3
ANI1	1×10^{-2}	1	0.045	400	0.010	≈ -3
ANI2	8×10^{-3}	2	0.045	400	0.010	≈ -3
ANI3	8×10^{-3}	3	0.045	420	0.007	$\approx -5/3$
ANI4	7×10^{-1}	3	0.045	420	0.006	$\approx -5/3$
ABC	7×10^{-1}	–	0.050	470	0.090	$\approx -5/3$

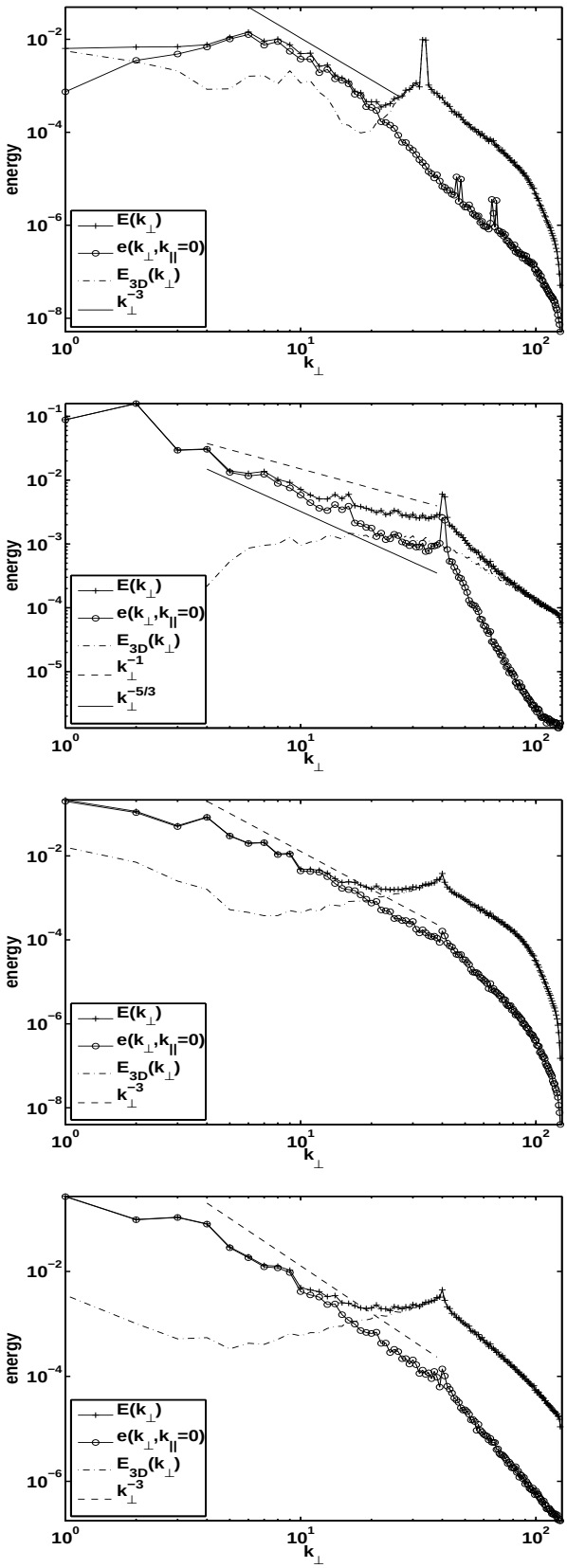

Figure 2.1: $E(k_\perp)$, $E_{3D}(k_\perp)$ and $e_\perp(k_\perp, k_\parallel = 0)$ at late times for TG, ABC, RND1 and RND4 forcing (from top to bottom).

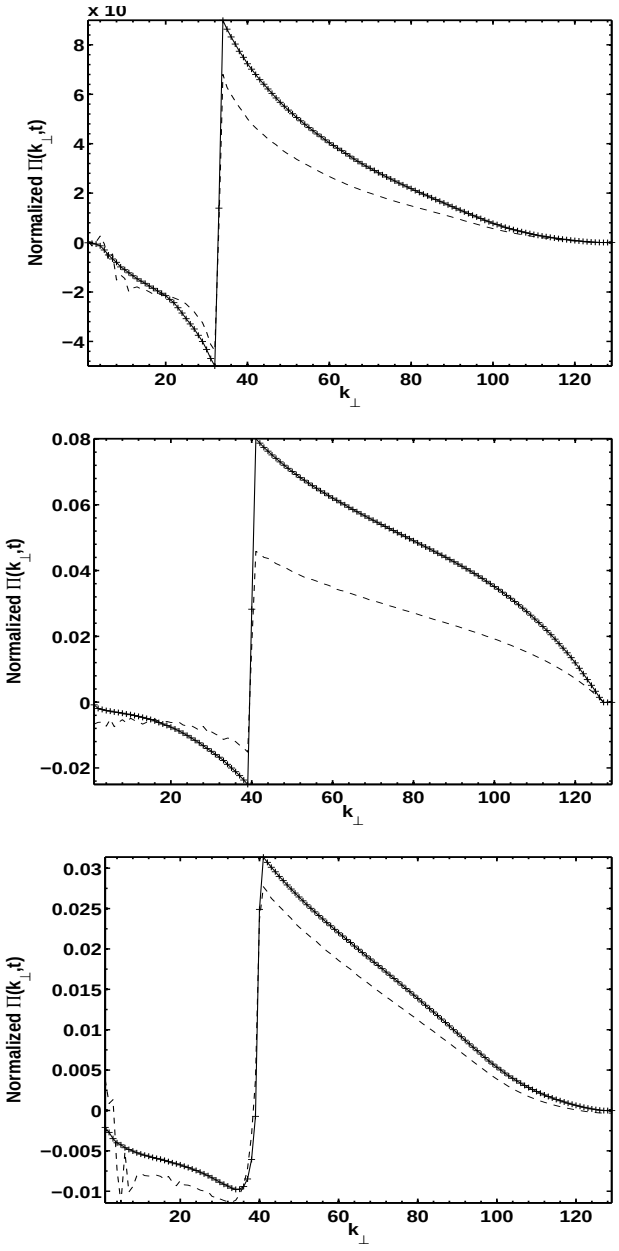

Figure 2.2: Energy flux $\Pi(k_\perp)$ for runs TG, ABC and RND1 (from top to bottom). Solid lines are time averaged while dashed are instantaneous fluxes at late times. The fluxes are normalized to the value at the forcing wavenumber.

numbers. The build up of energy at large scales observed in the spectra is associated with an inverse cascade of 2D energy in the presence of rotation. This can be verified from the energy flux that shows a positive range at wavenumbers larger than k_f (associated with a direct cascade of energy) and a negative range at wavenumbers smaller than k_f (associated with the inverse cascade). Figure (2.2) shows $\Pi(k_\perp)$ for runs TG, ABC, and RND1. The same behavior is observed in the isotropic flux $\Pi(k)$ (not shown). The growth of energy is clearly seen from the temporal plots of total energy as shown in [109]. The temporal evolution of enstrophy is shown in figure (2.3). Notably, Z_{2D} remains reasonably constant once the inverse cascade of energy starts.

2.2.6 Effect of anisotropic injection

Except for one case (ABC forcing), all simulations in figure (2.1) seem to show an inverse cascade of 2D energy with a $k_\perp^{-3}$ scaling. What is the origin of the KKBL-like $\sim k_\perp^{-5/3}$ spectrum in the ABC run? Previous studies obtained KKBL scaling with elongated boxes [28] or when all triadic interactions between 2D and 3D modes were shut down [113] (which in fact corresponds to the case of KKBL phenomenology). However, in our case we used a box with fixed unit aspect ratio and with all triadic interactions and coupling between modes were accounted for in the simulations. One of the distinguishing feature of an ABC forcing is its anisotropic spectral space geometry. Thus it is interesting to study the effect of anisotropic random forcing on the scaling index of the energy spectrum. Figure (2.4) underlines this point further. In the subsequent section, we will present phenomenological arguments to justify the observed scaling law for the energy spectrum.

It must be noted that varying the forcing wavenumber either in absolute terms or broadening the range of wave numbers excited by the external forcing mechanism do not have any discernible effect on the slope of the energy spectrum [109].

2.3 Waves and Eddies: a first glimpse of an interesting interplay

In the previous section, we have seen that if the forcing mechanism excites predominantly the 3D wave modes (e.g, TG, RND1, etc.), the energy spectrum scales differently than the case when

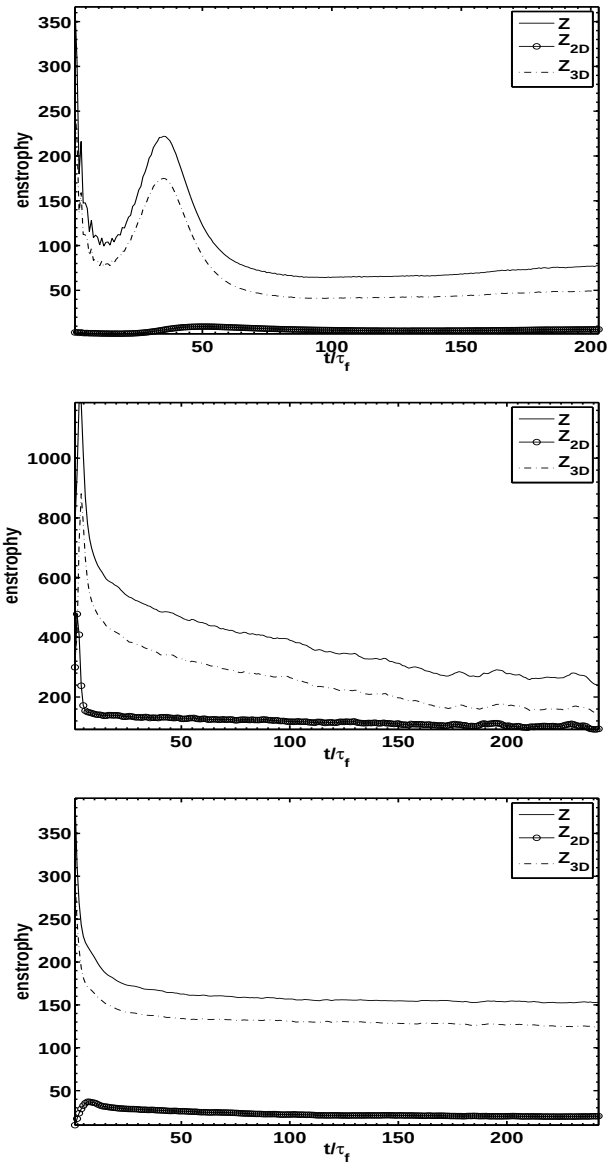

Figure 2.3: Time evolution of the total enstrophy Z, enstrophy in 2D modes Z_{2D}, and enstrophy in 3D modes Z_{3D} in runs TG, ABC and RND1 (from top to bottom).

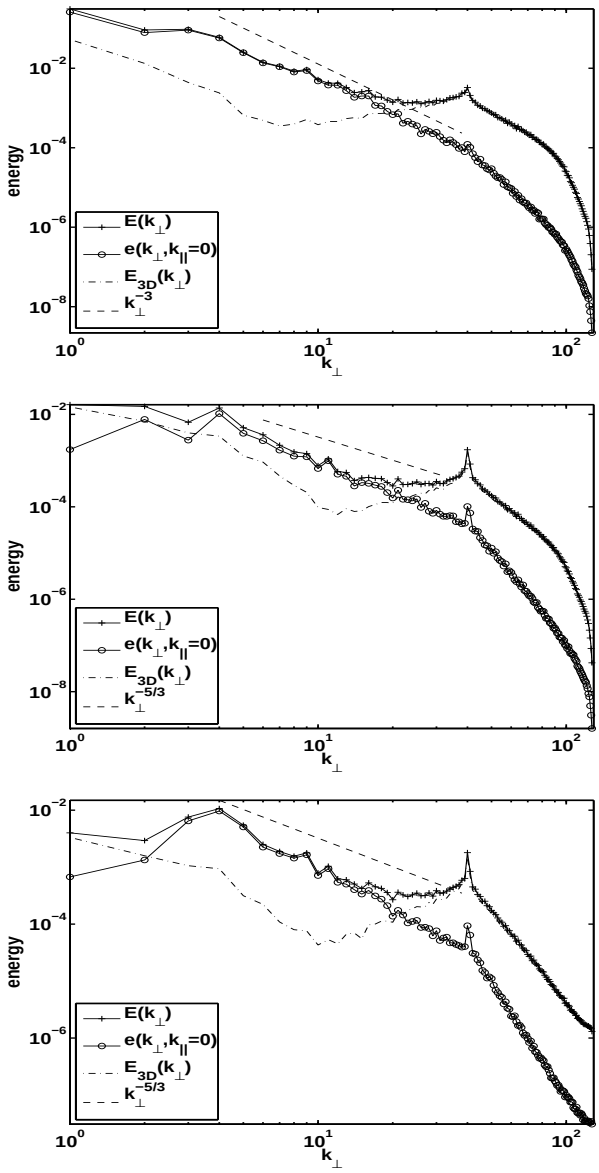

Figure 2.4: Energy spectra at late times for runs ANI1 (top), ANI3 (middle) and ANI4 (bottom).

the external forces excite the vortical modes. This perhaps should suggest an interplay between wave modes and vortical modes that ultimately changes the 2D energetics of the flow. Coupling between Waves and Eddies has been a rather contentious issue in the literature and will be looked at in greater detail in the next chapter. In this section, let us assume for now that Waves and Eddies do couple and the 2D energetics is influenced by the 3D wave dynamics in the flow.

2.3.1 Coupling and fluxes between slow and fast modes

Assuming that the 2D and 3D dynamics is driven not only by their respective external force components but also by one another, we can write the following equations for the evolution of 2D and 3D energy:

$$d_t E_{2D} = -\Pi_{2D\to 3D} - \Pi_{2D} + \epsilon_{2D}, \tag{2.21}$$

$$d_t E_{3D} = \Pi_{2D\to 3D} - \Pi_{3D} + \epsilon_{3D}. \tag{2.22}$$

Thus, in equation (2.21), the temporal change in energy is governed not only by the energy flux (energy exchange) across purely vortical modes and the 2D component of the external force but also by the energy pumped into the vortical modes by the purely 3D wave modes. The same holds true for the evolution of the 3D energy. $\Pi_{2D\to 3D}$ is the flux of energy across $k_{||} = 0$ in Fourier space, i.e., energy going from the 2D to the 3D modes when $\Pi_{2D\to 3D}(t) > 0$. This term is expected to be $\mathcal{O}(\mathcal{R}o)$ [16]. A completely decoupled system (at the leading order) would mean that $\Pi_{2D\to 3D} = 0$. Equations (2.21) and (2.22) are not merely model equation but are exact in the sense that they can be directly deduced form the governing equation (1.1) by integrating over the appropriate vortical and 3D wave numbers as shown in [16].

Note that $\Pi_{2D\to 3D} \equiv \Pi(k_{\|} = 0)$ can be explicitly calculated by using equation (2.18) and is plotted in figure (4.1) for the various runs tabulated in table (2.1). In most runs, the flux is negative for small values of $k_{\|}$ (indicating that energy goes from the 3D modes towards the 2D modes for larger scales), and positive for large values of $k_{\|}$ (indicating that energy goes away from the 2D modes for smaller scales). Note that as more energy is injected into the 2D modes (e.g., as β is

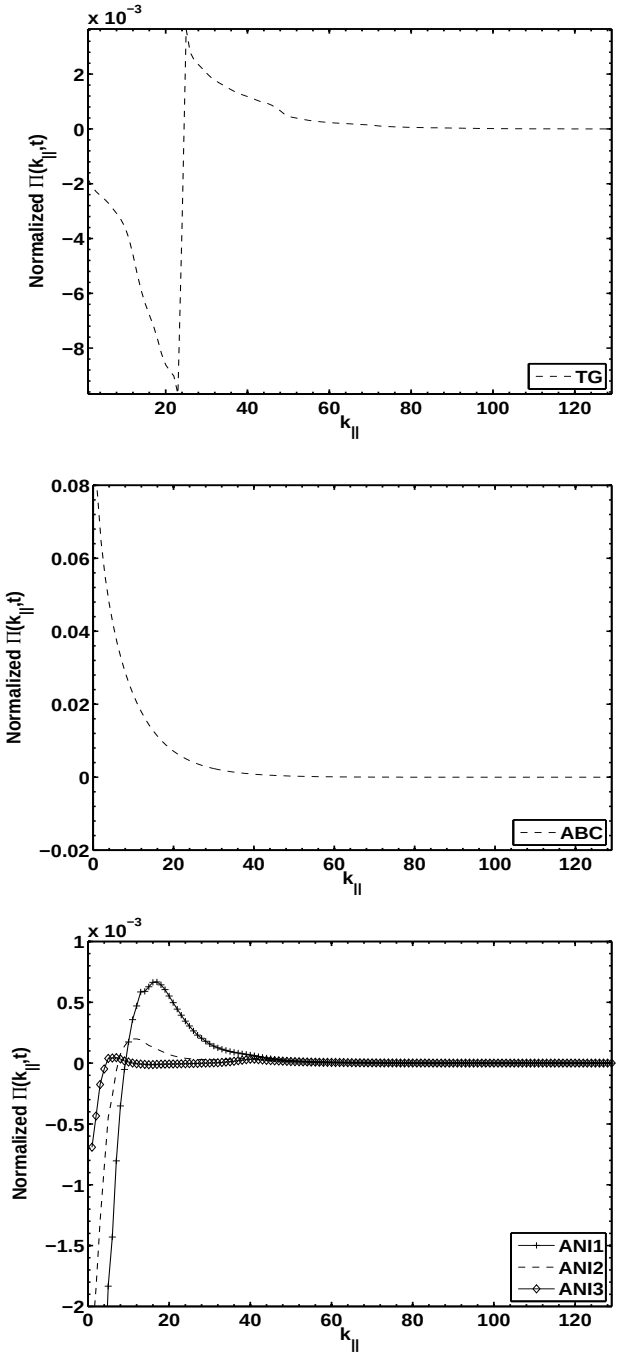

Figure 2.5: $\Pi(k_{\|})$ for runs TG, ABC, ANI1, ANI2 and ANI3 (top to bottom).

Table 2.2: Amplitude of the terms in Eq. (2.22). The time derivative dE_{3D}/dt was obtained using centered finite differences from the data. $\Pi(k_{\|}=0)$ represents energy per unit of time transferred from 2D to 3D modes, and ϵ_{3D} is the power injected in the 3D modes. $\Pi_{3D}^{\text{l.h.s.}}$ is the flux of energy in the 3D modes estimated from Eq. (2.23), $\Pi_{3D}^{\text{est.}}$ is estimated based on geometrical considerations, and $2\nu\int k^2 Z_{3D}(k)\,dk$ is an estimation based on the energy dissipation rate.

Run	dE_{3D}/dt	$\Pi(k_{\|}=0)$	ϵ_{3D}	$\Pi_{3D}^{\text{l.h.s.}}$	$\Pi_{3D}^{\text{est.}}$	$2\nu\int k^2 E_{3D}(k)dk$
TG	1.0×10^{-4}	-2.0×10^{-3}	3.0×10^{-2}	2.8×10^{-2}	1.0×10^{-2}	1.0×10^{-2}
RND1	1.0×10^{-4}	-6.8×10^{-3}	4.6×10^{-2}	3.9×10^{-2}	2.0×10^{-2}	2.0×10^{-2}
RND4	4.0×10^{-5}	-6.3×10^{-3}	4.6×10^{-2}	3.9×10^{-2}	2.0×10^{-2}	3.0×10^{-2}
ANI1	1.0×10^{-4}	-5.2×10^{-3}	8.9×10^{-3}	3.6×10^{-3}	4.0×10^{-2}	4.0×10^{-2}
ANI2	1.0×10^{-4}	-2.3×10^{-3}	9.3×10^{-3}	6.9×10^{-3}	2.0×10^{-2}	1.0×10^{-2}
ANI3	1.0×10^{-4}	-6.9×10^{-4}	6.5×10^{-3}	5.7×10^{-3}	2.0×10^{-3}	5.0×10^{-3}
ANI4	3.0×10^{-5}	-6.0×10^{-4}	5.4×10^{-3}	4.7×10^{-3}	2.0×10^{-3}	4.0×10^{-3}
ABC	-2.0×10^{-4}	8.3×10^{-2}	2.0×10^{-2}	1.0×10^{-1}	3.0×10^{-2}	3.0×10^{-2}

increased in the ANI runs), the wavenumber at which the fluxes change sign moves towards $k_{\|}=0$, and for the ABC flow the flux $\Pi(k_{\|})$ is positive everywhere (i.e., energy goes from the 2D modes to the 3D modes at all scales). The above observations imply that the ABC flow corresponds to the limiting case in which most of the energy is injected into the 2D modes and as a result of the imbalance, an excess of energy "leaks" from the 2D modes to the 3D modes. We will see later that this latter fact results in the build up of shear in the flow. This can be verified by computing each term in the energy balance Eqs. (2.22) and (2.21) (see tables 2.2 and 2.3). The flux of 3D and 2D energy can be estimated from Eqs. (2.22) and (2.21) as follows. Since all terms in these equations, with the exception of Π_{2D} and Π_{3D}, are known, the equations can be re-written as:

$$\Pi_{3D}^{\text{l.h.s}} = \Pi(k_{||}=0,t) + \epsilon_{3D} - d_t E_{3D}, \tag{2.23}$$

and

$$\Pi_{2D}^{\text{l.h.s}} = -\Pi(k_{||}=0,t) + \epsilon_{2D} - d_t E_{2D}. \tag{2.24}$$

The superscript "l.h.s." here and in the table indicates that the fluxes are obtained by solving for the l.h.s. of the balance equations above.

The fact that Π_{2D} is negative in the ABC run (see table 2.3) is evidence of an inverse cascade of energy in the slow manifold once the energy from the 3D modes is transferred to the 2D modes.

Table 2.3: Amplitude of the terms in Eq. (2.21). The time derivative dE_{2D}/dt was obtained using centered finite differences, ϵ_{2D} is the power injected in the 2D modes, and $\Pi_{2D}^{\text{l.h.s.}}$ is the flux of energy in 2D modes estimated from Eq. (2.24).

Run	dE_{2D}/dt	ϵ_{2D}	$\Pi_{2D}^{\text{l.h.s.}}$
TG	4.0×10^{-4}	1.0×10^{-10}	1.6×10^{-3}
RND1	1.0×10^{-3}	1.3×10^{-3}	7.1×10^{-3}
RND4	2.0×10^{-3}	1.5×10^{-3}	5.8×10^{-3}
ANI1	1.0×10^{-3}	1.1×10^{-3}	5.3×10^{-3}
ANI2	4.0×10^{-4}	7.0×10^{-4}	2.6×10^{-3}
ANI3	7.0×10^{-5}	5.0×10^{-4}	1.1×10^{-3}
ANI4	8.0×10^{-5}	6.4×10^{-4}	1.1×10^{-3}
ABC	5.0×10^{-4}	7.0×10^{-2}	-1.3×10^{-2}

For the other runs, even though Π_{2D} is positive and small in magnitude, it merely implies that more energy cascades to the smaller scales than to the larger scales. It is important to note that the positiveness of Π_{2D} hints at positive eddy viscosity and the possibility of the inverse cascade of energy in the slow manifold cannot be ruled out. It may also be worth pointing out that with increasing β (anisotropy), Π_{2D}, for the ANI runs, become less positive and seems to approach the nature of the energy cascade exhibited by the ABC run (see table 2.3).

The picture that emerges for the fluxes from the values in tables 2.2 and 2.3 is illustrated schematically in Fig. 2.6.

2.3.2 Wave-eddy coupling and resulting energetics, scaling laws

The relevant quantity for distinguishing a $\sim k_\perp^{-3}$ power law from a $\sim k_\perp^{-5/3}$ scaling in the inverse cascade energy spectrum is $\Pi(k_\parallel = 0)$. Indeed, if little energy goes into the 2D modes from the 3D modes, or if energy goes from the 2D modes into the 3D modes with the 2D modes being the most energetic and dominating the dynamics, we can assume that the cascade in the slow manifold is dominated by the turnover time $\tau_\perp \sim l_\perp/u_\perp$ (where $l_\perp$ is a characteristic length in the slow manifold and $u_\perp$ the 2D r.m.s. velocity at that length). With only one relevant timescale, KKBL

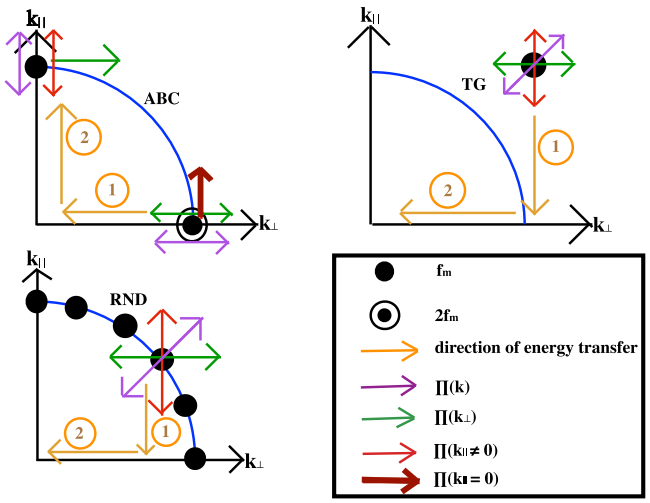

Figure 2.6: A schematic depiction of the direction of transfer of energy (and corresponding fluxes) in the case of forced rotating turbulence. Here f_m is the normalized unit amplitude of forcing in Fourier space. The black dots indicate the modes that are directly excited by the different forcing functions, with $2f_m$ indicating twice the energy injected in that mode compared to the energy injected into other modes.

phenomenology tells us that the energy flux goes as:

$$\Pi_{2D} \sim \frac{u_\perp^2}{\tau_\perp} \sim \frac{u_\perp^3}{l_\perp}, \tag{2.25}$$

which results in a $\sim k_\perp^{-5/3}$ scaling law based on dimensional arguments as shown below. Following Kolmogorov, in the inertial range, we have $E_{\mathbf{k}} \sim \Pi^a k^b$, where a, b are unknowns to be determined. For simplicity, here Π is actually Π_{2D} mentioned above and k is actually $k_\perp$. $[E_{\mathbf{k}}] = [\frac{u^2}{k}]$ where [ ] denotes the dimensionality of the related argument. Matching exponents, we have $a = 2/3$ and since $a + b = -1$, $b = -5/3$.

On the other hand, if energy goes from the 3D modes to the 2D modes, interactions with the 3D modes cannot be neglected. Besides the slow turnover time $\tau_\perp$, we have to consider now the 3D turnover time and the timescale associated with the fast waves, $\tau_\Omega \sim \frac{1}{\Omega}$. There is no unique dimensional solution in this case but we can borrow from the phenomenology developed by Kraichnan [65] for magnetohydrodynamic (MHD) turbulence where the effect of the waves modulates the dominant time-scale of the flow. This phenomenology has been successfully extended to rotating flows [136], including in the helical case [84]. It states that in the presence of waves, the nonlinear transfer is slowed down because of the waves and the relevant parameter of the problem is the Rossby number, i.e. the ratio of time-scales of the wave and the nonlinear turn-over time. Thus, we can assume that the flux will be slowed down by a factor proportional to the ratio τ_Ω/τ where τ is the relevant (and unknown) turnover time for the problem,

$$\Pi_{2D} \sim \frac{u_\perp^2}{\tau}\frac{\tau_\Omega}{\tau}. \tag{2.26}$$

It is interesting to point out that if the turnover time in the above expression is built upon the velocity at the forcing scale U_f as $\tau \sim l_\perp/U_f$ (i.e., assuming interactions are non-local in the inverse cascade range and that most of the energy in the slow manifold comes directly from the 3D forced modes, which is consistent with the large and negative values of $\Pi(k_\parallel = 0)$ in some of the runs), Eq. (2.26) results in a $\sim k_\perp^{-3}$ scaling for the energy spectrum of the 2D modes. Note that such a choice of the time-scale is consistent with the non-local transfers reported in [18], and that non locality of nonlinear transfer in rotating turbulence in the direct cascade was also observed in [82].

2.4 Large scale shear

In the ABC simulation run, since the large scale two dimensional modes leak energy to the 3D modes, the spatial z derivative of field variables become non-zero. This results in development of large scale shear. This point is further supported by plotting the spectrum of the largest eigenvalue of the rate of strain tensor, $\mathfrak{S}$ [109] as shown in figure (2.7).

It is interesting that once large-scale shear is present, a new constant time scale (i.e., independent of length scale) appears. Large scale shear is associated with the *shear time scale*,

$$\tau_{sh} := \frac{1}{\max\{\lambda_{max}\}}, \tag{2.27}$$

where $\lambda_{max}(x, y, z)$ is the largest eigenvalue (in magnitude) of $\mathfrak{S}$ at any given location (x, y, z). Dimensional analysis then hints at a flatter energy spectrum, and a k^{-1} energy spectrum (as observed for the total energy in the ABC run) is not uncommon in shear dominated flows [97].

2.5 Summary

In this chapter, we have seen that spectral space anisotropy of the forcing function plays an important role in the large scale energetics of the flow. We have also seen how Waves can interact with Eddies and regulate the energy transfer across scales in the inertial range thereby determining the scaling indices for the respective energy spectra. In the following chapters we will study the nonlinear wave dynamics of rotating turbulent flows in more details from a theoretical point of view.

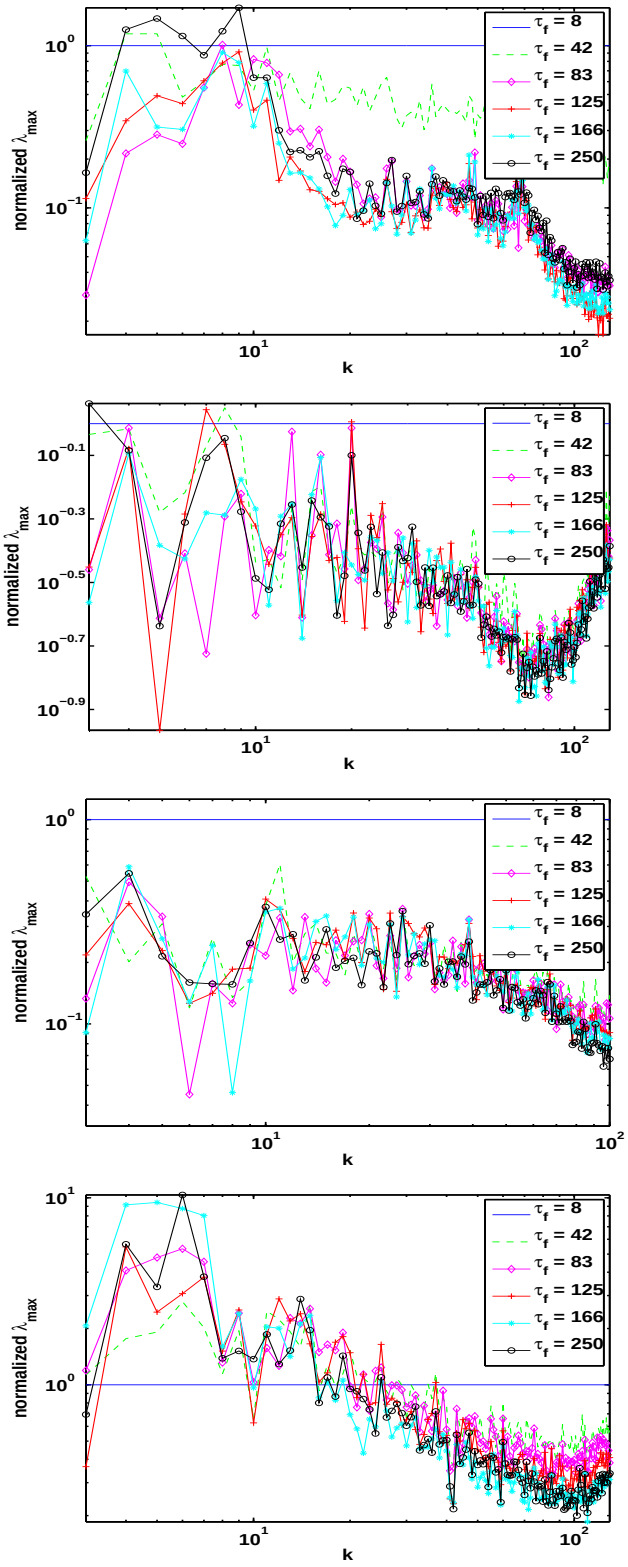

Figure 2.7: (Color online) Spectrum of the maximum eigenvalue of the rate of strain tensor in horizontal planes, for different runs as a function of time. The amplitudes of the spectra are normalized to their initial values (when the rotation is turned on corresponding to $\tau_f = 8$). From top to bottom: TG, RND1, RND4, and ABC.

Chapter 3

Introduction to Wave Turbulence Theory

"Everything has its beauty, but not everyone sees it."

Andy Warhol

In the preceding chapter, we have studied and developed phenomenological understanding of rotating turbulence by analyzing the flow variables produced by numerical simulations. This has given us useful insight into the several interesting dynamics of rotating flows. We now undertake a theoretical approach to study rotating turbulence in the subsequent chapters. In this chapter, we introduce the fundamental concepts of weak-wave turbulence in the Hamiltonian framework.

3.1 Weak wave turbulence theory: a first glimpse

Weak-wave turbulence is a theory of small amplitude weakly interacting nonlinear random waves that are in resonance in a dispersive medium. In this theory, the weak nonlinear interactions happen at an asymptotic order higher than that where linear effects are dominant. Thus, it is most suitable to describe the slow dynamics of the system that is embedded within the domineering linear effects and are thereby visually masked by the leading order dynamics of the flow. For example, in the case of purely rotating turbulent flows, the leading order geostrophic balance manifests as axially oriented columnar eddies as shown in figure 1.1.2. This leading order dynamics masks the underlying non-linear resonant wave interactions that serve as carriers of energy and helicity, the two invariants of the flow. The wave dynamics happens at a higher asymptotic order and thus

remains visually concealed. The importance and relevance of this nonlinear wave dynamics will become clear in the subsequent chapters.

In this thesis, we have presented a Hamiltonian formalism of weak-wave turbulence. The Hamiltonian, for any continuous media representing the equations of motion, embodies the invariants of the motion. As we will soon find out, the Hamiltonian of the system comprises of the wave dispersion relation ($\omega_{\mathbf{k}}$) and the interaction coefficient of the canonical wave amplitude functions, the latter encompassing the information about the nature of interaction between the resonating wave modes. The wave dispersion relation and the interaction coefficient together contain all the information for obtaining power law solutions of the spectral densities of the flow invariants. We will return to this point in chapter 6. Here, we summarize the two distinct approaches of the Hamiltonian formalism of wave turbulence.

3.2 Hamiltonian formalism: a perturbation approach in spectral space

This approach forms the basis of the theoretical presentation of this thesis in the subsequent chapters. The details will be presented in the following chapters, here we outline the essence in an informal manner. We begin with the incompressible reduced rotating hydrodynamic equations [60, 58] that are an asymptotically reduced version of the incompressible Euler equations in the limit of rapid rotation. We perform an asymptotic expansion of the wave field to extract the wave amplitude equation at the appropriate order in the wave space in terms of the canonical complex amplitude functions, $c_{\mathbf{k}}$. In the next chapter, we will show formally the relation between the wave field and $c_{\mathbf{k}}$ for purely rotating flows. Then, we construct the Hamiltonian involving the three wave process by multiplying the wave amplitude equation by the complex conjugate, $c^*_{\mathbf{k}}$. The Hamiltonian, H is generally a power series of the canonical variables, $c_{\mathbf{k}}$:

$$H = H^{(2)} + H^{(3)} + H^{(4)} + \cdots, \tag{3.1}$$

where the superscripts denote the order of the power series.

For any three wave decay process, it can be shown that the Hamiltonian takes the form,

$$H \approx H^{(3)} = \frac{1}{2}\int [V_{kpq} c^*_{\mathbf{k}} c_{\mathbf{p}} c_{\mathbf{q}} + c.c.]\delta_{\mathbf{k},\mathbf{pq}}\delta_{\omega_{\mathbf{k}},\omega_{\mathbf{p}}\omega_{\mathbf{q}}} d\mathbf{p}d\mathbf{q}, \tag{3.2}$$

since $H^{(2)} \equiv 0$ and $H^{(3)}$ is the first non-trivial term in the power series [135]. This is a very strong statement about the third order Hamiltonian, since it is unique for any three wave decay process up to the multiplier, V_{kpq}, known as the interaction coefficient.

For a four-wave process [135],

$$H^{(4)} = \frac{1}{4}\int W_{kpql} c^*_{\mathbf{k}} c^*_{\mathbf{p}} c_{\mathbf{q}} c_{\mathbf{l}} \delta_{\mathbf{k}+\mathbf{p}-\mathbf{q}-\mathbf{l}} d\mathbf{kpql} + \int G_{kpql} c_{\mathbf{k}} c^*_{\mathbf{p}} c^*_{\mathbf{q}} c^*_{\mathbf{l}} \delta_{\mathbf{k}-\mathbf{p}-\mathbf{q}-\mathbf{l}} d\mathbf{kpql} \tag{3.3}$$

$$+ \int R^*_{kpql} c_{\mathbf{k}} c_{\mathbf{p}} c_{\mathbf{q}} c_{\mathbf{l}} \delta_{\mathbf{k}+\mathbf{p}+\mathbf{q}+\mathbf{l}} d\mathbf{kpql}, \tag{3.4}$$

where W, G, R are the interaction coefficients.

The wave amplitude equation can then be written in terms of the Hamiltonian, H as follows:

$$i\partial_t c_{\mathbf{k}} = \frac{\delta H}{\delta c^*_{\mathbf{k}}}. \tag{3.5}$$

This equation is known as the *Jacobi Hamilton* equation in classical mechanics and precedes the derivation of the three-wave kinetic equation describing the evolution of the energy (and helicity) in the wave number space.

3.3 Hamiltonian formalism using Clebsch variables: a classical approach

A more natural way of obtaining the Hamiltonian for the resonant wave process is to construct it in the physical space with appropriate co-ordinates. Here, we will explain this point in terms of the presentation by Lvov and Tabak [75] applicable for stratified fluid turbulence given by the equations,

$$\partial_t \mathbf{u} + \frac{\nabla p}{\rho} = 0, \quad p_z + \rho g = 0, \tag{3.6}$$

$$\partial_t \rho = 0, \quad \nabla \cdot \mathbf{u} + w_z = 0, \tag{3.7}$$

where $\mathbf{u}$ and w are the horizontal and vertical velocities, p is the pressure, ρ is the density and g is the gravity. The reason we have chosen equations (3.6) and (3.7) to explain the formalism

at hand will become clear soon. Broadly speaking, there is a more suitable co-ordinate frame, (x, y, ρ), known as the *isopycnal* coordinate axes, where the Hamiltonian formalism of this section is applicable [75]. Here, the coordinate transformation, $(x, y, z) \rightarrow (x, y, \rho)$ is implicit. In this case, the Hamiltonian can be expressed in the general form as:

$$H = \int f(\mathbf{r}, \rho, \nabla\rho, \nabla^{(2)}\rho, ...)d\mathbf{r}d\rho, \tag{3.8}$$

where f is an appropriate functional describing the system (refer [75] to see the exact functional form of f for the system described by equations (3.6)) and (3.7)). The functional form of f stated above is important to construct the Hamiltonian such that the functional derivative of H: $\frac{\delta H}{\delta \rho} = \frac{\partial f}{\partial \rho} - \nabla \cdot \frac{\partial f}{\partial \nabla \rho}$ yields the requisite *Jacobi Hamilton* equations in the canonical physical variables: $\partial_t \phi = -\frac{\delta H}{\delta \Pi}, \quad \partial_t \Pi = \frac{\delta H}{\delta \phi}$. Here, $\mathbf{u} = \nabla\phi$ and Π is a suitable re-normalization of ρ.

The canonical variables in physical space, (ϕ, Π) are the Clebsch variables for this system and are related to the velocity field, $\mathbf{v} = \Pi\nabla\phi + \nabla\Phi$, where the Φ dependence can be eliminated by using the incompressibility condition. The Hamiltonian in the physical space given by equation (3.8), is now transformed to spectral space via a Fourier transformation and is formally equivalent to that given by equations (3.1), (3.2) and (3.4) in terms of the canonical complex amplitude functions, $c_{\mathbf{k}}$.

3.4 The equivalence of the two Hamiltonian formalism of wave turbulence

It must be noted that the choice of approach for the Hamiltonian wave turbulence theory depends entirely on the problem at hand. Two points are important in this regard.

(1) To obtain the appropriate coordinate axes is a non-trivial exercise (in the above example: the isopycnal coordinates are most suitable). It must be emphasized that the proper choice of the coordinate axes is essential for expressing the functional form of the integrand in the Hamiltonian expression (3.8) in the proper form. In this regard, it may be more convenient to opt for the first approach to construct the Hamiltonian as has been done in the subsequent chapters in this thesis.

(2) The Clebsch variables, (ϕ, Π) are related to the canonical complex amplitude functions, $c_{\mathbf{k}}$ in the following manner:

$$\phi_{\mathbf{k}} = iA(c_{\mathbf{k}} - c^*_{\mathbf{k}}), \quad \Pi_{\mathbf{k}} = B(c_{\mathbf{k}} + c^*_{\mathbf{k}}), \tag{3.9}$$

where A, B are determinate constants (see [75] for details). Equivalently,

$$c_{\mathbf{k}} = \frac{1}{2}(\Pi_{\mathbf{k}} - i\phi_{\mathbf{k}}), \quad c^*_{\mathbf{k}} = \frac{1}{2}(\Pi_{\mathbf{k}} + i\phi_{\mathbf{k}}), \tag{3.10}$$

with $A, B = 1$. Thus, $c_{\mathbf{k}}$ and $c^*_{\mathbf{k}}$ are related to the annihilation and creation (or succinctly, *ladder*) operators of the quantum mechanical description of the harmonic oscillator [50]. This is the basis of the formalism presented in [135] and establishes the equivalence of the two Hamiltonian formalisms of wave turbulence.

Clebsch variables are often used as canonical variables to study incompressible fluids which have inherent symmetries and thereby permit reduction of the given Hamiltonian system to the one of smaller dimension [90]. This formalism is widely used in the study of ideal fluids; e.g., generalization of the equations of motion described by the incompressible Navier-Stokes equations for the Weber-Clebsch potentials have been derived by Cartes et. al. [24] and explain the phenomena of vortex re-connections.

3.5 Summary

In this chapter, we have given an introductory flavor to Hamiltonian wave turbulence theory. We have also shown that one of two approaches mentioned in the sections 2 and 3 of this chapter can be applied to construct the Hamiltonian as they are equivalent. It is however imperative to understand their intimate relationship to obtain a deeper understanding of the ensuing physical and mathematical formulation.

Chapter 4

Rotating Turbulence II: wave amplitude equation for slow inertial waves

"I only give expression to the instincts from my soul."

M. F. Husain

In this chapter, we derive the canonical equations of motion for the wave amplitudes of an incompressible rapidly rotating fluid system. We will begin by introducing the governing equations of the flow within the slow manifold that is populated by geostrophically balanced slow inertial waves. These amplitude equations can be shown to be derived from the equation of motions in Hamiltonian mechanics, the latter being a reformulation of classical mechanics [135]. Here, the presentation will be slightly different as we will construct the amplitude equations from the governing fluid equation in spectral space.

4.1 Slow manifold revisited

4.1.1 Slow inertial waves

We have seen in chapter 2 that inertial Rossby waves in a rotating flow transport energy from the three dimensional modes towards the two dimensional manifold in an efficient manner. The frequency of these waves in spectral space is a function of the axial wavenumber: $\omega_{\mathbf{k}} = \pm\frac{1}{\mathcal{R}o}\frac{k_z}{k}$, where $k = \sqrt{k_\perp^2 + k_z^2}$ is the total wavenumber expressed in terms of the horizontal and the vertical (axial) wavenumbers, $\pm$ implies the circularly polarized nature of the waves. As the resonating waves move energy towards the 2D modes, i.e. towards the slow manifold where k_z becomes

progressively small; the inertial waves become geostrophically balanced where the wave time scale and the advective time scales are of the same order. This region is known as the *slow manifold* due to the *slowness* of the oscillating wave modes as evident from the dispersion relation:

$$\omega_{\mathbf{k}} = \pm \frac{1}{\mathcal{R}o} \frac{k_z}{k}. \tag{4.1}$$

4.1.2 Classical wave turbulence theory in the slow manifold: singular solutions

We recall that the underlying hypothesis of rotating wave turbulence is stated in [40] as:

(1) the separation of inertial and advective time scales, i.e. $\mathcal{R}o \ll 1$, and

(2) the non-interaction between geostrophically balanced and inertial waves dynamics.

Hypothesis (1) above is no longer valid in the slow manifold in the classical weak-wave turbulence treatment of Galtier [45] which does not account for slow geostrophic waves. This results in *singular* solutions for the energy and helicity evolution equations as stated in [45] primarily because the governing equations therein are not valid in the slow manifold. This necessitated that the resonant wave theory be applied to equations that are valid in the slow manifold. In the next section, we introduce a recently developed asymptotically reduced set of equations henceforth referred to here as the R-RHD (*reduced rotating hydrodynamic* equations)[59, 58]. It must be noted that a wave turbulence analysis for reduced equations in the context of MHD has been developed by Nazarenko [92].

4.2 Asymptotically reduced equations: the R-RHD

We will consider inviscid incompressible flow dynamics described by the Euler equation:

$$\partial_t + (\mathbf{u} \cdot \nabla)\mathbf{u} + \frac{1}{\mathcal{R}o}\hat{\mathbf{z}} \times \mathbf{u} = -\frac{1}{\mathcal{R}o}\nabla p, \quad \nabla \cdot \mathbf{u} = 0. \tag{4.2}$$

The analysis presented in this thesis will be on the asymptotically reduced version of equation(4.2). The original detailed derivations of the reduced equation can be found in the paper by Julien and

Knobloch [58]. A summary of the approach is presented in this section to keep the analysis in context. We propose a multiple-scale expansion in the axial direction, $\partial_z = \partial_{\mathrm{z}} + \mathcal{R}o\partial_Z$ with the isotropic scale $\mathrm{z} = z \sim (x, y)$ and the anisotropic columnar length scale $Z = \mathcal{R}oz$. The flow variable, $\mathbf{v} = (\mathbf{u}, p)^T$ is now expressed as an asymptotic series as:

$$\mathbf{v} = \mathbf{v_0} + \mathcal{R}o\mathbf{v_1} + \mathcal{R}o^2\mathbf{v_2} + \mathcal{O}(\mathcal{R}o^3). \tag{4.3}$$

4.2.1 Leading order dynamics

At leading order in $\mathcal{R}o$, equation (4.2) becomes,

$$\widehat{\mathbf{z}} \times \mathbf{u}_0 = -\nabla p_0. \tag{4.4}$$

Equation (4.4) describes geostrophic balance and the ensuing fluid motion is horizontally non-divergent, i.e. $\nabla_\perp \cdot \mathbf{u}_{0\perp} = 0$, with $\mathbf{u}_{0\perp} = \nabla^\perp\psi$ where $p_0 = \psi$ is the geostrophic stream function. The axial invariance of the flow variables, as entailed by the Taylor-Proudman theorem [49], holds because we have, $\partial_{\mathrm{z}}\mathbf{v}_0 \equiv 0$. However, in agreement with the Taylor-Proudman theorem, the variations on Z-scale is permissible as shown in [59, 58]. This formally defines the slow manifold as $k_z \leq \mathcal{O}(\mathcal{R}o)$.

4.2.2 $\mathcal{O}(\mathcal{R}o)$ dynamics: the R-RHD (*reduced rotating hydrodynamic equations*)

At the order $\mathcal{R}o$, the solvability condition ensuring non-secular of $\mathbf{v}_1$ gives us the R-RHD. The R-RHD is stated below,

$$\partial_t\zeta + \mathbf{u}_\perp \cdot \nabla_\perp\zeta = \partial_Z W \tag{4.5}$$

$$\partial_t W + \mathbf{u}_\perp \cdot \nabla_\perp W = -\partial_Z\psi \tag{4.6}$$

Here $\mathbf{u}_\perp = \nabla^\perp\psi$, and $\zeta := \nabla^2_\perp\psi$ and W are the $\widehat{\mathbf{z}}$ components of the vorticity and velocity fields. Equations (4.5) and (4.6) are the governing equations in this chapter and the wave-turbulence treatment presented in the subsequent chapters and will henceforth be referred to as the governing equations unless otherwise specified.

4.3 Features of the R-RHD

In the context of this thesis and for the purposes of the wave-turbulence treatment presented here, we will state two relevant features of the governing equations. The overall detailed features of the equations can be found in [59, 58].

4.3.1 Invariants of the R-RHD

The R-RHD conserves the temporal volume-averaged kinetic energy, $\mathcal{E}_V$ and helicity, $\mathcal{H}_V$:

$$\mathcal{E}_V \equiv \int \mathbf{u}\cdot\mathbf{u}dV = \frac{1}{2}\int \left(|\nabla_\perp\psi|^2 + W^2\right) dV, \tag{4.7}$$

$$\mathcal{H}_V \equiv \int \mathbf{u}\cdot\nabla\times\mathbf{u}dV = 2\int (W\zeta)\, dV. \tag{4.8}$$

4.3.2 Natural helical basis for circularly polarized waves

4.3.2.1 Circularly polarized waves

The resonant wave analysis that will be applied to the R-RHD will be presented in the spectral wavenumber space. This approach is chosen for mathematical convenience in presenting the analysis in its totality in an appropriate helical wave basis. Recall our brief introductory statements about the geostrophically balanced slow inertial waves in section 4.1. Formally, we represent the slow inertial waves with circular polarity as follows:

$$\mathbf{\Psi}_{\mathbf{k}}^{s_k} e^{i\mathbf{\Phi}(\mathbf{k},s_k\omega_{\mathbf{k}})}, \quad \omega_{\mathbf{k}} = \frac{k_Z}{k_\perp}. \tag{4.9}$$

with planar phase function $\mathbf{\Phi}(\mathbf{k}, s_k\omega_{\mathbf{k}}) = (\mathbf{k}_\perp\cdot\mathbf{x}_\perp + k_Z Z - s_k\omega_{\mathbf{k}}t)$. Clearly, $k_Z = 0$ represents vertically invariant modes with $\omega_k = 0$. These 2D modes are generally referred to as *eddies* in this thesis. Here, $\mathbf{\Psi}_{\mathbf{k}}^{s_k}$ is a vector function defined below:

$$\mathbf{\Psi}_{\mathbf{k}}^{s_k} \equiv \begin{pmatrix} \psi_{\mathbf{k}}^{s_k} \\ \\ W_{\mathbf{k}}^{s_k} \end{pmatrix} = \begin{pmatrix} s_k/k_\perp \\ \\ 1 \end{pmatrix} c_{\mathbf{k}}^{s_k} \tag{4.10}$$

where $s_k = \pm$ denotes the handedness, '+' for right-handed circularly polarized waves (with positive helicity) and '$-$' for left-handed circularly polarized waves (with negative helicity). $c_{\mathbf{k}}^{s_k}$ is a complex amplitude function and we will later see they are the canonical variables for the wave-turbulence analysis.

4.3.2.2 Orthogonal basis for helical waves

We first define an orthogonal 'right-handed' basis in the wavenumber basis as follows: $(\widehat{\mathbf{k}}_\perp, \widehat{\mathbf{k}}^\perp, \widehat{\mathbf{z}})$, where $\widehat{\mathbf{k}}_\perp = \mathbf{k}_\perp/k_\perp$ and $\widehat{\mathbf{k}}^\perp = \mathbf{k}^\perp/k_\perp$. The complex helical basis is then defined as:

$$\mathbf{h}_{\mathbf{k}}^{s_k} := i s_k \widehat{\mathbf{k}}^\perp + \widehat{\mathbf{z}}. \tag{4.11}$$

The orthogonality condition is satisfied because,

$$\frac{1}{2}\mathbf{h}_{\mathbf{k}}^{-s_k} \cdot \mathbf{h}_{\mathbf{k}}^{s_k} = 1. \tag{4.12}$$

Moreover, the incompressibility criteria, $\nabla_\perp \cdot \mathbf{u} = 0$, can be stated in terms of this basis as: $\mathbf{k}_\perp \cdot \mathbf{h}_{\mathbf{k}}^{s_k} = 0$. Note that subscripts, representing the order in the asymptotic expansion, have been dropped here and henceforth as it is understood that the analysis of the R-RHD is undertaken at the same order at which they were derived, i.e. $\mathcal{O}(\mathcal{R}o)$.

The velocity field can now be expressed in terms of the helical basis as follows:

$$\begin{aligned} \mathbf{u}_{\mathbf{k}} &= \left(U_{\mathbf{k}}^{s_k}\widehat{\mathbf{k}}^\perp + W_{\mathbf{k}}^{s_k}\widehat{\mathbf{z}}\right) e^{i\mathbf{\Phi}(\mathbf{k},\omega_{\mathbf{k}})} + c.c. \\ &= c_{\mathbf{k}}^{s_k}\mathbf{h}_{\mathbf{k}}^{s_k} e^{i\mathbf{\Phi}(\mathbf{k},\omega_{\mathbf{k}})} + c.c., \end{aligned}$$

where $U_{\mathbf{k}}^{s_k} := i k_\perp \psi_{\mathbf{k}}^{s_k}$.

It can be verified that the helical basis $\mathbf{h}_{\mathbf{k}}^{s_k}$ has a very useful symmetry property.

$$\mathbf{h}_{\mathbf{k}}^{-s_k} = \mathbf{h}_{-\mathbf{k}}^{s_k} = \mathbf{h}_{\mathbf{k}}^{s_k *}. \tag{4.13}$$

This ensures that we can seamlessly transcend polarity (or handedness) through the complex conjugation operation. The most useful point to note is that the R-RHD are naturally set up in the helical wave basis as shown in the figure (4.1).

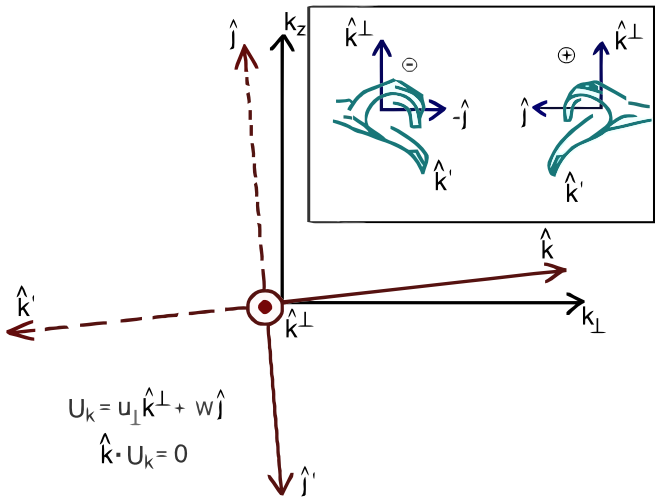

Figure 4.1: Helical wave basis: $(\widehat{\mathbf{k}}, \widehat{\mathbf{k}}'^{\perp}, \widehat{\boldsymbol{\jmath}})$ forms a right-handed coordinate system with $\mathbf{k} \cdot \mathbf{k}'^{\perp} = \mathbf{k} \cdot \widehat{\boldsymbol{\jmath}} = 0$ where $\widehat{\boldsymbol{\jmath}} = \frac{\widehat{\mathbf{k}}'^{\perp} \times \widehat{\mathbf{k}}}{k_{\perp}^2}$. The wave propagation direction is given by the wave vector, $\hat{\mathbf{k}}$. Within the *slow manifold* where $k_z = \mathcal{R}ok_Z$, $(\widehat{\mathbf{k}}, \widehat{\mathbf{k}}'^{\perp}, \widehat{\boldsymbol{\jmath}}) \to (\widehat{\mathbf{k}}_{\perp}, \widehat{\mathbf{k}}^{\perp}, \widehat{\mathbf{z}})$.

4.4 Wave amplitude equation

Inertial wave amplitudes can be of the magnitude of $o(\mathcal{R}o^{-1})$ outside the slow manifold. These waves can also have strong nonlinear interactions. However, for the presentation here, we will assume that the slow inertial waves have progressively (in time) attenuated in power sufficiently such that small amplitude dynamics is dominant in the slow manifold. Hence we introduce another small parameter, ϵ that is a measure of the strength of the wave amplitude. Thus, small amplitude dynamics demands $\epsilon \ll 1$ in the multiple scales expansion in time, $\partial_t = \partial_t + \epsilon\partial_\tau$, where $\tau = \epsilon t$.

4.4.1 Small amplitude weak non-linear interactions

We begin by writing an asymptotic expansion for the wave field,

$$\begin{aligned}\mathbf{\Psi}^\epsilon(\mathbf{x}_\perp, Z, t, \tau) = \epsilon\mathbf{\Psi}_1(\mathbf{x}_\perp, Z, t, \tau)|_{\tau=t/\epsilon} \\ + \epsilon^2\mathbf{\Psi}_2(\mathbf{x}_\perp, Z, t, \tau)|_{\tau=t/\epsilon} + \mathcal{O}(\epsilon^3);\end{aligned} \tag{4.14}$$

It is important to note that τ denotes the advective time scale of the geostrophically balanced slow waves as opposed to the fast inertial wave time scale represented by t. Thus, the resonant wave interactions within the slow manifold happen on a slow time scale, τ.

Recall, that even though the governing equations are nonlinear, the perturbative approach is *linear* in every successive order. Thus, a nonlinear system can be transformed into a hierarchy of linear systems in successive order.

4.4.1.1 Leading order wave dynamics

At leading order, $\mathcal{O}(\epsilon^0)$, we have:

$$\mathcal{L}_\mathcal{H}\mathbf{U}^{s_k}_{1\mathbf{k}} = \mathbf{0}, \qquad \mathcal{L}_\mathcal{H} \equiv \left[-i\omega^{s_k}_\mathbf{k}\mathbf{I}_2 - \frac{k_Z}{k_\perp}\mathbf{J}_2\right]. \tag{4.15}$$

Here $\mathbf{J}_2 = \begin{pmatrix} 0 & 1 \\ -1 & 0 \end{pmatrix}$ is the Hamiltonian matrix and $\mathbf{I}_2$ is the identity matrix. The solution to this system is the helical base vector $\mathbf{U}^{s_k}_{1\mathbf{k}} \equiv \mathbf{h}^{s_k}_\mathbf{k}$. This means that the wave field can now be written as

a superposition of slow inertial helical waves,

$$\mathbf{U}_1 = \sum_{s_k} \int c_{\mathbf{k}}^{s_k}(\tau)\mathbf{h}_{\mathbf{k}}^{s_k} e^{i\mathbf{\Phi}(\mathbf{k},s_k\omega_{\mathbf{k}})} d\mathbf{k}. \tag{4.16}$$

We note that the complex modal amplitude function, $c_{\mathbf{k}}^{s_k}$ is a function of the advective time scale, τ.

4.4.1.2 $\mathcal{O}(\epsilon)$ wave dynamics

At order $\mathcal{O}(\epsilon)$, we have,

$$\mathcal{L}_{\mathcal{H}}\mathbf{U}_{2\mathbf{k}}^{s_k} = -\partial_\tau c_k^{s_k}\mathbf{h}_{\mathbf{k}}^{s_k} - \sum_{s_p,s_q}\int \frac{\mathbf{p}^\perp\cdot\mathbf{q}_\perp}{p_\perp}\begin{pmatrix} \frac{q_\perp}{k_\perp}U_{\mathbf{p}}^{s_p}U_{\mathbf{q}}^{s_q} \\ U_{\mathbf{p}}^{s_p}W_{\mathbf{q}}^{s_q}\end{pmatrix} \times e^{i(\mathbf{\Phi}(\mathbf{p},s_p\omega_{\mathbf{p}})+\mathbf{\Phi}(\mathbf{q},s_q\omega_{\mathbf{q}})-\mathbf{\Phi}(\mathbf{k},s_k\omega_{\mathbf{k}}))} d\mathbf{p}d\mathbf{q}. \tag{4.17}$$

where the subscript 1 has been dropped from the right hand side of the above equations. To ensure non-secular behavior, we impose the solvability condition: $\frac{1}{2}(\mathbf{h}_{\mathbf{k}}^{-s_k}\cdot\mathcal{L}_{\mathcal{H}}\mathbf{U}_{2\mathbf{k}}^{s_k}) = 0$ and thus obtain the wave amplitude equation,

$$i\partial_\tau c_{\mathbf{k}}^{s_k} = \frac{1}{2}\sum_{s_p,s_q}\int V_{kpq}^{s_k s_p s_q} c_{\mathbf{p}}^{s_p} c_{\mathbf{q}}^{s_q}\delta_{\mathbf{k},\mathbf{pq}}\delta_{\omega_{\mathbf{k}},\omega_{\mathbf{p}}\omega_{\mathbf{q}}} d\mathbf{p}d\mathbf{q}d\mathbf{k}, \tag{4.18}$$

where $V_{kpq}^{s_k s_p s_q} := \frac{\mathbf{p}^\perp\cdot\mathbf{q}_\perp}{p_\perp}\left(\frac{q_\perp}{k_\perp}s_k s_p s_q + s_p\right)$ is the interaction coefficient. We note here that the inner product in the solvability condition involves the fast time scale, t. It is also important to note that for $s_k = +$, we have forbidden the possibility of $(s_p, s_q) = (-,-)$ and vice versa in the summation over the polarities. This is because in such cases, resonance cannot be attained.

4.4.2 Large amplitude strong nonlinear interactions

It must be emphasized here that for the perturbation analysis to work out, it is imperative that we have $\epsilon \ll 1$ such that $\epsilon\mathcal{R}o$ is even smaller. However, it is clear that if $\epsilon \gg 1$, then $\epsilon\mathcal{R}o \sim \mathcal{O}(1)$ and the entire asymptotic analysis breaks down. This is also true if $\epsilon \sim \mathcal{O}(1)$. Thus, any wave turbulence treatment falls outside the realm of large amplitude strongly interacting inertial waves, the latter being an open research topic.

4.5 Summary

In this chapter, we began by formally defining the slow manifold and the dynamics within its scope. We also formally introduced the R-RHD which serve as the governing equations for our wave-turbulence analysis in the subsequent chapters. Application of perturbation theory enabled us to derive the wave-amplitude equation that are a suitable version of Hamilton's equation of classical mechanics.

Chapter 5

Rotating Turbulence III: energy and helicity equations

"If I could say it in words there would be no reason to paint."

Edward Hopper

In this chapter, we will derive the equations that describe the energetics of rotating flows within the realm of the governing equations. Moreover, we will also derive the equation that describes the evolution of helicity. The calculations involving helicity are known to be intensive and very mathematically rigorous [46]. We have applied a novel strategy here to accomplish the above mentioned goals. We first begin with the case where the fluid flow is devoid of helicity, i.e. a state where the waves are not polarized rendering it to be free of 'handedness '. For this case, we derive the energy evolution equation describing scale by scale energy transfer by resonating wave modes. We then extend this approach to the more general case of a fully helical flow by using suitable arguments.

5.1 Velocity spectral tensor and symmetries in canonical variables

5.1.1 Definition of velocity spectral tensor

The velocity spectral tensor is defined as the outer product of the complex wave field for every spectral mode as follows:

$$\begin{aligned}\mathcal{U}_{\mathbf{k}} := 2\left(\mathbf{U}_{\mathbf{k}} \otimes \mathbf{U}^*_{\mathbf{k}'}\right)\delta_{\mathbf{k},\mathbf{k}'} &= 2\begin{pmatrix} \sum\limits_{s_k=\pm} c^{s_k}_{\mathbf{k}} c^{s_k *}_{\mathbf{k}'} & \sum\limits_{s_k=\pm} i s_k \frac{k_\perp}{k_\perp} c^{s_k}_{\mathbf{k}} c^{s_k *}_{\mathbf{k}'} \\ \sum\limits_{s_k=\pm} -i s_k \frac{k_\perp}{k_\perp} c^{s_k}_{\mathbf{k}} c^{s_k *}_{\mathbf{k}'} & \sum\limits_{s_k=\pm} c^{s_k}_{\mathbf{k}} c^{s_k}_{\mathbf{k}'} \end{pmatrix}\delta_{\mathbf{k},\mathbf{k}'} \\ &= 2\begin{pmatrix} c^+_{\mathbf{k}} c^{+*}_{\mathbf{k}'} + c^-_{\mathbf{k}} c^{-*}_{\mathbf{k}'} & i\frac{k_\perp}{k_\perp}(c^+_{\mathbf{k}} c^{+*}_{\mathbf{k}'} - c^-_{\mathbf{k}} c^{-*}_{\mathbf{k}'}) \\ -i\frac{k_\perp}{k_\perp}(c^+_{\mathbf{k}} c^{+*}_{\mathbf{k}'} - c^-_{\mathbf{k}} c^{-*}_{\mathbf{k}'}) & c^+_{\mathbf{k}} c^{+*}_{\mathbf{k}'} + c^-_{\mathbf{k}} c^{-*}_{\mathbf{k}'} \end{pmatrix}\delta_{\mathbf{k},\mathbf{k}'} \\ &= 2\begin{pmatrix} e^+_{\mathbf{k}} + e^-_{\mathbf{k}} & i\frac{h^+_{\mathbf{k}} + h^-_{\mathbf{k}}}{k_\perp} \\ -i\frac{h^+_{\mathbf{k}} + h^-_{\mathbf{k}}}{k_\perp} & e^+_{\mathbf{k}} + e^-_{\mathbf{k}} \end{pmatrix} = 2\begin{pmatrix} e_{\mathbf{k}} & i\frac{h_{\mathbf{k}}}{k_\perp} \\ -i\frac{h_{\mathbf{k}}}{k_\perp} & e_{\mathbf{k}} \end{pmatrix}. \end{aligned} \tag{5.1}$$

Note, $\mathcal{U}_{\mathbf{k}}$ is Hermitian. Here, $e_{\mathbf{k}} := \sum_{s_k} c^{s_k}_{\mathbf{k}} c^{s_k *}_{\mathbf{k}} = \sum_{s_k} e^{s_k}_{\mathbf{k}}$ and $h_{\mathbf{k}} := \sum_{s_k} s_k k_\perp e^{s_k}_{\mathbf{k}}$. We can now establish the relationship between the modal energy and helicity in terms of the energy density tensor, $e^{s_k}_{\mathbf{k}}$ as follows:

$$e^+_{\mathbf{k}} + e^-_{\mathbf{k}} = e_{\mathbf{k}}, \tag{5.2}$$

$$e^+_{\mathbf{k}} - e^-_{\mathbf{k}} = \frac{h_{\mathbf{k}}}{k_\perp}. \tag{5.3}$$

Equivalently,

$$\begin{aligned} e^+_{\mathbf{k}} &= \frac{1}{2}\left(e_{\mathbf{k}} + \frac{h_{\mathbf{k}}}{k_\perp}\right), \\ e^-_{\mathbf{k}} &= \frac{1}{2}\left(e_{\mathbf{k}} - \frac{h_{\mathbf{k}}}{k_\perp}\right). \end{aligned} \tag{5.4}$$

5.1.2 Mirror symmetry and parity conservation (Noether's theorem)

Noether's (first) theorem states that any differentiable symmetry of the action of a physical system has a corresponding conservation law [95]. Here, we illustrate this further in the context of

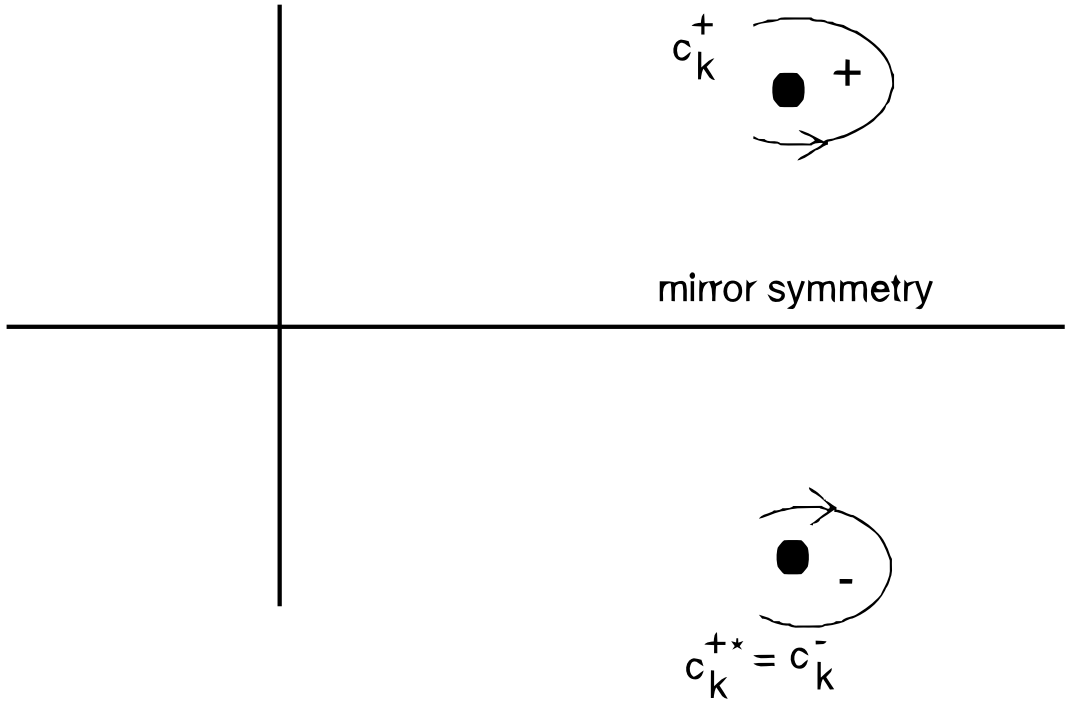

Figure 5.1: Mirror symmetry in non-helical flow is shown in a complex plane. By Noether's theorem, the wave field is invariant under parity transformation.

a rotating flow. Clearly, from equation (5.4) above, we have that for a zero helicity flow ($h_{\mathbf{k}} = 0$), $e^+_{\mathbf{k}} = e^-_{\mathbf{k}} = \frac{1}{2}e_{\mathbf{k}}$. This implies that given a specific flow of unique handedness, energy is not transferred or leaked to a differently handed mode. In fact, the flow retains its unique handedness at all times.

What does this mean in terms of the symmetry in the canonical complex amplitude functions that make up the velocity spectral tensor? By carefully analyzing the structural components of the tensor in equation (5.1), we see that $h_{\mathbf{k}} = 0$ implies that the minor diagonal terms are absent in the tensor representation involving the terms $e_{\mathbf{k}}$ and $h_{\mathbf{k}}$. This in turn demands that the corresponding terms in the representation involving the canonical variables, $c^{s_k}_{\mathbf{k}}$ be also absent. For this to be true, we must have:

$$c^{-s_k}_{\mathbf{k}} = c^{s_k *}_{\mathbf{k}} (\text{for convenience, } c^{+*}_{\mathbf{k}} \equiv c^{*}_{\mathbf{k}}). \tag{5.5}$$

This shows that a non-helical flow is characterized by mirror symmetry (see figure 5.1). This should not be surprising since helicity measures departure from mirror symmetry. The existence of mirror symmetry is equivalent to the conservation of *parity* transformation by *Noether's theorem*. Thus in a non-helical flow, parity (or handedness) is preserved (for more details, see [88]). To make this point formally precise, we first define parity transformation, $\mathbb{P}$ as follows:

$$\mathbb{P}\psi(\mathbf{r}) = \psi(-\mathbf{r}), \tag{5.6}$$

representing a reflection about the real axis on the complex plane followed by an inversion (180 degrees flip). It is easy to check (see figure (5.1)) that for the non-helical case this means that *handedness* of the wave field, ψ is preserved, i.e.

$$\text{for } h_{\mathbf{k}} = 0, \quad \mathbb{P}(\psi^s) = \psi^s, \text{ where } s = \{+, -\}$$

$\mathbb{P}$ acts as the identity operator and hence $d_t\mathbb{P} = 0$ meaning $\mathbb{P}$ is conserved. Also note that using the definition of total derivative, the following is true,

$$d_t\mathbb{P}(\psi^+) = \partial_{\psi^+}\mathbb{P}(\psi^+)d_t\psi^+ + \partial_{\psi^-}\mathbb{P}(\psi^+)d_t\psi^- = d_t\psi^+ = 0, \tag{5.7}$$

because $\partial_{\psi^-}\psi^+ = 0$ and $\mathbb{P}(\psi^+) = \psi^+$. Similarly, we have

$$d_t\mathbb{P}(\psi^-) = d_t\psi^- = 0. \tag{5.8}$$

Following [110], $d_t\psi^s$ can be written in *symplectic* form as,

$$d_t\psi^s = J_{ss'}\partial_{\psi^s}H, \tag{5.9}$$

where $J = \begin{pmatrix} 0 & 1 \\ -1 & 0 \end{pmatrix}$ and the variation of the Hamiltonian, H under the parity transformation, denoted by $\delta_{\mathbb{P}}H$, becomes

$$\delta_{\mathbb{P}}H = \partial_{\psi^+}H\delta_{\mathbb{P}}\psi^+ + \partial_{\psi^-}H\delta_{\mathbb{P}}\psi^- = 0, \tag{5.10}$$

after using equations (5.7), (5.8) and (5.9). Thus, we have shown that reflection symmetry of the wave field in a non-helical flow is equivalent to the invariance of the Hamiltonian under parity transformation (i.e., that variation represents a symmetry of the Hamiltonian).

We will see shortly in the subsequent sections that this mirror (reflection) symmetry of the canonical system will make our calculations of deriving the wave kinetic equation much simpler.

5.2 Non-helical flow dynamics

We impose the mirror symmetry in the wave amplitude equation (4.18) with $s_k = +$ and multiply it by $c^*_{\mathbf{k}}$, upon symmetrization to obtain the Hamiltonian, $H \approx H^{(3)}$ that was introduced in chapter 3.

$$\begin{aligned} &H \approx H^{(3)} \\ &= \frac{1}{2}\left\{\int \frac{1}{2}(V^{+++}_{kpq} + V^{+++}_{kqp})c^*_{\mathbf{k}}c_{\mathbf{p}}c_{\mathbf{q}}\delta_{\mathbf{k},\mathbf{pq}}\delta_{\omega_{\mathbf{k}},\omega_{\mathbf{p}}\omega_{\mathbf{q}}} + (V^{++-}_{kpq} + V^{+-+}_{kqp})c^*_{\mathbf{k}}c_{\mathbf{p}}c^*_{\mathbf{q}}\delta_{\mathbf{k},\mathbf{pq}}\delta_{\omega_{\mathbf{k}},\omega_{\mathbf{p}}\omega_{\mathbf{q}}}d\mathbf{kpq}\right\} + c.c.. \end{aligned} \tag{5.11}$$

The second term, $(V^{++-}_{kpq} + V^{+-+}_{kqp}) = \frac{\mathbf{p}^\perp\cdot\mathbf{q}_\perp}{k_\perp p_\perp q_\perp}(q_\perp - p_\perp)(k_\perp - p_\perp - q_\perp)$, is zero because of the delta function $\delta_{\mathbf{k},\mathbf{pq}}$. Hence, in final form we have,

$$H^{(3)} = \int\left[\tilde{L}_{kpq}c^*_{\mathbf{k}}c_{\mathbf{p}}c_{\mathbf{q}} + c.c.\right]\delta_{\mathbf{k},\mathbf{pq}}\delta_{\omega_k,\omega_p\omega_q}d\mathbf{kpq} \tag{5.12}$$

where the interaction coefficient, $\tilde{L}_{kpq} := \frac{1}{4}(V^{+++}_{kpq} + V^{+++}_{kqp}) = \frac{1}{4}\frac{\mathbf{p}^{\perp}\cdot\mathbf{q}_{\perp}}{k_{\perp}p_{\perp}q_{\perp}}(q_{\perp} - p_{\perp})(p_{\perp} + q_{\perp}) = \frac{1}{4}\frac{\mathbf{p}^{\perp}\cdot\mathbf{q}_{\perp}}{p_{\perp}q_{\perp}}(q_{\perp} - p_{\perp})$ is symmetric in the second and third arguments, i.e. $\tilde{L}_{kpq} = \tilde{L}_{kqp}$. The last equality is again due to the delta function $\delta_{\mathbf{k},\mathbf{pq}}$, notably, the interaction coefficient is independent of $\mathbf{k}$.

The total derivative, $\frac{\delta H^{(3)}}{\delta c^*_{\mathbf{k}}} = \frac{\partial H^{(3)}}{\partial c^*_{\mathbf{k}}} + \frac{\partial H^{(3)}}{\partial c^*_{\mathbf{p}}}\frac{\delta c^*_{\mathbf{p}}}{\delta c^*_{\mathbf{k}}} + \frac{\partial H^{(3)}}{\partial c^*_{\mathbf{q}}}\frac{\delta c^*_{\mathbf{q}}}{\delta c^*_{\mathbf{k}}}$ and the limit, $\delta c^*_{\mathbf{k}} \to 0$ is applied to show that Hamilton's equation $i\partial_{\tau} c_{\mathbf{k}} = \frac{\delta H}{\delta c^*_{\mathbf{k}}}$ is satisfied, where

$$\frac{\delta H}{\delta c^*_{\mathbf{k}}} = \int \left[\tilde{L}_{kpq} c_{\mathbf{p}} c_{\mathbf{q}} \delta_{\mathbf{k},\mathbf{pq}} \delta_{\omega_{\mathbf{k}},\omega_{\mathbf{p}}\omega_{\mathbf{q}}} + 2\tilde{L}^*_{qpk} c^*_{\mathbf{p}} c_{\mathbf{q}} \delta_{\mathbf{q},\mathbf{pk}} \delta_{\omega_{\mathbf{k}},\omega_{\mathbf{p}}\omega_{\mathbf{q}}} \right] d\mathbf{p} d\mathbf{q} d\mathbf{k}.$$

5.2.1 Wave kinetic equation: general form

The steps in this and the subsequent section is broadly based on the presentation in [135]. We first define the third order correlation functions of $c_{\mathbf{k}}$ as follows:

$$J_{kpq}\delta_{\mathbf{k},\mathbf{pq}} :=< c^*_{\mathbf{k}} c_{\mathbf{p}} c_{\mathbf{q}} > .$$

We then take ensemble averages in equation (5.13) and obtain the general wave kinetic equation:

$$\partial_{\tau} e_{\mathbf{k}} = \frac{1}{2}\Im\left\{ \int \tilde{L}_{kpq} J_{kpq} \delta_{\mathbf{k},\mathbf{pq}} \delta_{\omega_{\mathbf{k}},\omega_{\mathbf{p}}\omega_{\mathbf{q}}} - 2\tilde{L}_{pkq} J_{pkq} \delta_{\mathbf{p},\mathbf{kq}} \delta_{\omega_{\mathbf{p}},\omega_{\mathbf{k}}\omega_{\mathbf{q}}} d\mathbf{p} d\mathbf{q} \right\}.$$

Here, $\Im(\cdots)$ refers to imaginary part of the argument within the parenthesis. Equation (5.13) is *not closed* since the left hand side, which is a second order correlation, is expressed in terms of J_{kpq}, which is a third order correlation function.

5.2.2 Wave kinetic equation: closed form

In this section, we will assume Gaussian distribution of the wave field and apply the random phase approximation that will enable us to express fourth order correlation functions as sum of the product of second order correlation function, i.e. $< c^*_{\mathbf{k}} c^*_{\mathbf{p}} c_{\mathbf{q}} c_{\mathbf{m}} >:= 2e_{\mathbf{k}} e_{\mathbf{p}} \delta_{\mathbf{kp},\mathbf{qm}}$. Note, that the left hand side is a fourth order correlation and $e_{\mathbf{k}}$ on the right hand side is a correlation function of second order, $\delta_{\mathbf{kp},\mathbf{qm}}$ represents a summation over the appropriate wave numbers.

We then take a fast time derivative (note: $\partial_t \to \partial_t + \epsilon\partial_\tau$) of the correlation function, J_{kpq}:

$$
\begin{aligned}
i\partial_t\Big(J_{kpq} =& < c^*_{\mathbf{k}} c_{\mathbf{p}} c_{\mathbf{q}} > \delta_{\mathbf{k},\mathbf{pq}}\Big), \\
i\partial_t J_{kpq} &\to \delta_\omega J_{kpq} + i\epsilon\partial_\tau J_{kpq} \\
&\to \delta_\omega J_{kpq} + i\epsilon\partial_\tau < c^*_{\mathbf{k}} c_{\mathbf{p}} c_{\mathbf{q}} > \delta_{\mathbf{k},\mathbf{pq}}.
\end{aligned} \tag{5.13}
$$

Here $\delta_\omega \equiv (\omega_{\mathbf{k}} - \omega_{\mathbf{p}} - \omega_{\mathbf{q}})$ and is unity only when a three- wave resonance is attained. We apply the product rule to evaluate the term $i\epsilon\partial_\tau < c^*_{\mathbf{k}} c_{\mathbf{p}} c_{\mathbf{q}} > \delta_{\mathbf{k},\mathbf{pq}}$. This means we will have terms of the form $\partial_\tau c_{\mathbf{k}}$ which can be expressed in terms of the correlation functions by using equation (4.18) and simplified in terms of the second order correlation functions by applying the random phase approximation stated in the previous paragraph.

Thus, we have derived an ordinary differential equation for J_{kpq} as follows:

$$
\partial_t J_{kpq} = -i\delta_\omega J_{kpq} + \epsilon\tilde{L}_{kpq}(e_{\mathbf{k}}e_{\mathbf{p}} + e_{\mathbf{k}}e_{\mathbf{q}} - e_{\mathbf{p}}e_{\mathbf{q}}). \tag{5.14}
$$

The steady state solution, $\partial_t J_{kpq} = 0$ is,

$$
J_{kpq}(\tau) = \frac{\epsilon}{i\delta_\omega}\tilde{L}_{kpq}(e_{\mathbf{k}}e_{\mathbf{p}} + e_{\mathbf{k}}e_{\mathbf{q}} - e_{\mathbf{p}}e_{\mathbf{q}}), \tag{5.15}
$$

or equivalently,

$$
J_{kpq}(\tau) = \frac{\epsilon}{\delta_\omega}\tilde{L}^*_{kpq}(e_{\mathbf{k}}e_{\mathbf{p}} + e_{\mathbf{k}}e_{\mathbf{q}} - e_{\mathbf{p}}e_{\mathbf{q}}). \tag{5.16}
$$

where i is absorbed in the interaction coefficient, $\tilde{L}_{kpq}$, i.e. $\tilde{L}_{kpq} \to i\tilde{L}_{kpq}$. The singularity owing to δ_ω is averted by using the complex identity $\Im\{\omega + i\tilde{\delta}\} = -\pi\delta(\omega)$ for some $\tilde{\delta} \ll 1$, the details are available in the compendium paper by the author of this thesis and in [135]. We now substitute the steady state solution for J_{kpq} given by equation (5.16) in the general wave kinetic equation (5.13) and obtain the following closed equation for $e_{\mathbf{k}}$,

$$
\partial_\tau e_{\mathbf{k}} = \frac{\pi}{2}\int\Big[|\tilde{L}_{kpq}|^2(e_{\mathbf{p}}e_{\mathbf{q}} - e_{\mathbf{k}}e_{\mathbf{p}} - e_{\mathbf{k}}e_{\mathbf{q}})\delta_{\mathbf{k},\mathbf{pq}}\delta_{\omega_k,\omega_p\omega_q} + 2|\tilde{L}_{pkq}|^2(e_{\mathbf{k}}e_{\mathbf{q}} - e_{\mathbf{p}}e_{\mathbf{k}} - e_{\mathbf{p}}e_{\mathbf{q}})\delta_{\mathbf{p},\mathbf{kq}}\delta_{\omega_p,\omega_k\omega_q}\Big]d\mathbf{p}d\mathbf{q}. \tag{5.17}
$$

Equation (5.17) is known as the three-wave kinetic equation in the closed form that satisfies the applicability criterion for three-wave interaction [135] because $\xi_{\mathbf{k}} = |\tilde{L}_{kkk}|^2\mathcal{E}_V\omega_{\mathbf{k}} \approx 0 \ll 1$ holds true at the appropriate order in the multiple scale analysis.

Recall, that the energetics described by the three-wave kinetic equation (5.17) is for a non-helical fluid flow. In the next section, we will extend the formulation for a fully helical flow. It will become clear how the two invariants of a rotating flow, viz. energy and helicity, are intertwined vìa a set of coupled differential equation.

5.3 Fully helical flow dynamics

We now relax the special case, $h_{\mathbf{k}} = 0$ and allow for $h_{\mathbf{k}} \neq 0$, i.e. non-trivial helicity. Clearly, now $c_{\mathbf{k}}^{+*} = c_{\mathbf{k}}^{*} \neq c_{\mathbf{k}}^{-}$ implying that the mirror symmetry, and hence the parity, in the flow is broken. If we follow the same procedure to derive the three-wave kinetic equation in this case as we did for the non-helical flow, the calculations become very tedious and it becomes extremely difficult to define the correlators. Therefore, in this section, we take a novel approach to extend the results of the previous section to the fully helical case by using symmetry arguments.

5.3.1 General solutions of equations with inherent symmetries

Before we extend our results of the previous section to the more general fully helical flow, we present the steps here for a general (in (x and y) polynomial system. The important thing to note is that if x and y are independent variables, then we can represent the system in a complex plane by introducing a new complex variable, $z = x + iy$. Then, if we have a functional form of the system that is valid in the positive real line, i.e. $x > 0$, we can extend it to the complex right half plane and hence to the general bi-variate form as long as the functional form is *analytic* in the entire domain. Here, we will look at the case where x and y are not independent, and yet we would want to extend the system from the special case where, $y = 0$ to the more general case where, $x + \beta y$ is on the real line, for some real valued β.

We have a new variable z (not complex-valued) defined such that $z = x + \beta y, \forall \beta \in \mathcal{R}$. Let us suppose that we know a formal description of the system in terms of z when $\beta = 0$ as follows:

$$Az^2 + Dz + F = 0, \tag{5.18}$$

or equivalently,

$$Ax^2 + Dx + F = 0, \tag{5.19}$$

where A, D and F are system constants that represent the strength of the variable they are associated with, e.g., D is the strength of the contribution of x and A is the strength of the contribution of x^2 and so on. The goal is to construct the more general system describing z in terms of both x and y. We will assume for sake of convenience that both x and y have identical contributions, a symmetry in x and y.

We then substitute $z^{\pm} = x \pm y$ in equation (5.18) to get:

$$4Axy + 2Dy = 0, \tag{5.20}$$

$$2Ax^2 + 2Ay^2 + 2Dx + 2F = 0. \tag{5.21}$$

Adding equations (5.20) and (5.21) gives us the generalized system (5.23):

$$Ax^2 + 2Axy + Ay^2 + Dx + Dy + F = 0. \tag{5.22}$$

Equation (5.22) can be re-written as:

$$Ax^2 + \Big(A + A\Big)xy + Ay^2 + Dx + Dy + F = 0, \tag{5.23}$$

or

$$Ax^2 + Bxy + Cy^2 + Dx + Ey + F = 0, \tag{5.24}$$

where A, B, C, D, E and F are system constants with $B = 2A$ implying the symmetrical contributions of x and y. Thus we have shown that by simple algebraic manipulations and symmetry arguments, it is possible to extract a more general bi-variate polynomial system from a simpler mono-variate one. We will now show how this strategy is useful in deriving the general three-wave kinetic equation for a fully helical case in closed form.

5.4 Coupled equations of energy and helicity: general form

Recall, $e_{\mathbf{k}}$ in equation (5.17) is actually $e^{+}_{\mathbf{k}} \equiv e^{-}_{\mathbf{k}}$. Thus the closed form coupled energy-helicity equation becomes,

$$\begin{aligned}
&\partial_\tau \left(e_{\mathbf{k}} \pm \frac{h_{\mathbf{k}}}{k_\perp} \right) \\
&= \frac{\pi}{4} \int \Bigg[|\tilde{L}_{kpq}|^2 \Bigg\{ \left(e_{\mathbf{p}} \pm \frac{h_{\mathbf{p}}}{p_\perp} \right) \left(e_{\mathbf{q}} \pm \frac{h_{\mathbf{q}}}{q_\perp} \right) - \left(e_{\mathbf{k}} \pm \frac{h_{\mathbf{k}}}{k_\perp} \right) \left(e_{\mathbf{p}} \pm \frac{h_{\mathbf{p}}}{p_\perp} \right) - \left(e_{\mathbf{k}} \pm \frac{h_{\mathbf{k}}}{k_\perp} \right) \left(e_{\mathbf{q}} \pm \frac{h_{\mathbf{q}}}{q_\perp} \right) \Bigg\} \delta_{\mathbf{k},\mathbf{pq}} \delta_{\omega_k, \omega_p \omega_q} \\
&\quad + 2 |\tilde{L}_{pkq}|^2 \Bigg\{ \left(e_{\mathbf{k}} \pm \frac{h_{\mathbf{k}}}{k_\perp} \right) \left(e_{\mathbf{q}} \pm \frac{h_{\mathbf{q}}}{q_\perp} \right) - \left(e_{\mathbf{p}} \pm \frac{h_{\mathbf{p}}}{p_\perp} \right) \left(e_{\mathbf{k}} \pm \frac{h_{\mathbf{k}}}{k_\perp} \right) - \left(e_{\mathbf{p}} \pm \frac{h_{\mathbf{p}}}{p_\perp} \right) \left(e_{\mathbf{q}} \pm \frac{h_{\mathbf{q}}}{q_\perp} \right) \Bigg\} \delta_{\mathbf{p},\mathbf{kq}} \delta_{\omega_p, \omega_k \omega_q} \Bigg] d\mathbf{p} d\mathbf{q}.
\end{aligned} \tag{5.25}$$

The individual evolution equations for $e_{\mathbf{k}}$ (and $h_{\mathbf{k}}$) are obtained by adding (and subtracting) the two set of equations expressed concisely by equation (5.25) and is given as follows:

$$\begin{aligned}
\partial_\tau e_{\mathbf{k}} = \frac{\pi}{4} \int \Bigg[& |\tilde{L}_{kpq}|^2 \Bigg\{ \left(e_{\mathbf{p}} e_{\mathbf{q}} + \frac{h_{\mathbf{p}} h_{\mathbf{q}}}{p_\perp q_\perp} \right) - \left(e_{\mathbf{k}} e_{\mathbf{p}} + \frac{h_{\mathbf{k}} h_{\mathbf{p}}}{k_\perp p_\perp} \right) - \left(e_{\mathbf{k}} e_{\mathbf{q}} + \frac{h_{\mathbf{k}} h_{\mathbf{q}}}{k_\perp q_\perp} \right) \Bigg\} \delta_{\mathbf{k},\mathbf{pq}} \delta_{\omega_k, \omega_p \omega_q} \\
& + 2 |\tilde{L}_{pkq}|^2 \Bigg\{ \left(e_{\mathbf{k}} e_{\mathbf{q}} + \frac{h_{\mathbf{k}} h_{\mathbf{q}}}{k_\perp q_\perp} \right) - \left(e_{\mathbf{k}} e_{\mathbf{p}} + \frac{h_{\mathbf{k}} h_{\mathbf{p}}}{k_\perp p_\perp} \right) - \left(e_{\mathbf{p}} e_{\mathbf{q}} + \frac{h_{\mathbf{p}} h_{\mathbf{q}}}{p_\perp q_\perp} \right) \Bigg\} \delta_{\mathbf{p},\mathbf{kq}} \delta_{\omega_p, \omega_k \omega_q} \Bigg] d\mathbf{p} d\mathbf{q},
\end{aligned} \tag{5.26}$$

and

$$\begin{aligned}
\partial_\tau h_{\mathbf{k}} = \frac{\pi}{4} \int k_\perp \Bigg[& |\tilde{L}_{kpq}|^2 \Bigg\{ \left(e_{\mathbf{p}} \frac{h_{\mathbf{q}}}{q_\perp} + e_{\mathbf{q}} \frac{h_{\mathbf{q}}}{q_\perp} \right) - \left(e_{\mathbf{k}} \frac{h_{\mathbf{p}}}{p_\perp} + e_{\mathbf{p}} \frac{h_{\mathbf{k}}}{k_\perp} \right) - \left(e_{\mathbf{k}} \frac{h_{\mathbf{q}}}{q_\perp} + e_{\mathbf{q}} \frac{h_{\mathbf{k}}}{k_\perp} \right) \Bigg\} \delta_{\mathbf{k},\mathbf{pq}} \delta_{\omega_k, \omega_p \omega_q} \\
& + 2 |\tilde{L}_{pkq}|^2 \Bigg\{ \left(e_{\mathbf{k}} \frac{h_{\mathbf{q}}}{q_\perp} + e_{\mathbf{q}} \frac{h_{\mathbf{k}}}{k_\perp} \right) - \left(e_{\mathbf{k}} \frac{h_{\mathbf{p}}}{p_\perp} + e_{\mathbf{p}} \frac{h_{\mathbf{k}}}{k_\perp} \right) - \left(e_{\mathbf{p}} \frac{h_{\mathbf{q}}}{q_\perp} + e_{\mathbf{q}} \frac{h_{\mathbf{q}}}{q_\perp} \right) \Bigg\} \delta_{\mathbf{p},\mathbf{kq}} \delta_{\omega_p, \omega_k \omega_q} \Bigg] . \, d\mathbf{p} d\mathbf{q}.
\end{aligned} \tag{5.27}$$

To summarize, we have taken a special case of the wave-kinetic equations which has the functional form $\partial_t e_{\mathbf{k}} = f(\mathbf{k})$ (think of $f(\mathbf{k})$ as the right hand side of equation (5.17)) where $h_{\mathbf{k}} = 0$, and extended it to the more general case where $h_{\mathbf{k}} \neq 0$. In this general case, the domain of $f(\mathbf{k})$ is still the positive real line because the inequality $|h_{\mathbf{k}}| \leq k_\perp e_{\mathbf{k}}$ implies that $h_{\mathbf{k}}$ and $e_{\mathbf{k}}$ are not independent variables and $e_{\mathbf{k}} \pm \frac{h_{\mathbf{k}}}{k_\perp} \geq 0$ is always true. Hence, we have extended the applicability of the wave kinetic equation from the simpler symmetric case (where $c^{*}_{\mathbf{k}} = c^{-}_{\mathbf{k}}$ because $h_{\mathbf{k}} = 0$) to the more general case with non-trivial helicity.

5.5 Summary

In this chapter, we have argued for the importance of symmetries in the canonical description of rotating flows in deriving the three-wave kinetic equations. This has made the calculations tractable and mathematically convenient despite the rigor in the formalism. We have then extended the scope of the wave kinetic equation from the simpler case to a more general fully helical case. The newly derived coupled equations (5.26) and (5.27) from the R-RHD is most suitable for understanding the flow dynamics in the slow manifold.

Chapter 6

Stationary solutions and the wave-turbulence schematic

"Everything you can imagine is real."

Pablo Picasso

In this chapter, we will present the stationary solutions of the three-wave kinetic equation for the energy and helicity spectral densities. We identify the solution corresponding to the constant energy flux Kolmogorov solution. We then review the power law solutions for different flow regimes and place our results in perspective with the anisotropic turbulence schematic proposed by Nazarenko and Schekochihin. Finally, we end the chapter by showing how near-resonant wave interactions are the dominant players in wave-eddy coupling.

6.1 Stationary solutions of the wave kinetic equation

The detailed procedure for obtaining stationary solutions for the energy and helicity spectral densities can be found in [135]. The key step is to find the conditions that make the integrand of the integro-differential equation (5.17) equal to zero. Thus, the four possible stationary solutions for the anisotropic spectrum, $e_{\mathbf{k}} \sim k_Z^{-x_i} k_\perp^{-y_i}, \forall k_z \neq 0$, are listed as follows:

(i) $x_1 = 1$ and $y_1 = -1$.

(ii) $x_2 = 1$ and $y_2 = 0$.

(iii) $x_3 = (1 + u)$ and $y_3 = (2 + v)$, where $2u$ and $2v$ are respectively the powers of k_z and $k_\perp$ in $|\tilde{L}_{kpq}|^2$. Clearly, in our case, $u = 0, v = 1$ (equation (5.12)). Thus, $x_3 = 1$ and $y_3 = 3$.

(iv) $x_4 = 1$ and $y_4 = 7/2$. This solution corresponds to the constant flux in the z-component of the momentum.

Solution (iii), above, corresponds to the constant energy flux solution. Therefore, the exact solution for the Kolmogorov-Zakharov-Kuznetsov spectra with constant flux is as follows:

$$e_{\mathbf{k}} = e(k_\perp, k_Z) \sim k_\perp^{-3} k_Z^{-1}. \tag{6.1}$$

This result is also reported in recent numerical simulations [122, 85, 120].

Therefore, the cylindrically symmetrical solutions for the corresponding spectral quantitates are

$$E_{k_\perp} = (2\pi k_\perp e_k) \sim k_\perp^{-2}, \text{ and } H_{k_\perp} = (2\pi k_\perp h_k) \sim k_\perp^{-1}. \tag{6.2}$$

It is important to note that within this set up of weak turbulence theory, where we have assumed that helicity scales proportional to energy as stated above, obtaining multiple power law solutions for helicity, as shown in numerical simulations by Mininni and Pouquet [84], is beyond the scope of this study. Moreover, the treatment of wave interactions presented thus far is restricted to a strongly anisotropic limit, $\mathcal{R}o \to 0$ and that of mildly fluctuating waves. Where and how does all this fit in the big picture of rotating turbulence as a whole? This is a difficult question that has plagued researchers for sometime. We have tried to bring together certain important ideas proposed in the recent literature and the current theory presented in this thesis in the subsequent section.

6.2 Critical balance: at the confluence of weak and strong turbulence

It is important to re-emphasize the fact that the common theme of the weak-wave turbulence theory is to identify a small (or weak) parameter in the perturbation analysis, the small parameter representing weak-nonlinear interactions between small amplitude wave fields. In a real fluid flow, this *weak interaction* assumption is not always true and moreover wave amplitudes can be very large. Unfortunately, we do not have theory for the later yet. Motivated by the treatment of strong

magnetohydrodynamic (MHD) turbulence [48], Nazarenko and Schekochihin [93] have proposed that the *critical balance* phenomenology be applied as a universal scaling conjecture in all anisotropic turbulence. The conjecture is a balance between the linear wave time scale, τ_ω and nonlinear advective time scale, τ_{NL}; i.e. $\omega \sim \tau_{NL}^{-1}$, where ω is the fast inertial wave frequency related to the time scale τ_ω.

6.2.1 Weak-turbulence vis-à-vis critical balance, polarization alignment and path to recovery of isotropic turbulence

We will list three possible regimes in the context of rotating turbulence [93] in terms of the micro-Rossby number, $\mathcal{R}o_\omega := \frac{1}{\mathcal{R}o_\Omega}\frac{k_z}{k_\perp}$, where $\mathcal{R}o_\Omega$ is defined in chapter 1 in the paragraph following equations (1.1) and (1.2).

(1) $\omega\tau_{NL} \equiv \mathcal{R}o_\omega \gg 1$, such that nonlinear perturbations of the wave field are small since $\delta U \sim \mathcal{R}o_\omega^{-1}\mathbf{U}$ (c.f. U is the horizontal wave field as introduced in chapter 4). This the regime of the weak-wave turbulence presentation of Galtier [[45].

(2) Nazarenko and Schekochihin propose that as the nonlinear interactions become stronger, eventually a critical balance state is reached where $\mathcal{R}o_\omega \approx 1$. Note, that this definition of critical balance is disputed as Galtier et. al. [47] have argued that the constant does not have to be unity but of order unity, the schematic presented in this section and in figure (6.1) does not change on account of this slight disparity in the definition of critical balance. They propose that beyond this limit, the turbulent interactions take a path towards recovery of isotropic scales [85] (for wave numbers larger than the Zeman scale) through an intermediary balance that accounts for polarization of the fluctuating wave field known as *polarization alignment* (for the case of the helical waves, the nonlinear decorrelation time is multiplied by a polarization factor to account for the helical waves; see [93] for details). Here, Zeman scale is defined as the scale at which the eddy turnover time scale and the inertial wave time scale become equal and thereby the connection with critical

balance.

(3) The third regime corresponds to $\mathcal{R}o_\omega \ll 1$ pertains to the analysis presented in this dissertation; i,e, the slow manifold. In fact, as the energy cascades to higher horizontal wave numbers, the flow spans a *hierarchy of slow manifold* regimes with progressively diminishing $\frac{k_z}{k_\perp}$. While Nazarenko and Schekochihin, in their paper, had hinted at this regime and suggested a possible wave-turbulence treatment within the slow manifold using asymptotically reduced equations, it is for the first time to our knowledge that such an attempt has been made in a mathematically rigorous manner as presented in this thesis.

There is at least one experimental study, that of Di Leoni et. al. [37], that gives evidence that in rapidly rotating turbulent flows the energy is concentrated in modes that are far away from modes where critical balance is true, i.e. energy is concentrated in regimes of the flow shown by the blue arrow in figure (6.1). This means that for rapidly rotating flows, the $k_\perp^{-2}$ spectra observed in numerical simulations falls within the realm of the highly anisotropic weak turbulence analysis presented in this thesis and is not due to critical balance as proposed by Nazarenko and Schekochihin [93].

6.2.2 Wave turbulence schematic for rotating turbulent flows

We emphasize that a formal theory of strong turbulence is non-existent as yet, critical balance serves as a phenomenological scaling conjecture to describe strong wave interactions. Hence, proposing a wave turbulence schematic based on scaling conjectures and a theory (that of weak-wave turbulence) leaves a lacuna from a theoretical standpoint. Yet, it helps us to visualize what the physics of a complete wave turbulence theory (including both weak and strong turbulence theory) can entail if and when such a theory is indeed developed. Figure (6.1) depicts this schematic in a concise manner.

We note that in the schematic presented in figure 6.1 as well as in the wave-turbulence theory presented in this thesis and also that by Galtier [45] and Nazarenko et. al. [93], the cascade across

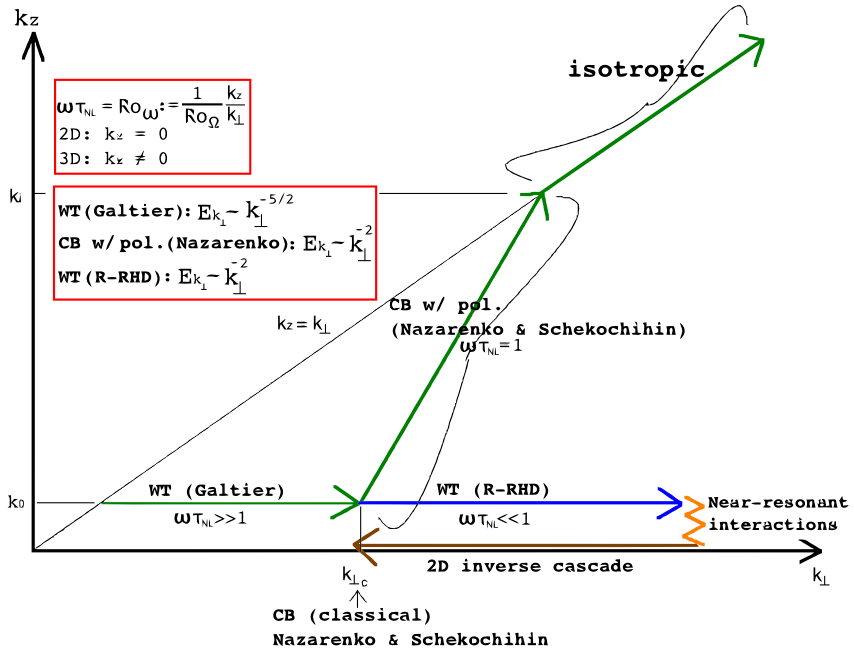

Figure 6.1: A sketch of cascade paths for rotating turbulence shows the different flow regimes depending on $\mathcal{R}o_\omega (\equiv \omega\tau_{NL})$ and the corresponding energy spectra. Here, k_i is the isotropic wavenumber, $k_{\perp c}$ is the classical critical balance wavenumber, k_0 is the injection wavenumber corresponding to an initial wave field. Three distinct regimes are shown: (i) WT (Galtier) corresponding to the wave-turbulence regime with $\mathcal{R}o_\omega \gg 1$, (ii) CB w/ pol. (i.e. critical balance with polarization alignment) as explained in [93] leading towards isotropy, and (iii) WT (R-RHD) corresponding to the R-RHD equations of this paper with $\mathcal{R}o_\omega \ll 1$. As we move along the horizontal axis from left to right, the flow traverses a hierarchy of slow manifolds with successively rescaled (decreasing) $k_Z/k_\perp$ wave number ratio.

the vertical wave numbers is ignored. For the latter, we refer to the work by Bellet et. al. [8].

6.3 Wave-eddy coupling

Within the realm of wave-turbulence theory, energy trapped in the resonating wave modes does not leak to non-resonating modes. However, numerical simulations and experimental evidences have supported transfer of energy to non-resonating modes including the 2D manifold. Here it is important to recognize the subtle distinction between the 2D manifold and the slow manifold, the former refers to $k_z = 0$ and the latter has already been defined in chapter 4 as a regime where slow inertial waves propagate at advective timescales.

So the important question that stays unresolved is if a formal theory can capture this conundrum about 2D-3D coupling to support the passage of energy to the barotropic wave modes. Here we refer to this phenomena as the *wave-eddy coupling*. Does this demand for an extension of the wave-turbulence analysis from a three-wave to a four-wave resonant interaction at the next order of asymptotic series? A four-wave process will make the calculations extremely tedious. Can we present an alternative evidence of the wave-eddy coupling within the framework of the formal approach pursued in this thesis? We make an attempt to address this issue in the following paragraphs of this section. It must be said that other researchers in the past have attempted to resolve this quandary in the recent past, one such example being the work of [114] who have argued, in an informal manner, the importance of near-resonant three-wave interactions.

Let us formally see what happens when $k_Z = 0$ in equation (5.17). Clearly, $\tilde{L}_{kpq}$ becomes *zero* because $p_\perp = q_\perp$ in this case. This can be shown as follows: when $\mathbf{k} = \mathbf{p} + \mathbf{q}$ or equivalently, $k_Z = p_Z + q_Z, k_\perp = p_\perp + q_\perp$, we have $p_Z = -q_Z$. Next, the frequency resonance condition $\omega_\mathbf{k} = \omega_\mathbf{p} + \omega_\mathbf{q}$, or equivalently, $\frac{k_Z}{k_\perp} = \frac{p_Z}{p_\perp} + \frac{q_Z}{q_\perp}$ becomes $\frac{p_Z}{p_\perp} = -\frac{q_Z}{q_\perp}$ and consequently, $p_\perp = q_\perp$ since we have already established $p_Z = -q_Z$. Note that we have intentionally ignored the polarity, s here to keep the expressions clean, it can be easily checked that the facts hold true even when we take the polarity into consideration.

Recall that the frequency delta function in equation (4.18) appeared as a result of applying the solvability condition to ensure bounded growth in the perturbation analysis. This involved a fast time integral (actually a fast time averaging, i.e. $\frac{1}{t}\int(\cdot)dt$) as part of applying the inner-product that changed the exponential term, $e^{i(\mathbf{\Phi}(\mathbf{p},s_p\omega_\mathbf{p})+\mathbf{\Phi}(\mathbf{q},s_q\omega_\mathbf{q})-\mathbf{\Phi}(\mathbf{k},s_k\omega_\mathbf{k}))}$ in equation (4.17) to the delta function, $\delta_{\omega_\mathbf{k},\omega_\mathbf{p}\omega_\mathbf{q}}$ in equation (4.18). Instead, we stop for a while at equation (4.17) and carefully analyze the information encompassed by the exponential term before applying the fast time integral. Let us define a parameter, δ_ω as $s_k\omega_k - s_p\omega_p - s_q\omega_q = \delta_\omega \ll \epsilon, \delta_\omega \neq 0$. Next, considering the *smallness* of $\frac{\delta_\omega}{\epsilon}\tau$, we Taylor expand the exponential term to obtain,

$$e^{i\frac{\delta_\omega}{\epsilon}\tau} \approx 1 + i\frac{\delta_\omega}{\epsilon}\tau + ... \tag{6.3}$$

i.e.,

$$e^{i\frac{\delta_\omega}{\epsilon}\tau} \approx \left(\delta_{\omega_k^{s_k},\omega_p^{s_p}\omega_q^{s_q}}\right)_{\delta_\omega=0} + i\frac{\delta_\omega}{\epsilon}\tau + \dots \,. \tag{6.4}$$

Thus, using equation (6.4) in equation (4.18), we get,

$$i\partial_\tau \tilde{c}_{\mathbf{k}}^{s_k} = \frac{1}{2t}\sum_{s_p,s_q}\int V_{kpq}^{s_k s_p s_q} c_{\mathbf{p}}^{s_p} c_{\mathbf{q}}^{s_q}\Bigg[\underbrace{\left(\delta_{\omega_k^{s_k},\omega_p^{s_p}\omega_q^{s_q}}\right)_{\delta_\omega=0}}_{\text{res}} + \underbrace{i\frac{\delta_\omega}{\epsilon}\tau + \dots}_{\text{non-res}}\Bigg]\delta_{\mathbf{k},\mathbf{pq}}d\mathbf{p}d\mathbf{q}dt.$$

Here $\tilde{c}$ denotes that non-resonant terms have been retained here. Comparing equation (6.5) and equation (4.18), we see that the second term responsible for the wave-eddy coupling (because here, $\delta_\omega \neq 0$ in the second term) is absent in the formal wave-turbulence treatment. Thus, broadly speaking, we have,

$$\partial_\tau e_{\mathbf{k}} = T_{\text{res}}(\mathbf{k},\tau) + T_{\text{non-res}}(\mathbf{k},\tau), \tag{6.5}$$

where $T(\mathbf{k},\tau)$ denotes nonlinear transfer of energy to mode $\mathbf{k}$. However, there is a very crucial implication of retaining the non-resonant terms in the manner prescribed above. In doing so, we lose the ability to extract a stationary *Kolmogorov* solution for the energy and helicity spectral densities. This is because it is the frequency delta function that is associated with the constant flux Kolmogorov solution. For details, we refer the reader to [135]. However, the three other stationary solutions, listed in section 6.1 in the beginning of this chapter, can be retained.

6.4 Summary

In this chapter, we have presented the stationary solutions of the three-wave kinetic equation of the R-RHD. We have identified three special regimes of rotating turbulent flows following [93]. This has enabled us to expand upon the wave turbulence schematic proposed by [93] and collate weak and strong turbulence phenomena within the broader picture of rotating flows. By no means do we claim that this is close to being the final word on the understanding of rotating turbulence. This is merely an attempt at engaging the weak-wave turbulence of R-RHD in the slow manifold with the findings in recent literature. We have also shown a possible way of accounting for wave-eddy coupling within the framework of the work presented in this thesis.

Chapter 7

Conclusion and future research

"The future belongs to those who believe in the beauty of their dreams."

Eleanor Roosevelt

7.1 Scope of the thesis: a concise review

In this thesis, we have studied the dynamics of rotating turbulent flows from a phenomenological point of view through numerical simulations as well as theoretical investigation using resonant wave theory. In doing so, we have ignored several important phenomena like the effect of density stratification, buoyancy forces, role of convection and boundary layer effects, to name a few. Several interesting studies are available in the literature [115, 61, 77] that investigate the role of one or more of these phenomena in the context of understanding turbulent flow dynamics. The combined influence of some of these physical processes become key to understanding geophysical and planetary flows. However, the goal here is to understand the energetics of flows where rotation is the dominant force. This lays the foundation for extending the investigation by including other physical processes.

7.2 Applicability of kinetic wave turbulence theory

The theoretical investigation presented here relies on resonant wave theory. Resonating waves serve as efficient carriers of energy across scales. However, several numerical simulations have given

enough evidence of the role of non-resonant wave interactions in the energy transfer process. A robust theory on strongly interacting wave modes including non-resonant interactions may shed deeper insight into the various dynamical processes involved in turbulent flows.

Moreover, the applicability of kinetic wave turbulence theory relies on two other simplifying assumptions, viz.,

(1) $\frac{L}{\lambda} \to \infty$, where L is the domain size of the fluid system and λ here refers to the characteristic wavelength. This means that boundary effects are not accounted for in this theory, and

(2) the *locality* of wave interactions, i.e. for two waves corresponding to $\omega_{\mathbf{p}}$ and $\omega_{\mathbf{q}}$ interacting to trigger a wave, $\omega_{\mathbf{k}}$, locality would imply that $\omega_{\mathbf{p}} \approx \omega_{\mathbf{q}}$.

The second implication is naturally true within the slow manifold. This is because the frequency resonance condition, when $\omega_{\mathbf{k}} \approx 0$, would imply that $\omega_{\mathbf{p}} \approx \omega_{\mathbf{q}}$, thereby permitting only local interactions within the slow manifold. This is not so obvious in the general case, outside the slow manifold. In the general case, to ensure the convergence of the *collision integral*, a locality of wave interactions is implicitly required. Thus, kinetic wave turbulence does not support non-local wave interactions [135].

To relax the above mentioned constraints, a *discrete* wave turbulence analysis has been undertaken recently [74, 63]. Two key points are worth discussing in this regard.

7.2.1 Boundary effects

Boundary effects are studied by imposing a finite box size, i.e. assuming $1 \ll \frac{L}{\lambda} \ll \infty$. This discretization naturally traps the energy in a few discrete modes (clusters) and forbids leakage of energy between clusters.

7.2.2 Non-local interactions

Since, only a few modes (those within a cluster) participate in the energy exchange process and there is no inter-cluster energy transfer, *non-local wave interactions* are dominant. This may be

most suitable outside the slow manifold in rotating turbulent flows to study the effect of non-local interactions in the energy cascade.

Thus, it is possible that natural processes can be best studied by accommodating a combination of discrete and kinetic wave turbulence investigations; thereby re-enforcing the importance of a *laminated wave turbulence* theory [63].

7.3 Information content in the wave turbulence formalism

A careful observation of the mathematical formalism of this theory presented here entails that all the important information about the wave dynamics and energetics of the flow is contained in the interaction coefficient, $\tilde{L}_{kpq}$ and the wave dispersion relation, $s_k\omega_{\mathbf{k}}$. As a concluding remark, it is useful to review the information contained in $\tilde{L}_{kpq}$. The strategy employed in this thesis to obtain the fully helical representation of the flow dynamics given by equations (5.26) and (5.27) is to superimpose the positive and negative solutions obtained independently. As has been noted before, the Hamiltonian of the system is such that the polarity of the interacting wave modes, $(\mathbf{p}, \mathbf{q}) \to \mathbf{k}$ must be similar, either $(+,+) \to +$ or $(-,-) \to -$. The interaction coefficient $\tilde{L}_{kpq}$ captures this information as only $\tilde{L}^{+++}_{kpq}$ and $\tilde{L}^{---}_{kpq}$ have non-trivial contribution to the Hamiltonian. The other cases, e.g. $(+,-) \to +$ represent a destructive (meaning, out of phase) configuration with a null contribution to the Hamiltonian as has been stated in chapter 5 in the paragraph after equation (5.11).

Should this be surprising? The answer is no because $(s_p, s_q) = (+,-)$ represents a fully helical configuration of the two interacting wave modes, $(\mathbf{p}, \mathbf{q})$, in a given wave triad, $(\mathbf{k}, \mathbf{p}, \mathbf{q})$. As is known, helical states retard nonlinear energy transfer, so it is not surprising that such a configuration would make no contribution to the Hamiltonian that makes up the nonlinear energy transfer term. It is important to note that $|\tilde{L}^{+++}_{kpq}|^2 = |\tilde{L}^{---}_{kpq}|^2 \equiv |\tilde{L}_{kpq}|^2$ and both $\tilde{L}^{+++}_{kpq}$ and $\tilde{L}^{---}_{kpq}$, representing the helical state of the flow, are implicitly present in the wave kinetic equations (5.26) and (5.27). The over-arching point here is that destructive wave interactions (i.e. out of phase wave modes) do not contribute to the resonant three wave dynamics of the flow. This

point can also be re-enforced by recalling that energy is conserved in every wave-triad and no leakage is permissible. This implies that out of phase configurations have zero energy (information) content. Of course, a quasi-resonant or non-resonant interaction would encompass out of phase wave interactions as has been outlined in the section on wave-eddy coupling in chapter 6. Such out of phase configurations will not conserve energy in every wave triad as some energy will always leak to the non (near) resonating wave modes. This is the disadvantage of a non-resonant analysis and will demand investigations at the four-wave resonance interactions thereby increasing the complexity of the theoretical approach. Again, it is important to note that the comments made in this section pertain to the formal theoretical framework of resonating waves only. If one relaxes the *resonance* constraint, like in [10], then such out of phase interactions are permissible.

7.4 Future research directions

Here we will mention only two applications, the first being an applied field where the investigation presented here may be useful and the second a purely theoretical question.

7.4.1 Resonant wave theory to understand planetary dynamics

From a purely application point of view, the analysis can be applied to fluid models developed to understand planetary dynamics. The weak wave turbulence formalism can be applied to the more general Boussinesq equations that serve as canonical models for several geophysical and planetary flows. These equations model the effect of stratification in addition to the effects of rotation. The linear wave dispersion relation of these equations is, $\omega_k = \pm\sqrt{\frac{f^2k_z^2+k_\perp^2N^2}{k_\perp^2+k_z^2}}$, where f and N are the *Coriolis* and *Brunt-Vaisala* frequencies, respectively. It can be shown that in the limit of $\mathcal{R}o^2k^2 \ll 1$ and finite stratification, the dispersion relation reduces to $\omega_k = \sqrt{gh}k$ and embodies non-dispersive waves. This should not be surprising because Boussinesq equations are known to have solitary wave solutions. Coherent structures observed in geophysical and planetary flows can be regarded as manifestations of solitary waves and hence this line of research serves as an interesting starting point to better understand such flows.

7.4.2 Importance of symmetries in developing general theories in fluid turbulence

The importance of exploiting symmetries to reduce the dimensionality of a Hamiltonian (or equivalently Lagrangian) system is one of mechanic's grand themes [20, 90] and is closely related to the invariants of the system by Noether's theorem [95]. E.g., Davidson et. al. [35, 34] show that the conservation of angular momentum that is related to rotational symmetry (axisymmetry) in rotating turbulent flows can be exploited to explain the growth of columnar structures in such flows. In this thesis, we have used reflection symmetry to obtain a special solution corresponding to the non-helical dynamics of the flow and then extended the solution to the more general case. An interesting question is if such simplification or reductions in the system description is always possible. Can this always be used as general theme for solving complex problems? If not, why?

Certainly, there are several instances in other related areas of physics where symmetries in the Hamiltonian formalism have been used to find new conservation laws; e.g. Philbin [98] has shown that conservation of optical *zilch* (measure of chirality of light) can be derived from simple symmetry of the standard electromagnetic action, Yahalom [132] has derived helicity conservation in ideal baratropic fluids by introducing a new symmetry group called the alpha group of translations, Webb et. al. [129] have used the Noether's theorem to derive the canonical Alfv́en wave mixing equations for the wave energy by exploiting linearity symmetry of the equations. These theoretical efforts have shown the importance of using symmetries in the canonical system in unraveling deeper insight about the system through conservation laws as a general strategic principle.

7.5 Summary

In this concluding chapter of the thesis, we have made brief remarks about the loopholes in the kinetic weak wave turbulence theory. We have also noted recent efforts made in the scientific community to address some of these short comings. Finally, we have identified two potential research directions that spawn naturally based on the investigations pursued in this dissertation research.

Bibliography

[1] V. I. Arnold. Sur la topologie des écoulements stationnaires des fluides parfaits. C. R. Hebd. Seances Acad. Sci., 17:261, 1965.

[2] P. Arras, O. Blaes, and N. J. Turner. Quasi-periodic oscillations from magnetorotational turbulence. The AstroPhys. Jour., 645:L65–L68, 2006.

[3] J. Baerenzung, H. Politano, and Y. Ponty. Spectral modeling of turbulent flows and the role of helicity. Phys. Rev. E, 77:046303:1–15, 2008.

[4] J. Baerenzung, H. Politano, Y. Ponty, and A. Pouquet. Spectral modeling of magnetohydrodynamic turbulent flows. Phys. Rev. E, 78:026310:1–11, 2008.

[5] A. M. Balk. On the kolmogorov-zakharov spectra of weak turbulence. Physica D, 139:137–157, 2000.

[6] A. M. Balk and S. V. Nazarenko. Physical realizability of anisotropic weak turbulence kolmogorov spectra. Zh. Eksp. Teor. Fiz, 97:1827–1846, 1990.

[7] G. K. Batchelor. Computation of the energy spectrum in homogeneous two dimensional turbulence. Phys. Fluids, 12 (II):233–239, 1969.

[8] F. Bellet, F. S. Godeferd, J. F. Scott, and C. Cambon. Wave turbulence in rapidly rotating flows. J. Fluid Mech., 562:83–121, 2006.

[9] D. Bernard, G. Boffetta, A. Celani, and G. Falkovich. Conformal invariance in two dimensional turbulence. Nature Physics, 2:124–128, 2006.

[10] L. Biferale, S. Musacchio, and F. Toschi. Split energy-helicity cascades in three-dimensional homogeneous and isotropic turbulence. J. Fluid Mech., 730:309–327, 2013.

[11] B. Bigot and S. Galtier. Two-dimensional state in driven magnetohydrodynamic turbulence. Phys. Rev. E., 83:026405:1–9, 2011.

[12] G. Boffetta and R. E. Ecke. Two-dimensional turbulence. Annu. Rev. Fluid Mech., 44:427–451, 2012.

[13] J. Boisson, C. Lamriben, L. R. M. Maas, P. P. Cortet, and F. Moisy. Inertial waves and modes excited by the libration of a rotating cube. Phys. Fluids, 24:076602, 2012.

[14] G. Bordes, F. Moisy, T. Dauxois, and P. P. Cortet. Experimental evidence of a triadic resonance of plane inertial waves in a rotating fluid. Phys. Fluids, 24:014105:1–15, 2012.

[15] G. Bordes, F. Moisy, T. Dauxois, and P.P. Cortet. Experimental evidence of a triadic resonance of plane inertial waves in a rotating fluid. Phys. Fluids, 24:014105, 2012.

[16] L. Bourouiba. Model of a truncated fast rotating flow at infinite reynolds number. Phys. Fluids, 20:075112:1–14, 2008.

[17] L. Bourouiba and P. Bartello. The intermediate rossby number range and two-dimensional-three-dimensional transfers in rotating decaying homogeneous turbulence. Jour. Fluid Mech., 587:139–161, 2007.

[18] L. Bourouiba, D. N. Straub, and M. L. Waite. Non-local energy transfers in rotating turbulence at intermediate rossby number. Jour. Fluid Mech., 690:129–147, 2011.

[19] J. C. Bowman. Casimir cascades in two-dimensional turbulence. Adv. in Turbulence XII, 132:685–688, 2009.

[20] J. Butterfield. On Symmetries and Conserved Quantities in Classical Mechanics in W. Demopoulos and I. Pitowsky (eds.), Physical Theory and its Interpretation, pp. 43-99. Springer, 2006.

[21] C. Cambon and L. Jacquin. Spectral approach to non-isotropic turbulence subject to rotation. Jour. Fluid Mech., 202:295–317, 1989.

[22] C. Cambon, R. Rubinstein, and F. S. Godeferd. Advances in wave turbulence: rapidly rotating flows. New Jour. Phys., 6:73: 1–29, 2004.

[23] P. Cargill and I. De Moortel. Waves galore. Nature, 475:463–464, 2011.

[24] C. Cartes, M. D. Bustamante, A. Pouquet, and M. E. Brachet. Capturing reconnection phenomena using generalized eulerianlagrangian description in navierstokes and resistive mhd. Fluid Dyn. Res., 41:011404:1–14, 2009.

[25] S. Chandrasekhar. On heisenberg's elementary theory of turbulence. Proc. R. Soc. London A, 200:20–33, 1949.

[26] J. G. Charney. The dynamics of long waves in baroclinic westerly current. J. Meteorol., 4:135–162, 1947.

[27] J. G. Charney. On the scale of atmospheric motions. Geof. Publ., XVII (2):1–15, 1948.

[28] Q. Chen, S. Chen, G. L. Eyink, and D. D. Holm. Resonant interactions in rotating homogeneous three-dimensional turbulence. Jour. Fluid Mech., 542:139–164, 2005.

[29] S. Childress and A. Gilbert. Stretch, Twist, Fold: The Fast Dynamo. Springer-Verlag, Berlin, 1995.

[30] Y. Choi, Y. V. Lvov, and S. Nazarenko. Wave turbulence. Recent Res. Devel. Fluid Dyn., 5, 2004.

[31] R. A. Craig. A solution of the nonlinear vorticity equation for atmospheric motion. J. Meteorol., 2 (3):175–178, 1945.

[32] A. Craya. Contribution à lanalyse de la turbulence associée à des vitesses moyennes. Publications scientifiques et techniques du Ministère de lair, Paris, 345, 1958.

[33] P. A. Davidson. Turbulence: an introduction for scientists and engineers. Oxford University Press, 2004.

[34] P. A. Davidson. The role of angular momentum conservation in homogeneous turbulence. J. Fluid Mech., 632:329–358, 2009.

[35] P. A. Davidson, P. J. Staplehurst, and S. B. Dalziel. On the evolution of eddies in a rapidly rotating system. J. Fluid Mech., 557:135–144, 2006.

[36] S. S. Davis, D. P. Sheeman, and J. N. Cuzzi. On the persistence of small regions of vorticity in the protoplanetary nebula. The AstroPhys. Jour., 545:494–503, 2000.

[37] P. C. Di Leoni, P. J. Cobelli, P D. Mininni, P. Dmitruk, and W. H. Matthaeus. Quantification of the strength of inertial waves in a rotating turbulent flow. arXiv:1310.4214 [physics.flu-dyn], 2013.

[38] B. Dubrulle and L. Valdetarro. Conseuences of rotation in energetics of accretion disks. Astronom. Astrophys., 263:387–400, 1992.

[39] Robert Ecke. The turbulence problem: An experimentalist's perspective. Los Alamos Science, 29, 2005.

[40] P. F. Embid and A. J. Majda. Low froude number limiting dynamics for stably stratified flow with small or finite rossby numbers. Geo. Astrophys. Fluid Dyn., 87:1–30, 1998.

[41] R. Fjørtoft. On the changes in the spectral distribution of the kinetic energy for two-dimensional, non-divergent flow. Tellus, 5:225–230, 1953.

[42] Bengt Fornberg. A numerical study of 2-d turbulence. Jour. Comp. Phys., 25 (1):1–31, 1977.

[43] Uriel Frisch. Turbulence: The Legacy of A. N. Kolmogorov. Cambridge University Press, 1995.

[44] A. A. Galeev, V. I. Karpman, and R. Z. Sagdeev. Multiparticle aspects of turbulent plasma theory. Nuclear Fusion, 5 (120):20, 1965.

[45] S. Galtier. Weak inertial-wave turbulence theory. Phys. Rev. E, 68:015301(R):1–4, 2003.

[46] S. Galtier, S. Nazarenko, A. C. Newell, and A. Pouquet. A weak turbulence theory for incompressible magnetohydrodynamics. J. Plasma Phys., 63 (5):447–488, 2000.

[47] S. Galtier, A. Pouquet, and A. Mangeney. On spectral scaling laws for incompressible anisotropic magnetohydrodynamic turbulence. Phys. Plasma, 12:092310, 2005.

[48] P. Goldreich and S. Sridhar. Toward theory of interstellar turbulence. 2: Strong alfv́enic turbulence. Astrophys. J., 438:763–775, 1995.

[49] H. P. Greenspan. The theory of rotating fluids. Cambridge University Press, 1968.

[50] D. J. Griffiths. Introduction to quantum mechanics. Prentice Hall, 1995.

[51] I. Grooms, K. Julien, J. B. Weiss, and E. Knobloch. Model of convective taylor columns in rotating rayleigh-benard convection. Phys. Rev. Letts., 104:224501:1–4, 2010.

[52] B. Haurwitz. The motion of atmospheric disturbances. J. Marine Res., 3 (1):35–50, 1940.

[53] B. Haurwitz. The motion of atmospheric disturbances on the spherical earth. J. Marine Res., 3 (3):254–267, 1940.

[54] J. R. Herring. Approach of axisymmetric turbulence to isotropy. Phys. Fluids, 17:859–872, 1974.

[55] J. V. Hollweg, S. R. Cranmer, and B. D. G. Chandran. Coronal faraday rotation fluctuations and a wave-turbulence driven model of the solar wind. The AstroPhys. Jour., 722:1495–1503, 2010.

[56] S. S. Hough. On the application of harmonic analysis to the dynamical theory of the tides (part i). Philos. Trans. R. Soc. London A, 189:201–257, 1897.

[57] B. A. Hughes. Nonlinear resonant inertial wave interactions. Phys. Fluids, 16 (11):1805–1809, 1973.

[58] K. Julien and E. Knobloch. Reduced models for fluid flow with strong constraints. Jour. Math. Phys., 48:065405, 2007.

[59] K. Julien, E. Knobloch, R. Milliff, and J. Werne. Generalized quasi-geostrophy for spatially anisotropic rotationally constrained flows. Jour. Fluid Mech., 555:233–274, 2006.

[60] K. Julien, E. Knobloch, and J. Werne. A new class of equations for rotationally constrained flows. Jour. Theo. Comp. Fluid Mech., 11:151–161, 1998.

[61] K. Julien, A. M. Rubio, I. Grooms, and E. Knobloch. Statistical and physical balances in low rossby number rayleigh-bénard convection. Geo. Astro. Fluid Dyn., 106:392–428, 2012.

[62] B. B. Kadomstev. Plasma turbulence, collection: Problems in plasma theory. Atomizdat, 4 (188), 1964.

[63] Elena Kartashova. Nonlinear Resonance Analysis. Cambridge University Press, 2011.

[64] R. Kraichnan and D. Montgomery. Two-dimensional turbulence. Rep. Prog. Phys., 43:547–619, 1980.

[65] R. H. Kraichnan. Inertial-range spectrum of hydromagnetic turbulence. Phys. Fluids, 8:1385:1–3, 2008.

[66] Robert H. Kraichnan. Inertial ranges in two-dimensional turbulence. Phys. Fluids, 10:1417–1423, 1967.

[67] Robert H. Kraichnan. Helical turbulence and absolute equilibrium. Jour. Fluid Mech., 59 (4):745–752, 1973.

[68] K. D. Krouse, A. H. Sobel, and L. M. Polvani. On the wavelength of the rossby waves radiated by tropical cyclones. Jour. Atmos. Sci., 65:644–654, 2007.

[69] E. A. Kuznetsov. Turbulence of ion sound in a plasma located in a magnetic field. Zh. Eksp. Teor. Fiz, 62:584–592, 1972.

[70] M. P. Lelong and E. Kunze. Can barotropic tide-eddy interactions excite internal waves? J. FLuid Mech., 721:1–27, 2013.

[71] M. Lesieur. Décomposition d'un champ de vitesse non divergent en ondes d'hélicité. Revue Turbulence, Observatoire de Nice, 1972.

[72] Q. Li, H. Graf, and C. Xuefeng. The role of stationary and transient planetary waves in the maintenance of stratospheric polar vortex regimes in northern hemisphere winter. Adv. Atmos. Sci., 28 (1):187–194, 2011.

[73] R. V. E. Lovelace, H. Li, S. A. Colgate, and A. F. Nelson. Rossby wave instability of keplerian accretion disks. The AstroPhys. Jour., 513:805–810, 1999.

[74] V. S. Lvov and S. Nazarenko. Discrete and mesoscopic regimes of finite-size wave turbulence. Phys. Rev. E, 82:056322:1–11, 2010.

[75] Y. V. Lvov and E. G. Tabak. Hamiltonian formalism and the garrett-munk spectrum of internal waves in the ocean. Phys. Rev. Lett., 87 (16):168501–1–4, 2001.

[76] Dana Mackenzie. The Universe in Zero Words. Princeton University Press, 2012.

[77] R. Marino, P. D. Mininni, D. Rosenberg, and A. Pouquet. Emergence of helicity in rotating stratified turbulence. Phys. Rev. E., 87:033016:1–9, 2013.

[78] E. Marsch. Waves and turbulence in the solar corona, The Sun and the Heliosphere as an Integrated System. Astro. Space Sci. Lib. (317), 2004.

[79] H. P. Mazumdar, Gr. Tsagas, and S. C. Ghosh. On the breaking of mirror symmetry in homogeneous isotropic turbulence-helicity effect. Balkan Journal of Geometry and Its Applications, 5:119–128, 2000.

[80] S. W. McIntosh, B. De Pontieu, M. Carlsson, V. Hansteen, P. Boerner, and M. Goossens. Alfvénic waves with sufficient energy to power the quiet solar corona and fast solar wind. Nature Letts., 475:477–480, 2011.

[81] J. C. McWilliams. Fundamentals of Geophysical Fluid Dynamics. Cambridge University Press, 2006.

[82] P. D. Mininni, A. Alexakis, and A. Pouquet. Scale interactions and scaling laws in rotating flows at moderate rossby numbers and large reynolds numbers. Phys. Fluids, 21:015108:1–14, 2009.

[83] P. D. Mininni and A. Pouquet. Rotating helical turbulence. I. Global evolution and spectral behavior. Phys. Fluids, 22:035105:1–9, 2010.

[84] P. D. Mininni and A. Pouquet. Rotating helical turbulence. II. Intermittency, scale invariance and structures. Phys. Fluids, 22:035106:1–10, 2010.

[85] P. D. Mininni, D. Rosenberg, and A. Pouquet. Isotropization at small scales of rotating helically driven turbulence. Jour. Fluid Mech., 699:263–279, 2012.

[86] P. D. Mininni, D. Rosenberg, R. Reddy, and A. Pouquet. A hybrid MPI-OpenMP scheme for scalable parallel pseudospectral computations for fluid turbulence. Parallel Computing, 37:316–326, 2011.

[87] H. K. Moffatt. The degree of knottedness of tangled vortex lines. Jour. Fluid Mech., 35:117–129, 1969.

[88] H. K. Moffatt and A. Tsinober. Helicity in laminar and turbulent flow. Annu. Rev. Fluid Mech., 24:281–312, 1992.

[89] C. Morize and F. Moisy. Energy decay of rotating turbulence with confinement effects. Phys. Fluids, 18:065107:1–9, 2006.

[90] P. J. Morrison. Hamiltonian description of the ideal fluid. Rev. Modern Phys., 70 (2):467–521, 1998.

[91] B. T. Nadiga and J. M. Aurnou. A table top demonstration of atmospheric dynamics: baroclinic instability. Oceanography, 21 (4):196201, 2008.

[92] S. Nazarenko. Wave Turbulence. Springer, 2011.

[93] S. Nazarenko and A. Scheckochihin. Critical balance in magnetohydrodynamics, rotating and stratified turbulence. Jour. Fluid Mech., 677:134–153, 2011.

[94] S. M. Neamtan. The motion of harmonic waves in the atmosphere. J. Meteorol., 3:53–56, 1946.

[95] E. Noether. Invariante variationsprobleme. Math-phys. Klasse, pages 235–257, 1918.

[96] J. Pedlosky. Geophysical Fluid Dynamics. Springer (NY), 1987.

[97] A. E. Perry, S. Henbest, and M.S. Chong. A theoretical and experimental study of wall turbulence. Jour. Fluid Mech., 165:163–199, 2006.

[98] T. G. Philbin. Lipkin's conservation law, noether's theorem, and the relation to optical helicity. Phys. Rev. A, 87:043843:1–7, 2013.

[99] A. Pouquet and P. D. Mininni. The interplay between helicity and rotation in turbulence: implications for scaling laws and small-scale dynamics. Phil. Trans. R. Soc. A, 368:1635–1662, 2010.

[100] A. Pouquet and G. S. Patterson. Numerical simulation of helical magnetohydrodynamic turbulence. Jour. Fluid Mech., 85:305–323, 1978.

[101] J. Proudman. On the motion of solids in a liquid possessing vorticity. Proc. R. Soc. London A, 92:408–424, 1916.

[102] Lewis Fry Richardson. Weather Prediction by Numerical Process. Cambridge University Press, 1922.

[103] P. A. Robinson. Nonlinear wave collapse and strong turbulence. Revs. Modern Phys., 69:507–573, 1997.

[104] C. G. Rossby. Relations between variations in the intensity of the zonal circulation of the atmosphere and the displacements of the semipermanent centers of action. J. Marine Res., 2 (1):38–55, 1939.

[105] G. Rude and F. A. Ringwald. Waves in accretion disks, observed with fresno state's station at sierra remote observatories: Hv andromedae, lq pegasi, and ln ursae majoris. American Astronomical Society Meeting Abstracts, 219:348.20, 2012.

[106] C. Salyk, A.P. Ingersoll, J. Lorre, A. Vasavada, and A.D DelGenio. Interaction between eddies and mean flow in jupiter's atmosphere: Analysis of cassini imaging data. Icarus, 185:422–430, 2007.

[107] J. F. Scinocca and P. H. Haynes. Dynamical forcing of stratospheric planetary waves by tropospheric baroclinic eddies. Jour. Atmos. Sci., 55 (14):2361–2392, 1998.

[108] A. Sen, K. Julien, and A. Pouquet. Hamiltonian wave dynamics on the genesis of eddies from slow waves in rotating flows. (to be submitted to JFM soon), 2012.

[109] A. Sen, P. D. Mininni, D. Rosenberg, and A. Pouquet. Anisotropy and non universality in scaling laws of the large-scale energy spectrum in rotating turbulence. Phys. Rev. E, 86:036319: 1–15, 2012.

[110] T.G. Shepherd. Hamiltonian dynamics. In Encyclopedia of Atmospheric Sciences (J.R. Holton et al., eds.), pp. 929-938,. Academic Press, 2003.

[111] A. A. Simon-Miller, J. H. Rogers, P. J. Gierasch, D. Choi, M. D. Allison, A. Adamoli, and H. J. Mettig. Longitudinal variation and waves in jupiter's south equatorial wind jet. Icarus, 218:817–830, 2012.

[112] L. M. Smith, J. R. Chasnov, and F. Waleffe. Crossover from two-to three-dimensional turbulence. Phys. Rev. Lett., 77:2467–2470, 1996.

[113] L. M. Smith and Y. Lee. On near resonances and symmetry breaking in forced rotating flows at moderate rossby number. Jour. Fluid Mech., 535:111–142, 2005.

[114] L. M. Smith and F. Waleffe. Transfer of energy to two-dimensional large scales in forced, rotating three-dimensional turbulence. Phys. Fluids A, 11:1608:1–15, 1999.

[115] L. M. Smith and F. Waleffe. Generation of slow large scales in forced rotating stratified turbulence. J. Fluid Mech., 451:145–168, 2002.

[116] P. Tabeling. Two-dimensional turbulence: a physicist approach. Phys. Rep., 362:1–62, 2002.

[117] G. I. Taylor. Motion of solids in fluids when the flow is not irrotational. Proc. R. Soc. London A, 93:92–113, 1917.

[118] G. I. Taylor and A.E. Green. Mechanism of the production of small eddies from large ones. Proc. R. Soc. Lond. A, 158:499–521, 1937.

[119] T. Teitelbaum and P. D. Mininni. The decay of turbulence in rotating flows. Phys. Fluids, 23:065105:1–15, 2011.

[120] T. Teitelbaum and P. D. Mininni. The decay of batchelor and saffman rotating turbulence. arXiv:1203.2201, 2012.

[121] S. Thalabard, D. Rosenberg, A. Pouquet, and P.D. Mininni. Conformal invariance in three-dimensional rotating turbulence. Phys. Rev. Lett., 106:204503: 1–4, 2011.

[122] M. Thiele and W. C. Muller. Structure and decay of rotating homogeneous turbulence. Jour. Fluid Mech., 637:425–442, 2009.

[123] S. V. Nazarenko V. S. L'vov and O. Rudenko. Gradual eddy-wave crossover in superfluid turbulence. J. Low Temp. Phys., 153:140–161, 2008.

[124] G. K. Vallis. Atmospheric and Oceanic Fluid Dynamics: Fundamentals and Large-scale Circulation. Cambridge University Press, 2006.

[125] G. J. F. van Heijst and H. J. H. Clercx. Laboratory modeling of geophysical vortices. Annu. Rev. Fluid Mech., 41:143–164, 2009.

[126] F. Waleffe. The nature of triad interactions in homogeneous turbulence. Phys. Fluids A, 4:350–363, 1992.

[127] F. Waleffe. Inertial transfers in the helical decomposition. Phys. Fluids A, 5:677–685, 1993.

[128] A. Warmuth. Globally propagating waves in the solar corona. Plasma Phys. Control. Fusion, 53:124023:1–9, 2011.

[129] G. M. Webb, J. F. McKenzie, Q. Hu, and G. P. Zank. Alfv́en wave mixing and non-jwkb waves in stellar winds. J. Phys. A: Math. Theor., 46:125501:1–28, 2013.

[130] G. B. Whitham. Linear and Nonlinear Waves. A Wiley-Interscience publication, 1974.

[131] A. Wuthrich. The Genesis of Feynman Diagrams. Springer Science and Business Media B. V., 2010.

[132] A. Yahalom. Helicity conservation via the noether theorem. J. Math. Phys., 36 (3):1324–1327, 1995.

[133] V. E. Zakharov. Stability of periodic waves of finite amplitude on the surface of a deep fluid. Zh. Prikl. Mekh. Tekh. Fiz, 9:86–94, 1968.

[134] V. E. Zakharov and N. N. Filonenko. Weak turbulence of capillary waves. Jour. Appl. Mech. Phys., 8 (5):62–67, 1967.

[135] V. E. Zakharov, V. S. Lvov, and G. Falkovich. Kolmogorov Spectra of Turbulence: Wave Turbulence. Springer, 1992.

[136] Ye Zhou. A phenomenological treatment of rotating turbulence. Phys. Fluids, 7:2092–2094, 1995.

Appendix A

A brief summary on the origin of R-RHD equations

Detail explanations of this chapter can be found in the paper by Julien et. al. [60]. A brief overview of the origin of the reduced set of equations used in chapter (3) is presented here.

A.1 The governing equation

The Navier-Stokes equation for an incompressible flow are as follows:

$$D_t\mathbf{u} + \hat{\Omega} \times \mathbf{u} = -\nabla P + E\nabla^2\mathbf{u}, \tag{A.1}$$

$$\nabla \cdot \mathbf{u} = 0, \tag{A.2}$$

where, Ekman number, $E := \frac{\nu}{2\Omega d^2}$, ν is the kinematic viscosity, d is the typical length scale imposed by the domain size and $\mathbf{\Omega} = \Omega\hat{z}$ is the rotation vector. Here, time is scaled in units of $(2\Omega)^{-1}$, distances in units of d and velocities in units of $2\Omega d$.

A.2 Stream-function formulation of the governing equation

A choice of a vector valued function, $\chi = \phi\hat{\mathbf{z}} + \nabla \times \psi\hat{\mathbf{z}}$ is made such that $\mathbf{u} = (u, v, w) = \nabla \times \chi$ ensures the incompressibility condition automatically due to the vector identity, $\nabla \cdot (\nabla \times \chi) \equiv 0$. Then velocity and vorticity can be expressed in terms of the stream-functions, ϕ, ψ, as follows:

$$\mathbf{u} = \begin{pmatrix} \partial_y\phi + \partial_x\partial_z\psi \\ -\partial_x\phi + \partial_y\partial_z\psi \\ -\nabla_\perp^2\psi \end{pmatrix}, \quad \zeta = \begin{pmatrix} \partial_x\partial_z\phi - \nabla^2\partial_y\psi \\ \partial_y\partial_z\phi + \nabla^2\partial_x\psi \\ \nabla_\perp^2\phi \end{pmatrix}. \tag{A.3}$$

Using the form of equation (A.3), the governing equation (A.1) can be written as follows by taking $(\hat{\mathbf{z}} \cdot \nabla\times)$ and $(\hat{\mathbf{z}} \cdot \nabla\times)\nabla\times$ of the momentum equation (A.1):

$$\partial_t \nabla_\perp^2 \phi - (\hat{\mathbf{\Omega}} \cdot \nabla)\nabla_\perp^2 \psi + N_\phi(\phi, \psi) = E\nabla^2\nabla_\perp^2 \phi, \tag{A.4}$$

$$\partial_t \nabla^2\nabla_\perp^2 \psi + (\hat{\mathbf{\Omega}} \cdot \nabla)\nabla_\perp^2 \phi + N_\psi(\phi, \psi) = E\nabla^4\nabla_\perp^2 \psi, \tag{A.5}$$

where $N_\phi(\phi, \psi) \equiv (\zeta \cdot \nabla)w - (\mathbf{u} \cdot \nabla)\zeta_{(z)}$ and $N_\psi(\phi, \psi) \equiv \hat{\mathbf{z}} \cdot \nabla \times \nabla \times (\zeta \times \mathbf{u})$. Note that $\zeta_{(z)}$ is the vertical component of the vorticity, ζ. N_ϕ and N_ψ can then be written in terms of ϕ and ψ.

A.3 Asymptotic analysis

A multiple scale asymptotic analysis is then performed using equations (A.4) and (A.5), $E \ll 1$ is the small expansion parameter. The Taylor-Proudman theorem demands slow variation in the vertical direction, denoted here by $D := \partial_z$ and hence fast horizontal variables are introduced, $x' \equiv E^{-1/3}x, y' \equiv E^{-1/3}y$. Horizontal motion being in geostrophic balance demands the introduction of a slow time scale, $\tau = E^{1/3}t$. The stream-function is scaled as: $\phi = E\phi'$, $\psi = E^{4/3}\psi'$. The above implies that locally, $Ro \sim \mathcal{O}(E^{1/3})$ and is hence extremely small. Using the aforementioned scalings in equations (A.4) and (A.5), the following equations are obtained in terms of the new variables denoted by primes (except that the primes have been dropped):

$$\partial_\tau \nabla_\perp^2 \phi - J[\phi, \nabla_\perp^2 \phi] - D\nabla_\perp^2 \psi = \nabla_\perp^4 \phi + \mathcal{O}(E^{1/3}), \tag{A.6}$$

$$\partial_\tau \nabla_\perp^2 \psi - J[\phi, \nabla_\perp^2 \psi] + D\phi = \nabla_\perp^4 \psi + \mathcal{O}(E^{1/3}). \tag{A.7}$$

Then, using the fact that $w = -\nabla_\perp^2 \psi$ and $\zeta_{(z)} = -\nabla_\perp^2 \phi$ and ignoring viscosity, the reduced rotating hydrodynamic (R-RHD) equations are written in simple form as:

$$\partial_t \zeta_{(z)} + J[\psi, \zeta_{(z)}] = \partial_z w \tag{A.8}$$

$$\partial_t w + J[\psi, w] = -\partial_z \psi \tag{A.9}$$

Note, $\zeta_{(z)} = \nabla_\perp^2 \psi$ and $\mathbf{u}_\perp = \nabla^\perp \psi$ in this formulation. This is the main set of equations for our analysis in chapter (3).

Appendix B

Vanishing integrals to show invariance of energy

Here we have chosen a function, $f(k_\perp) = \frac{1}{k_\perp^2}$ but the result is true for any function of $k_\perp$ that decays slower than an exponential function.

First we show that $\int \frac{1}{k_\perp^2} e_{\mathbf{p}} e_{\mathbf{q}} \delta_{\mathbf{k},\mathbf{pq}} \delta_{\omega_k,\omega_p\omega_q} d\mathbf{k} = 0$. To show this, we approximate the delta function with a limiting exponential function as: $\delta_{\omega_k,\omega_p\omega_q} \approx \lim_{\sigma\to 0} e^{-\frac{\omega_k-\omega p-\omega_q}{\sigma}}$.

$$\begin{aligned}
\int \frac{1}{k_\perp^2} e_{\mathbf{p}} e_{\mathbf{q}} \delta_{\mathbf{k},\mathbf{pq}} \delta_{\omega_k,\omega_p\omega_q} d\mathbf{k} &\propto \int \delta_{k_z,p_zq_z} \int \frac{1}{k_\perp^2} \delta_{k_\perp,p_\perp q_\perp} \lim_{\sigma\to 0} e^{-\frac{\omega_k-\omega p-\omega_q}{\sigma}} dk_\perp dk_z \\
&= \int \delta_{k_z,p_zq_z} \lim_{\sigma\to 0} \int \frac{1}{k_\perp^2} e^{-(\frac{k_z}{k_\perp}-\frac{p_z}{p_\perp}-\frac{q_z}{q_\perp})\sigma^{-1}} \delta_{k_\perp,p_\perp q_\perp} dk_\perp dk_z \\
&= \int \delta_{k_z,p_zq_z} \lim_{\sigma\to 0} e^{(\frac{p_z}{p_\perp}+\frac{q_z}{q_\perp})\sigma^{-1}} \int \frac{1}{k_\perp^2} e^{-\frac{k_z}{\sigma k_\perp}} \delta_{k_\perp,p_\perp q_\perp} dk_\perp dk_z = 0. \qquad \text{(B.1)}
\end{aligned}$$

The above equation is zero on account of the integral $\int \frac{1}{k_\perp^2} e^{-\frac{k_z}{\sigma k_\perp}} \delta_{k_\perp,p_\perp q_\perp} dk_\perp$ being zero as shown below. Using integration by parts and the fact that for some arbitrary continuous function $f(x)$, $\int f(x)\delta_{x-a}dx = f(a)$, we have,

$$\begin{aligned}
I = \int \frac{1}{k_\perp^2} e^{-\frac{k_z}{\sigma k_\perp}} \delta_{k_\perp,p_\perp q_\perp} dk_\perp &= \frac{1}{k_\perp^2} \int e^{-\frac{k_z}{\sigma k_\perp}} \delta_{k_\perp,p_\perp q_\perp} dk_\perp + \int \frac{2}{k_\perp^3} e^{-\frac{k_z\sigma^{-1}}{p_\perp+q_\perp}} dk_\perp \\
&= \frac{1}{k_\perp^2} e^{-\sigma^{-1}\frac{k_z}{p_\perp+q_\perp}} - \frac{1}{k_\perp^2} e^{-\sigma^{-1}\frac{k_z}{p_\perp+q_\perp}} = 0. \qquad \text{(B.2)}
\end{aligned}$$

Next, by following a similar argument it can be shown that

$$\int \frac{1}{k_\perp^2} e_{\mathbf{k}} e_{\mathbf{p}} \delta_{\mathbf{k},\mathbf{pq}} \delta_{\omega_k,\omega_p\omega_q} d\mathbf{k} = 0$$

and

$$\int \frac{1}{k_\perp^2} e_{\mathbf{k}} e_{\mathbf{q}} \delta_{\mathbf{k},\mathbf{pq}} \delta_{\omega_k,\omega_p\omega_q} d\mathbf{k} = 0$$

Appendix C

Publications that resulted from this thesis

Publications

(1) **Sen, A.**, Mininni, P. D., Rosenberg, D., and Pouquet, A., *Anisotropy and nonuniversality in scaling laws of the large-scale energy spectrum in rotating turbulence*, Phys. Rev. E 86, 036319 (2012).

(2) Pouquet, A., **Sen, A.**, Rosenberg, D, Mininni, P. D., and Baerenzung, J., *Inverse cascades in turbulence and the case of rotating flows*, Phys. Scr., 2013, T-155, 014032 (2013).

(3) **Sen, A.**, Julien, K., and Pouquet, A., *A weak wave turbulence theory for rotationally constrained slow inertial waves*, http://arxiv.org/abs/1312.7497 (2013).

Research Funds

(1) NSF/CMG Grant No. 1025183 (NCAR, PI: Annick Pouquet, Jan 2011-April 2013)

(2) FRG/NSF, Award No. DMS 0855010 (CU Boulder, PI: Keith Julien, Summer 2012)

(3) Department of Applied Math for financial support.